International Pyrheliometer Comparison
IPC VIII
25 September - 13 October 1995

Results and Symposium

International Pyrheliometer Comparison
IPC VIII
25 September - 13 October 1995

Results and Symposium

Working Report No.188
Swiss Meteorological Institute
Davos and Zürich, May 1996

Table of Contents

1 Organization and Procedures

1.1 Introduction

The 8th International Pyrheliometer Comparisons were held, together with Regional Comparisons for the Regional Associations of Africa (RA I), Asia (RA II), North and Central America (RA IV), Europe and Near East (RA VI), from 25 September through 13 October 1995 at PMOD/WRC in Davos. The reason for this combination was the urgent need for Pyrheliometer Comparisons in some Regions and the lack of funds and time to organize them in the corresponding area. This led to the largest number of participants and instruments since the start of the IPC in 1959.

These Comparisons were *in memoriam* of and dedicated to Ron Latimer who died in early February 1995. He was with the Canadian Meteorological Service and participated in 5 IPC (2 to 6), the last one just before he retired from the Service. His profound knowledge and expertise in meteorological radiometry influenced the way IPC were performed. Not only by his voice "Please shade and heat the right hand strip ...." recorded in 1970 remains in the conscientious memory of all participants sharing the experience (for details see Sct.5: *In Memoriam* Ron Latimer).

The results presented in this report are based on 8 days of measurements with very good or excellent conditions. Time on other days was used for technical preparations and training of participants and a symposium on meteorological radiometry.

Figure 1.1: Most of the 62 Participants of IPC VIII in October 1995. Photo: PMOD/WRC

1.2 Participation

The group photo of Fig.1.1 shows most of the 62 participants from 15 Regional- and 28 National Radiation Centers and from 8 Institutions not directly linked to WMO structures. They operated a total of 77 pyrheliometers, 44 of which were already present at IPC VII and 33 instruments being compared to WRR for the first time.

Table 1.1-1.3 lists the participants according to Regions and the Institutions respectively. A complete list of participants with addresses can be found in Chapter 4.

Table 1.1: IPC VIII Participation: *World Radiation Centers*

Country	Institution	Participants
Russia	Main Geophysical Observatory, Leningrad	V. Klevantsova
Switzerland	Physikalisch-Meteorologisches Observatorium Davos	C. Fröhlich, R. Philipona, J. Romero, HJ. Roth, Ch. Wehrli

Table 1.2: IPC VIII Participation: *Regional and National Radiation Centers*

Country	*Institution*	*Participants*
RA I		
Algeria	Office National de Météorologie, Alger	A. Chabane
Egypt	Egyptian Meteorol. Authority, Cairo	M.A. Darwisch
Ethiopia	National Meteorol. Agency, Addis Ababa	E. Bekele
Nigeria	Meteorol. Dept., Lagos	I. Nnodu
Tunisia	Inst. National de la Météorologie., Tunis	S. Ben Abdallah, M. Bin Mihfood
Saudi Arabia	King Abdulaiz City for Science, Riyadh	M. Al-Muhaisini
South Africa	The Weather Bureau, Pretoria	C. Archer
Sudan	Meteorol. Dept., Khartoum	H. Abdalla
RA II		
India	Meteorol. Office, Pune	S. Naseeruddin
Japan	Meteorol. Agency, Tokyo	Y. Hirose
Mongolia	Hydromet. Inst. of Mongolia, Ulan Bataar	S. Gonchig
Philipines	Solar Rad. Center, Quezon City	J. Yunzal

Country	*Institution*	*Participants*
Thailand	Dept. of Meteorology, Bangkok	K. Khovadhana
Uzbekistan	Glavgidromet, Tashkent	A. Umarov
RA III		
Argentinia	Meteorol. Service, Buenos Aires	G. Atienza
Chile	Direction Meteol., Santiago	M. Vargas
Costa Rica	Escuela de Fisica, San José	V. Castro
Cuba	Inst. de Meteorol., Habana	F. Vigón del Busto
RA IV		
Canada	Atmospheric Environm. Service, Toronto	T. Grajnar, B. McArthur
USA	NOAA, Boulder	D. Nelson, E. Dutton
Mexico	Inst. de Geofisica, Coyoacan	J. Bravo-Cabrera
Mexico	Universidad de Colima, Colima	I. Galindo, G. Galindo-Rios
RA V		
Australia	Bureau of Meteorology, Melbourne	B. Forgan, P. Novotny
RA VI		
Austria	Meteorol. Zentralanstalt, Wien	E. Wessely
Austria	Inst. für Meteorologie, Wien	W. Laube
Belgium	Inst. Royal de Météorologie, Bruxelles	A. Joukoff, S. Ginion
Estonia	Meteorol. Inst., Tartu	A. Kallis
Finland	Meteorol. Inst., Helsinki	L. Laitinen
France	Centre Radiométrique, Carpentras	J. Oliviéri
Germany	Deutscher Wetterdienst, Potsdam	K. Behrens, K. Dehne
Spain	Observatorio Meteorol. Especial de Izaña, Tenerife	J. Pérez de la Puerta
Hungary	Inst. for Atmospheric Physics, Budapest	Z. Nagy
Israel	Meteorol. Service, Bet Dagan	A. Israeli, A. Manes
Republic of Iran	Meteorol. Organization, Teheran	F. Khani Moghanaki

Country	*Institution*	*Participants*
Netherlands	Meteorol. Institute, AE De Bilt	F. Kuik, A. Van Londen
Portugal	Inst. de Meteorologia, Lisbon	M. Rocha
Romania	Nat. Inst. of Meteorologia, Bucaresti	C. Oprea
Slovakia	Slovak Hydromet. Inst., Bratislava	V. Horecká
Spain	Inst. Nacional, Madrid	J. Pardo Mainez
Sweden	Meteorol. Institute, Norrköping	L. Dahlgren, Th. Persson
Switzerland	Schweiz. Meteorol. Anstalt, Payerne	-
United Kingdom	Meteorol. Office, Berkshire	M. Collins, St. Goldstraw

Table 1.3: IPC VIII Participation: *Various Institutions*

Country	*Institution*	*Participants*
DSET, USA	DSET Lab., Phoenix	-
Eppley, USA	Eppley Lab., Newport	J. Hickey, T. Kirk
JPL, USA	Jet Propulsion Lab., Pasadena	M. Cerezo
NREL, USA	Nat. Renewable Energy Lab., Golden	I. Reda, T. Stoffel, J. Treadwell
Inst. de Geophysica, Mexico	Universidad Nat. Autonómica, Mexico	A. Muhlia
Kipp & Zonen, Netherlands	Kipp & Zonen, Delft	L. Van Wely
NTI, Sweden	Nat. Testing Inst., Boras	L. Liedquist
VNIIO, Russia	All-Russian Research Inst., Moscow	S. Morozowa, M. Pavlovitch

1.3 Data Acquisition and Evaluation

The WSG instruments and some radiometers and auxiliary parameters are measured by an analog data acquisition system based on eight HP3478A voltmeters with relay scanners that are controlled by a HP9216 computer. Data from participating instruments are acquired via a number of micro terminals operated by the participants and controlled by the HP9216 computer. This scheme permits each instrument to be operated with its standard equipment and avoids electrical interface problems and mutual interferences. Each terminal can accept 3 different values from two instruments, identified by labels A through F. Due to the large number of instruments involved, not all of them could be accommodated simultaneously on micro terminals. Fortunately, some of the participants had their own computer controlled systems which they synchronized to the

timing of IPC's measurement runs. At the end of each day, they delivered their data on floppy disks which were then converted and incorporated into the data set residing on the HP computer for further processing.

Data from 77 pyrheliometers were acquired: 14 by the analog data acquisition system of PMOD/WRC, 45 through micro terminals and 18 via floppy disks. The final evaluation contains about 85'000 irradiance values.

1.3.1 Timing of the Measurements

The measurements are taken in runs lasting 21 minutes with a basic cadence of 90 seconds. Voice announcements ending in a buzzer signal are used to inform the participants about the sequence of operations. Timing for the different instrument types proceeds as follows:

a) Ångström pyrheliometers: during the first 90s the zero of the instrument is established. From then on, alternating right or left strip readings are performed, starting with the right hand strip exposed to the sun. The first reading is not taken into account. The following readings are paired as L-R, R-L, etc., yielding a total of 11 irradiance values per run.

b) PACRAD: the run starts with shutter closed, after 60s the heater is turned on for 30s (this was introduced after IPC III in order to have a well defined thermal state of the instrument independent of the operation sequence before the run). At 270s the zero of the thermopile is read and the heater switched on again. At 360s the heater voltage, current and thermopile is read, the heater turned off and the shutter opened. From 450s on readings are taken every 90s yielding 8 irradiance values per run. After the last reading the shutter is closed.

c) HF type pyrheliometers: the run starts with the shutter closed, after 90s the zero is read and the heater turned on until at 180s the voltage, current and thermopile are read. The heater is then turned off and the shutter opened. From 270s onward the instrument is read every 90s yielding 11 irradiance values per run.

d) TMI type pyrheliometers: the run starts with shutter closed and the calibration procedure is performed until the end of the first 90s. Starting at 180s readings are taken every 90s yielding 12 irradiance values per run.

e) Active cavity type pyrheliometers: the run starts with a reference phase (shutter closed) during the first 90s, followed by a measurement phase (shutter open) for the next 90s. This is repeated for the next 18 minutes. A total of 6 open and 7 closed readings are taken yielding a total of 6 irradiance values during a run. PMO2 is read at twice that pace, with a reference phase of 38s and a measurement phase of 52s, producing 13 irradiance values per run so that for all readings of the basic sequence a PMO2 irradiance is available.

f) Normal Incidence Pyrheliometers (NIP): they take 12 irradiance values every 90s after an initial zero reading at 90 seconds.

1.3.2 Data Evaluation

For each instrument the irradiance is obtained with the corresponding evaluation procedure. After each run, a summary of measured values and evaluated irradiances is printed and distributed to be checked by the participants. If necessary, the raw data can be edited for gross errors. Updated summaries with the mean and standard deviation of the ratio to PMO2 are made available for each instrument during the course of the comparison.

For each type of instrument the procedure used to calculate the irradiance S is described in the following. The notations are:

V_{th}	output of the thermopile
U_h,U_i	voltage across heater (h) or standard resistor (I)
R_n	standard resistor
C	calibration factor
C_2	correction factor for lead heating
P	electrical power in the active cavities

a) Å-pyrheliometers: the current through the right or left strip is measured as voltage drop across a standard resistor and the irradiance obtained as:

$$S=C\frac{U_i(left)U_i(right)}{R_n^2}$$

This corresponds to the geometric mean of the irradiances at the time of right and left readings. Thus, the ratio to WRR is calculated using the geometric mean of WSG irradiances at the corresponding instances.

b) PACRAD and HF type pyrheliometers: the irradiance is calculated from the thermopile output V_{th}(irrad) when the receiver is irradiated. The sensitivity is determined by the calibration during which the cavity is electrically heated and U_h and U_i are measured together with the corresponding thermopile output V_{th}(cal). Furthermore, the zero of the thermopile V_{th}(null) is measured and substracted.

$$S=C\frac{V_{th}(irrad)-V_{th}(zero)}{V_{th}(cal)-V_{th}(zero)}\frac{U_i}{R_n}(U_h-\frac{U_i}{R_n}C_2)$$

c) TMI type pyrheliometers: most are operated in the "normal" way, that is by calibrating the readout directly in units of $mWcm^{-2}$. The values are entered in Wm^{-2} and no irradiance calculation is needed. Others are operated and evaluated like HF pyrheliometers.

d) Active cavity pyrheliometers: the irradiance is obtained from *P(closed)* averaged from the closed values before and after the open reading *P(open)*. The power calculation is according to the prescription of the instrument type

$$S = C\,(P(closed)-P(open))$$

$$\text{with } P = U_h^2 \text{ or } P = U_hU_i \text{ or } P = U_h\frac{U_i}{R_n}$$

e) Normal Incidence Pyrheliometer (NIP): the thermopile reading is multiplied by the calibration factor after substraction of the zero point reading.

f) PMO2: As during preceding IPC's, PMO2 is used as the local reference instrument because it can be operated fast enough to provide an irradiance value every 90 seconds. The values of PMO2 are obtained with the algorithm for active cavity radiometers. At the end of the open phase, 8 readings are taken in rapid succession. The average of these 8 readings is used as the PMO2 value for further evaluation. For the on-line calculations the first value is used as reference for the values entered by the terminals while the remaining serve as reference for each scan position of the analog data acquisition system. The standard deviation of the 8 readings is used during the final evaluation as a quality control parameter to judge the stability of the radiation during each acquisition sequence (see para. 1.3.1).

1.3.3 Auxiliary Data

The meteorological parameters air temperature, relative humidity and atmospheric pressure are taken from the automatic weather station ASTA of the Swiss Meteorological Service located at PMOD/WRC. Direct-, global- and sky radiation are recorded by the RASTA (Radiometer for ASTA) Radiometer and the ASRB (Alpine Surface Radiation Budget) pyranometers on the roof of the Institute. The values from ASTA and RASTA are 10-minute averages and the one from the ASRB pyranometers 2-minute averages. The value allocated to each measurement run are averages of this period and the results are plotted in 2.21 and 2.23.

Sunphotometer measurements taken simultaneously with Pyrheliometer data are used to determine the vertical aerosol optical depth at 368, 500 and 778nm. Daily total Ozone values measured at Arosa (about 15 km south-west of Davos) are used for the evaluation of the 500nm channel. The total amount was: 260.6, 251.8, 276.3, 267.2, 274.9, 274.7 and 275.0 mcm (Dobson units) on 2, 3, 7, 9, 10, 11 and 12 October 1995 respectively. The optical depth results are plotted in 2.22.

2 Measurements and Results

During the Comparisons over 1200 measurements were taken on 10 days, four of which had excellent sky conditions. Data from the following 8 dates have been selected for the final evaluation: 2, 3, 7, 9, 10, 11 and 12 October 1995 with 1093 irradiances of PMO2.

2.1 Data Selection Criteria for Final Evaluation

Several criteria are used to select the data for final evaluation. A first criterion eliminates the influence of the local horizon entering the view limiting angle of the instruments. From known solar position and horizon, limits on measurement time are determined for circular and rectangular aperture instruments and listed in Table 2.1.

A second criterion rejects sequences where a standard deviation of the 8 rapid PMO2 readings larger than 0.3 Wm^{-2} indicates a radiation instability.

The third criterion applies on individual instruments: a filter rejects measurement with a deviation of more than 1% from the mean ratio to WRR of that instrument.

Table 2.1: Selection of measurement periods constrained by local horizon and view limiting geometry.

Date	Cavity pyrheliometers	Ångstrom pyrheliometers
2 October 1995	7 h 38 - 16 h 28	9 h 03 - 15 h 32
3 October 1995	7 h 41 - 16 h 27	9 h 05 - 15 h 30
7 October 1995	7 h 54 - 16 h 22	9 h 16 - 15 h 21
9 October 1995	7 h 38 - 16 h 28	9 h 22 - 15 h 17
10 October 1995	8 h 00 - 16 h 19	9 h 25 - 15 h 15
11 October 1995	8 h 7 - 16 h 16	9 h 27 - 15 h 12
12 October 1995	8 h 10 - 16 h 15	9 h 30 - 15 h 10

2.2 Determination of the WRR

The main objective of the periodic Pyrheliometer Comparisons is the dissemination of the World Radiometric Reference (WRR) in order to ensure worldwide homogeneity of meteorological radiation measurements. The WRR is realized by World Standard Group which is frequently inter-compared at PMOD/WRC to detect possible deviations of individual members of the group and to ensure the stability of WRR. Independently, the stability of the WRR can be checked by instruments that have participated in previous IPC's.

For the traceability of the WRR from IPC VII to IPC VIII four instruments of the WSG can be used: PMO-2, PMO-5, CROM-2L and CROM-3R; the remaining three, PAC3, MK67814 and HF18748, had different instrumental problems: In April 1993 a fly entered into the cavity of PAC3. It could be removed, but no further cleaning was performed and a rather large change was observed. The original control electronics of TMI MK67814 showed intermittent problems and had to be replaced. As stated in the IPC VII report the HF18748 had a bug in its cavity which was removed after the IPC; the new value was somewhat higher, but stayed very constant since then.

In a first step the irradiances of all WSG radiometers are scaled to WRR by their WRR factors either from IPC VII (PMO-2, PMO-5, CROM-2L and CROM-3R) or estimated from the results of interim comparisons (PAC3, MK67814 and HF18748); they are listed in the 2nd column of Table 2.2. For the 255 sequences where all 4 instruments had valid irradiance values their average is used as reference to calculate the ratio of each irradiance to that reference. In a second step, the mean and standard deviation of these ratios are calculated for all WSG pyrheliometers which are listed in column 3 and 4 of Table 2.2. The mean of the ratios for the 4 radiometers tracing the WRR from IPC VII amounts to 0.999998 with a standard deviation of 0.000222. The mean being very close to one demonstrates the stability of the 4 WSG instruments and the careful maintenance of the WRR

Table 2.2: Ratios of WSG to WRR realized by (*) using IPC VII factors.

Instrument	WRR factors IPC VII	Ratio to WRR IPC VIII	Standard. Deviation	Change [ppm] IPC VIII - VII
*PMO2	0.99944	1.00058	0.0015	-20
*PMO5	1.00063	1.99909	0.0014	279
*CROM2L	1.00294	0.99706	0.0018	5
*CROM3R	0.99890	1.00137	0.0033	-265
PAC3	1.00027	0.99818	0.0014	1552
MK67814	1.00094	0.99936	0.0015	-297
HF18748	0.99576	1.00402	0.0015	237

For the final evaluation of the participating instruments the ratios of Table 2.2 are used to calculate for each sequence the WRR reference as the mean irradiance of all WSG pyrheliometers that are available at a given sequence. This means that the final ratios of the WSG instruments as listed in Table 2.3 are slightly different from the ones in Table 2.2. Moreover, to remove outlier from the WSG the following criterion is used: If the standard deviation of the reference irradiance is greater than 5 Wm^{-2} the individual WSG value which causes this deviation is rejected.

The stability of the WRR can be further checked by calculating the average ratio over all pyrheliometers that have participated in IPC VII. Taking all instruments (39, including the WSG) the average amounts to 0.999658 with a standard deviation of 0.001334. If instruments with a ration lying more than 0.3% (0.2%) off, the average is 0.999710 (0.999832) with 37 (35) instruments remaining. These results are certainly confirming the conclusion from the results of the WSG alone.

2.3 Approvement and Dissemination of the Results

Formerly the CIMO Working Group on Radiation has taken the responsibility for the final results and the dissemination of the corresponding final calibration constants to each participating Pyrheliometer. A major problem arose from the fact that the next CIMO session had to be awaited. WMO therefore decided to nominate an *ad-hoc* Working Group from among the participants of IPC VIII, chaired by the CIMO-Rapporteur on Meteorological Radiation Measurements Klaus Dehne, Germany. The members designated are: D.M. Achmed (RA I), A. Chabane (RA I), Y.Hirose (RA II), B. McArthur (RA IV), I. Galindo (RA IV), B. Forgan (RA V), V. Klevantsova (RA VI), J. Olivieri (RA VI).

The procedure to evaluate the final results and the new WRR factors of the WSG instruments have been approved by the *ad-hoc* WG and the final results of IPC VIII have been calculated accordingly.

2.4 Results

The following Tables show the results: Tables 2.3-2.5 show the ratios and standard deviations for each individual instrument and the recommended WRR or calibration factors (Table 2.3/2.6.: WSG, Table 2.4/2.7.: Absolute Radiometers and Table 2.5/2.8. Å-Pyrheliometers and NIP). The results of each instrument are also plotted in Section 3 with the corresponding histograms.

Table 2.3: Final results of the WSG

Instrument	Ratio to WRR	Standard Deviation	Num	Min	Max	IPC VII	Owner
PMO2	1.00064	0.00074	518	0.9985	1.0060	1	WSG
PMO5	0.99909	0.00091	241	0.9949	1.0021	1	WSG
CROM2L	0.99711	0.00130	239	0.9916	1.0023	1	WSG
CROM3R	1.00103	0.00269	229	0.9919	1.0090	1	WSG
MK67814	0.99932	0.00099	243	0.9963	1.0027	1	WSG
PAC3	0.99814	0.00074	286	0.9949	1.0011	-	WSG
HF18748	1.00407	0.00064	417	1.0014	1.0065	-	WSG

Table 2.4: Final Results of the absolute radiometers

Instrument	Ratio to WRR	Standard Deviation	N	Min	Max	IPC VII	Owner
PMO6-5	1.00202	0.00103	211	1.0002	1.0068	1	Germany
PMO609	0.99684	0.00105	242	0.9941	1.0036	0	PMOD

Instrument	Ratio to WRR	Standard Deviation	N	Min	Max	IPC VII	Owner
PMO610	0.99772	0.00228	239	0.9881	1.0064	1	PMOD
PMO611	0.99671	0.00115	242	0.9944	1.0010	0	PMOD
R80022	1.00389	0.00118	242	1.0005	1.0099	1	PMOD
R79-121	1.00003	0.00114	209	0.9913	1.0053	1	Switzerland
R811103	0.99954	0.00171	231	0.9920	1.0069	0	Germany
R811104	1.00303	0.00144	227	0.9972	1.0082	1	Spain
R811106	1.00457	0.00106	217	1.0009	1.0079	0	India
R811107	0.99998	0.00155	239	0.9951	1.0084	1	Japan
R811108	0.99989	0.00095	218	0.9973	1.0048	1	Sweden
R850401	1.00113	0.00155	221	0.9964	1.0078	1	Finland
R850404	0.99977	0.00130	230	0.9941	1.0081	0	South Africa
R850405	0.99963	0.00093	239	0.9922	1.0027	0	ETHZ
R850410	0.99820	0.00125	241	0.9912	1.0030	0	Chile
MK67502	1.00134	0.00131	412	0.9969	1.0060	1	NOAA
MK67604	0.99762	0.00103	449	0.9929	1.0012	1	United Kingdom
MK67702	1.00250	0.00132	462	0.9976	1.0070	1	JPL
MK68016	0.99950	0.00140	408	0.9949	1.0025	1	France
MK68018	1.00112	0.00106	483	0.9920	1.0049	1	NREL
MK68024	0.99914	0.00125	295	0.9926	1.0028	0	Austria
MK68025	1.00014	0.00138	461	0.9952	1.0039	1	Austria
MK69137	0.99722	0.00093	491	0.9924	1.0009	0	Australia
MAR-1-1	1.00089	0.00112	205	0.9963	1.0056	0	VNIIO
MAR-1-2	1.00039	0.00201	67	0.9973	1.0053	0	VNIIO
P13219	1.00078	0.00499	377	0.9901	1.0101	1	India
HF14915	0.99954	0.00118	426	0.9956	1.0034	1	Eppley
HF15744	1.00053	0.00087	453	0.9961	1.0033	1	Sweden
HF17142	1.00114	0.00114	389	0.9968	1.0064	1	DSET
HF18747	0.99905	0.00080	416	0.9953	1.0020	1	Canada
HF19746	1.00081	0.00074	416	0.9985	1.0028	1	Hungary
HF20406	0.99863	0.00089	423	0.9926	1.0012	0	Canada
HF23725	1.00342	0.00158	425	0.9966	1.0081	1	Tunesia
HF27157	0.99962	0.00109	378	0.9952	1.0028	0	Germany

Instrument	Ratio to WRR	Standard Deviation	N	Min	Max	IPC VII	Owner
HF27159	1.00112	0.00124	404	0.9971	1.0052	1	The Netherlands
HF27160	1.00292	0.00111	500	0.9985	1.0069	1	Australia
HF27162	0.99904	0.00158	426	0.9945	1.0087	1	Israel
HF27798	1.00102	0.00115	421	0.9971	1.0047	1	Eppley
HF28553	1.00245	0.00093	409	0.9985	1.0057	0	NOAA
HF28558	1.00211	0.00136	376	0.9923	1.0097	0	Costa Rica
HF28965	1.00142	0.00096	405	0.9978	1.0067	0	Mexico
HF28968	1.00173	0.00095	497	0.9980	1.0051	0	NREL
HF29220	1.00138	0.00107	401	0.9979	1.0044	0	NREL
HF29223	1.00256	0.00153	437	0.9935	1.0091	0	Mexico
HF30110	1.00274	0.00072	422	1.0000	1.0052	0	Saudi Arabia
HF30710	0.99993	0.00106	413	0.9906	1.0033	0	NOAA

Table 2.5: Final Results for the Ångström and Normal Incidence Pyrheliometer

Instrument	Ratio to WRR	Standard Deviation	N	Min	Max	IPC VII	Owner
A7	0.99840	0.00256	385	0.9884	1.0055	1	Belgium
A171	1.00033	0.00293	404	0.9903	1.0097	1	Sweden
A212	0.99825	0.00215	338	0.9918	1.0060	1	Russia
A238	1.00983	0.00393	285	1.0001	1.0197	0	Uzbekistan
A556	0.96353	0.00580	121	0.9553	0.9749	0	Cuba
A564	1.00346	0.00263	412	0.9944	1.0130	1	Egypt
A576	0.99954	0.00389	385	0.9902	1.0099	1	Nigeria
A578	0.99829	0.00277	409	0.9911	1.0080	1	Australia
A585	1.00830	0.00397	215	0.9981	1.0177	0	Mongolia
A702	0.97172	0.00343	379	0.9627	0.9818	0	Rumania
A7190	0.99908	0.00329	392	0.9887	1.0083	1	Belgium
A7636	0.99837	0.00250	348	0.9893	1.0074	1	France
A12578	0.96027	0.00414	341	0.9513	0.9707	0	Philipines
A12579	0.97553	0.00363	241	0.9656	0.9849	0	Iran
A13439	0.97753	0.00245	424	0.9682	0.9874	0	Slovakia
A15192	0.99811	0.00246	402	0.9889	1.0065	1	Austria
A16491	1.00357	0.00495	343	0.9940	1.0137	1	Algeria

Instrument	Ratio to WRR	Standard Deviation	N	Min	Max	IPC VII	Owner
A18587	0.99399	0.00381	420	0.9844	1.0036	1	Mexico
A25783	0.99831	0.00241	426	0.9899	1.0078	0	Chile
M-59-8	1.00077	0.00344	363	0.9920	1.0108	0	Estonia
N-18649	0.97088	0.00246	470	0.9542	0.9809	0	Ethiopia
N-20110	0.98416	0.00528	436	0.9703	0.9958	0	Portugal
N-28335	0.99697	0.00404	457	0.9771	1.0050	0	Sudan

2.5 Recommended calibration and WRR factors

The Tables 2.6-2.8 list the recommended calibration and WRR factors as result from the comparisons.

Table 2.6: Recommended calibration and WRR factors for the WSG

Instrument	C used IPC VIII	C_1	C_2	C IPC VII	WRR IPC VII	Ratio to WRR	New WRR	New C	Change (ppm)
PMO2	24.18			24.1665	0.99944	1.00064	0.99936	24.1645	-81
PMO5	31.615			31.6349	1.00063	0.99909	1.00091	31.6438	281
CROM2L	127.687			128.062	1.00294	0.99711	1.00290	128.057	-38
CROM3R	127.549			127.409	0.99890	1.00103	0.99897	127.418	69
MK67814	10007	0	39.9961	10016.4	1.00094	0.99932	1.00068	10013.8	-259
PAC3	9962.6	0.07	75		0.00000	0.99814	1.00186	9981.17	
HF18748	19989	0.07	75		0.00000	1.00407	0.99595	19908	

Table 2.7: Recommended calibration and WRR factors for the absolute radiometers

Absolute Radiometers	C used IPC VIII	C_1	C_2	C from IPC VII	WRR IPC VII	Ratio to WRR	New WRR	New C	Change (ppm)
PMO6-5	23.729			23.6982	0.99870	1.00202	0.99798	23.6812	-719
PMO609	24.0392				0.00000	0.99684	1.00317	24.1154	
PMO610	22.6395			22.6911	1.00228	0.99772	1.00229	22.6912	6
PMO611	23.9442				0.00000	0.99671	1.00330	24.0232	
R80022	23.915			23.8461	0.99712	1.00389	0.99613	23.8223	-998
R79-121	599.44			23.9968	0.04003	1.00003	0.99997	599.422	
R811103	23.929				0.00000	0.99954	1.00046	23.94	
R811104	1194.905			23.8309	-	1.00303	0.99698	1191.3	
R811106	120.43				0.00000	1.00457	0.99545	119.882	
R811107	24.031			24.0187	0.99949	0.99998	1.00002	24.0315	532

Absolute Radiometers	C used IPC VIII	C_1	C_2	C from IPC VII	WRR IPC VII	Ratio to WRR	New WRR	New C	Change (ppm)
R811108	24.088			24.088	1.00000	0.99989	1.00011	24.0907	110
R850401	602.375			24.0608	-	1.00113	0.99887	601.695	
R850404	1207.29				0.00000	0.99977	1.00023	1207.57	
R850405	24.185				0.00000	0.99963	1.00037	24.194	
R850410	1210.7				0.00000	0.99820	1.00180	1212.88	
MK67502	1.0039			1.00276	0.99886	1.00134	0.99866	1.00256	-203
MK67604	1.0028			1.00514	1.00233	0.99762	1.00239	1.00519	52
MK67702	1.0035			1.00166	0.99817	1.00250	0.99751	1.001	-662
MK67915	1.00406			1.00277	0.99872	1.00086	0.99914	1.0032	426
MK68016	1.0045			1.00477	1.00027	0.99950	1.00050	1.005	231
MK68024	0.9936				0.00000	0.99914	1.00086	0.99446	
MK68025	1.002			1.00146	0.99946	1.00014	0.99986	1.00186	399
MK69137	1.002				0.00000	0.99722	1.00279	1.00479	
MAR-1-1	35600				0.00000	1.00089	0.99911	35568.3	
MAR-1-2	35600				0.00000	1.00039	0.99961	35586.1	
P13219	10079	0.06	1	10070.1	0.99912	1.00078	0.99922	10071.1	104
HF14915	20010	0.07	1000	19978	0.99840	0.99954	1.00046	20019.2	2058
HF15744	20020	0.07	1000	20013.6	0.99968	1.00053	0.99947	20009.4	-210
HF17142	19982	0.07	1000	19960.1	0.99890	1.00114	0.99886	19959.2	-43
HF18747	20014	0.07	1000	19997.2	0.99916	0.99905	1.00095	20033	1789
HF19746	20030	0.07	10000	20005.8	0.99879	1.00081	0.99919	20013.8	399
HF20406	20038	0.07	1000		0.00000	0.99863	1.00137	20065.5	
HF23725	20070.2	0.07	1000	19991.4	0.99607	1.00342	0.99659	20001.8	520
HF27157	20030	0.07	10000		0.00000	0.99962	1.00038	20037.6	
HF27159	20030.01	0.07	10000	20015.4	0.99927	1.00112	0.99888	20007.6	-390
HF27160	20030	0.07	10000	19975.3	0.99727	1.00292	0.99709	19971.7	-181
HF27162	20020	0.07	10000	20027.4	1.00037	0.99904	1.00096	20039.2	591
HF27798	20020	0.07	1000	19987.2	0.99836	1.00102	0.99898	19999.6	620
HF28553	19986	0.07	10000		0.00000	1.00245	0.99756	19937.2	
HF28558	19978.06	0.07	10000		0.00000	1.00211	0.99789	19936	
HF28965	19986	0.07	1000		0.00000	1.00142	0.99858	19957.7	
HF28968	19980.2	0.07	1000		0.00000	1.00173	0.99827	19945.7	

Absolute Radiometers	C used IPC VIII	C_1	C_2	C from IPC VII	WRR IPC VII	Ratio to WRR	New WRR	New C	Change (ppm)
HF29220	19999	0.07	1000		0.00000	1.00138	0.99862	19971.4	
HF29223	19998	0.07	1000		0.00000	1.00256	0.99745	19946.9	
HF30110	19999	0.07	10000		0.00000	1.00274	0.99727	19944.4	
HF30710	19999	0.07	10000		0.00000	0.99993	1.00007	20000.4	

Table 2.8: Recommended calibration and WRR factors for the Ångström and Normal Incidence Pyrheliometers

Å-Pyrheliometers & NIP	C used IPC VIII	C_1	C_2	C IPC VII	WRR IPC VII	Ratio to WRR	New WRR	New C	Change (ppm)
A7	30077		1000	30077	1.00000	0.9984	1.00160	30132.7	1848
A171	5717		1	5717.4	1.00007	1.00033	0.99967	5715.34	-360
A212	10535		500	10544.1	1.00086	0.99825	1.00175	10554.6	995
A238	10380		1000		0.00000	1.00983	0.99027	10275.9	
A556	6520		200		0.00000	0.96353	1.03785	6755.99	
A564	5925.3		1000	5924.8	0.99992	1.00346	0.99655	5904.05	-3515
A576	5885.6		1000	5891.9	1.00107	0.99954	1.00046	5885.13	-1150
A578	6241.2		1	6251.3	1.00162	0.99829	1.00171	6251.58	45
A585	5615		200		0.00000	1.0083	0.99177	5568.34	
A702	5969		200		0.00000	0.97172	1.02910	6141.14	
A7190	4605.2		1000	4605.2	1.00000	0.99908	1.00092	4611.38	1340
A7636	4321.4		1	4327.9	1.00150	0.99837	1.00163	4328.5	139
A12578	4263.8		1000		0.00000	0.96027	1.04137	4439.33	
A12579	4187		1000		0.00000	0.97553	1.02508	4291.72	
A13439	4312.4		1000		0.00000	0.97753	1.02299	4411.8	
A15192	4479		1	4475.1	0.99913	0.99811	1.00189	4487.89	2850
A16491	4540		1000	4520.5	0.99570	1.00357	0.99644	4522.77	502
A18587	4539.1		1000	4539.1	1.00000	0.99399	1.00605	4567.19	6150
A25783	5693		1		0.00000	0.99831	1.00169	5702.41	
M-59-8	1773200				0.00000	1.00077	0.99923	1771680	
N-18649	8.99				0.00000	0.97088	1.02999	9.26031	
N-20110	8.59				0.00000	0.98416	1.01609	8.72888	
N-28335	8.33				0.00000	0.99697	1.00304	8.3559	

3 Graphical Representation of Results

3.1 PMO2, PMO5, CROM2L and CROM3L

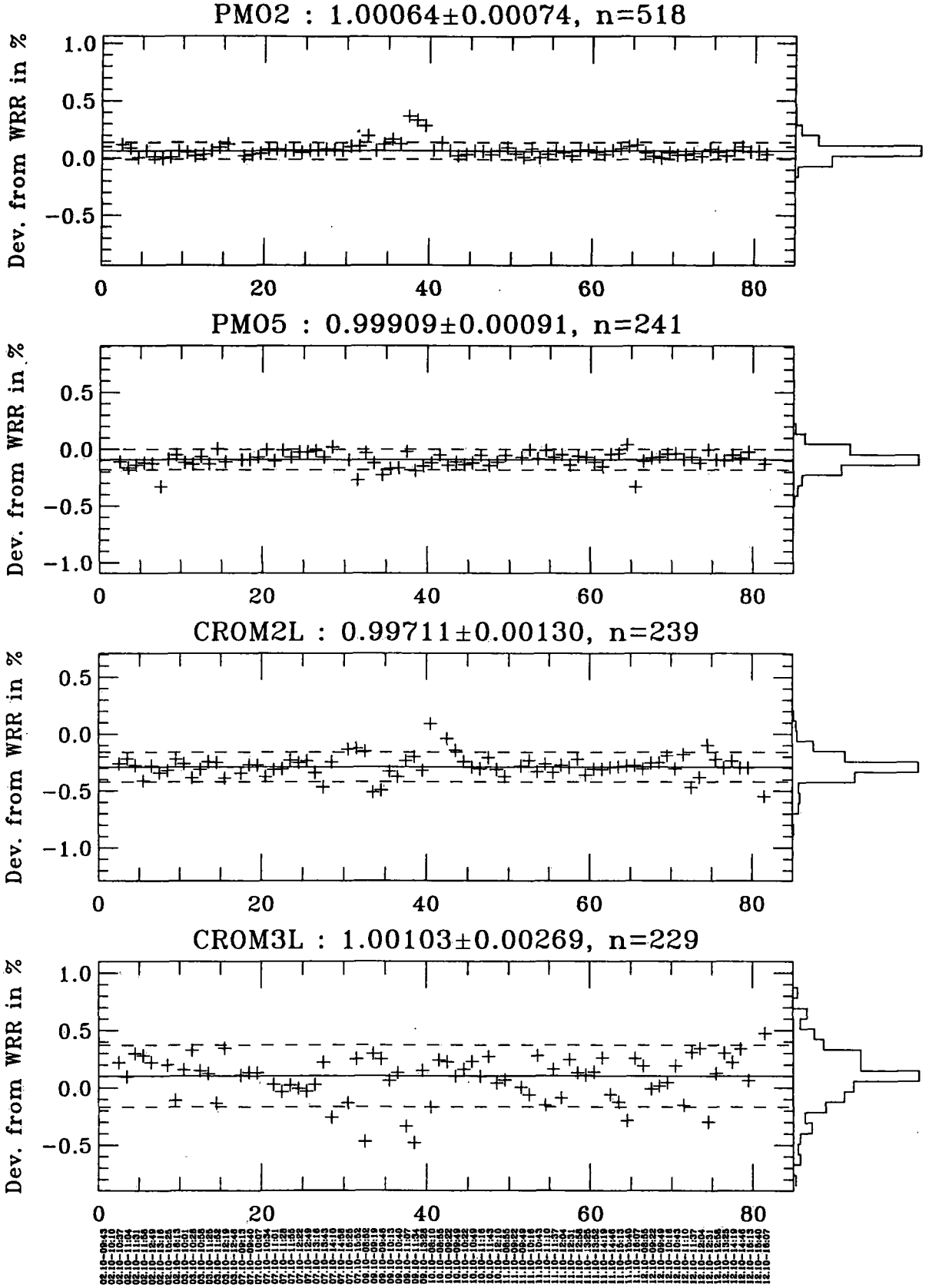

3.2 MK67814, PAC3, HF18748, PMO6-5

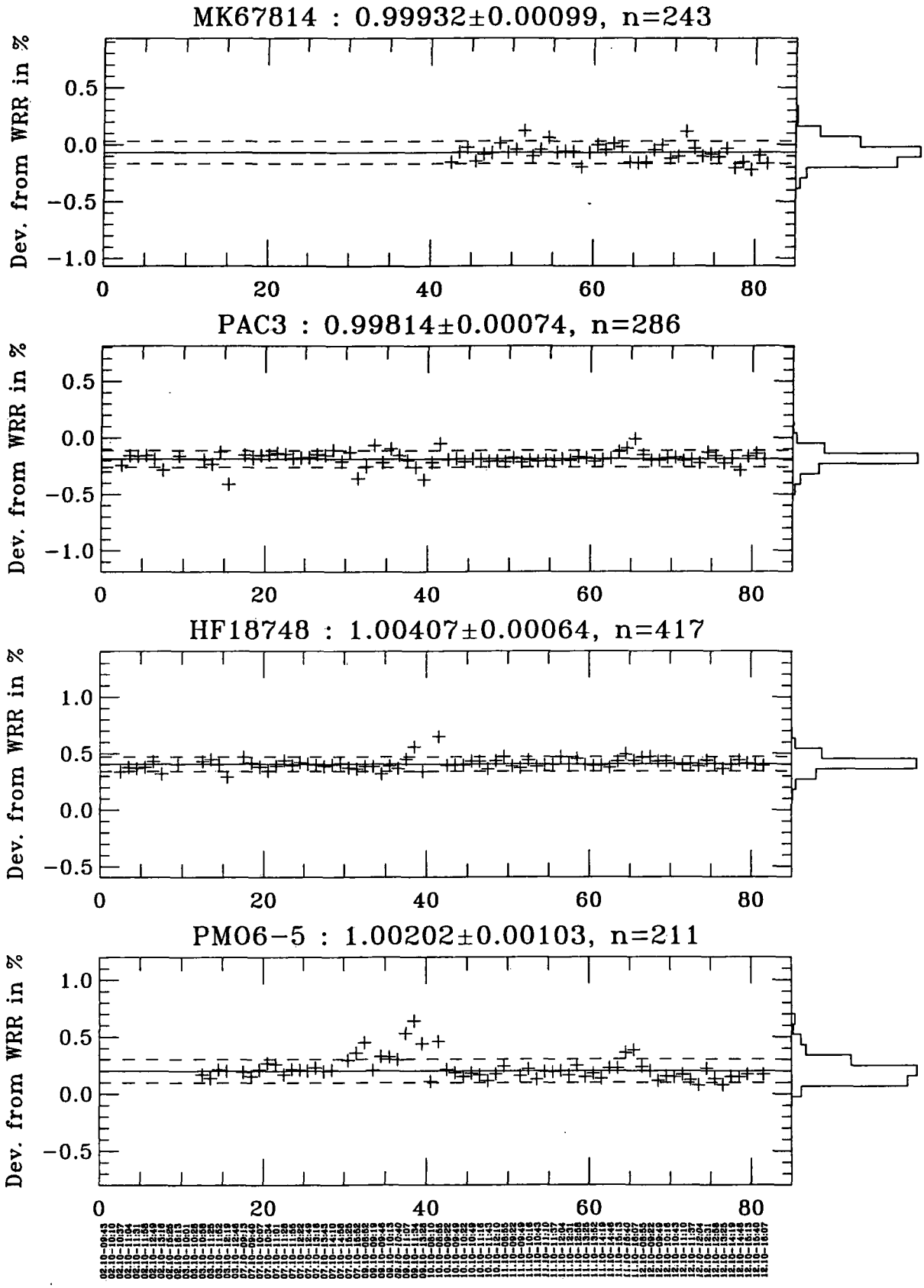

3.3 PMO609, PMO610, PMO611, R80022

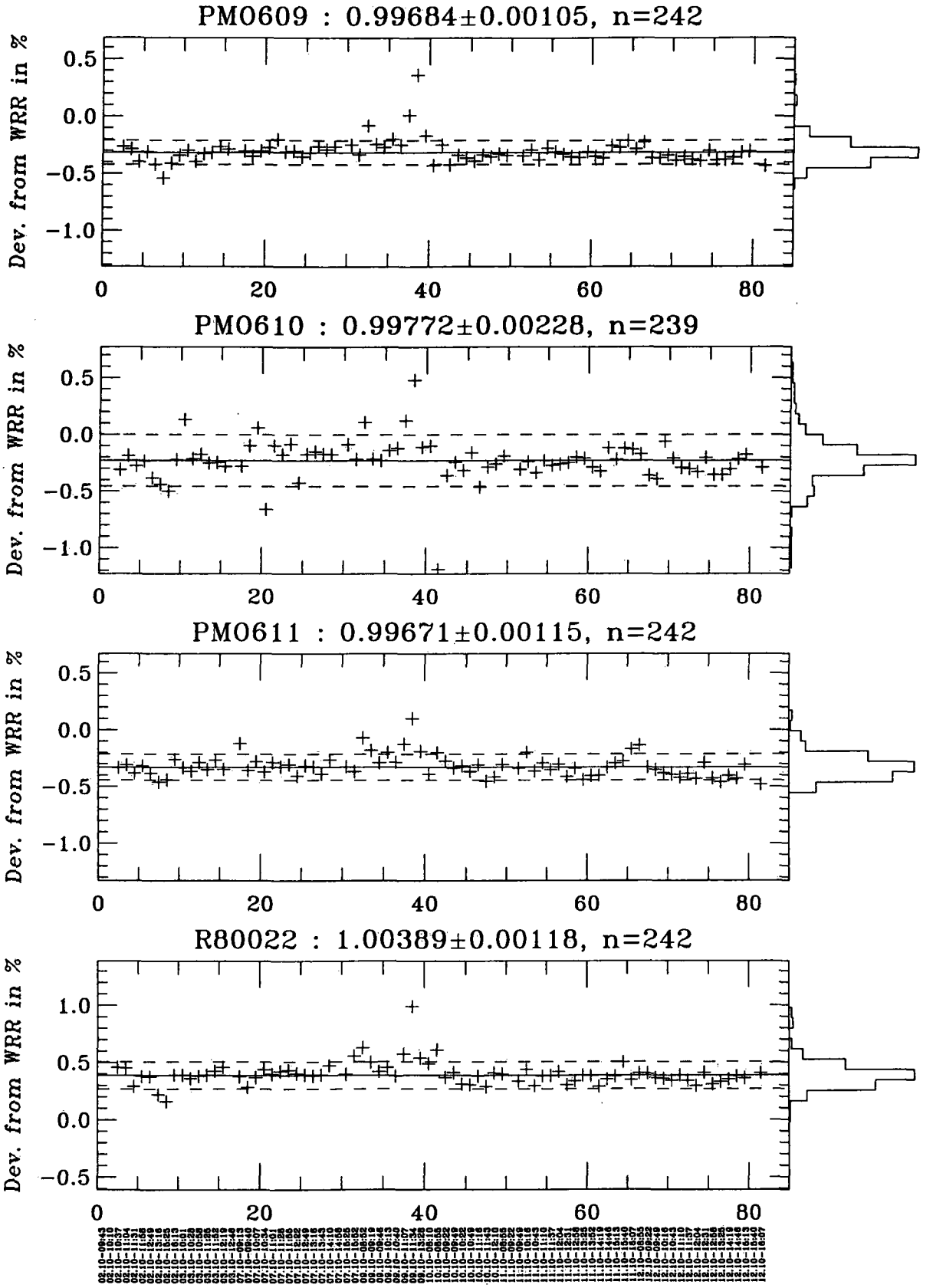

3.4 R79-121, R811103, R811104, R811106

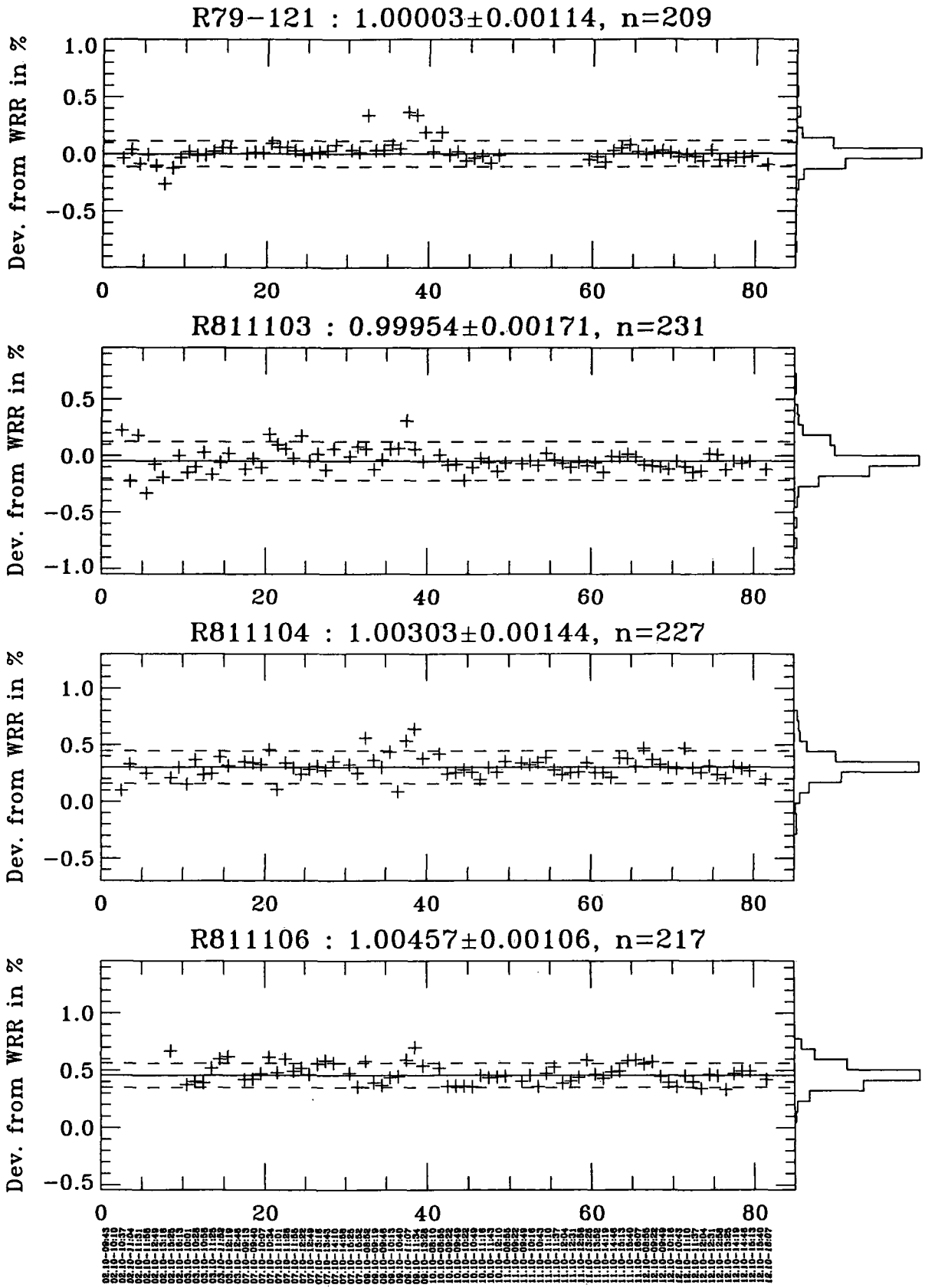

3.5 R811107, R811108, R850401, R850404

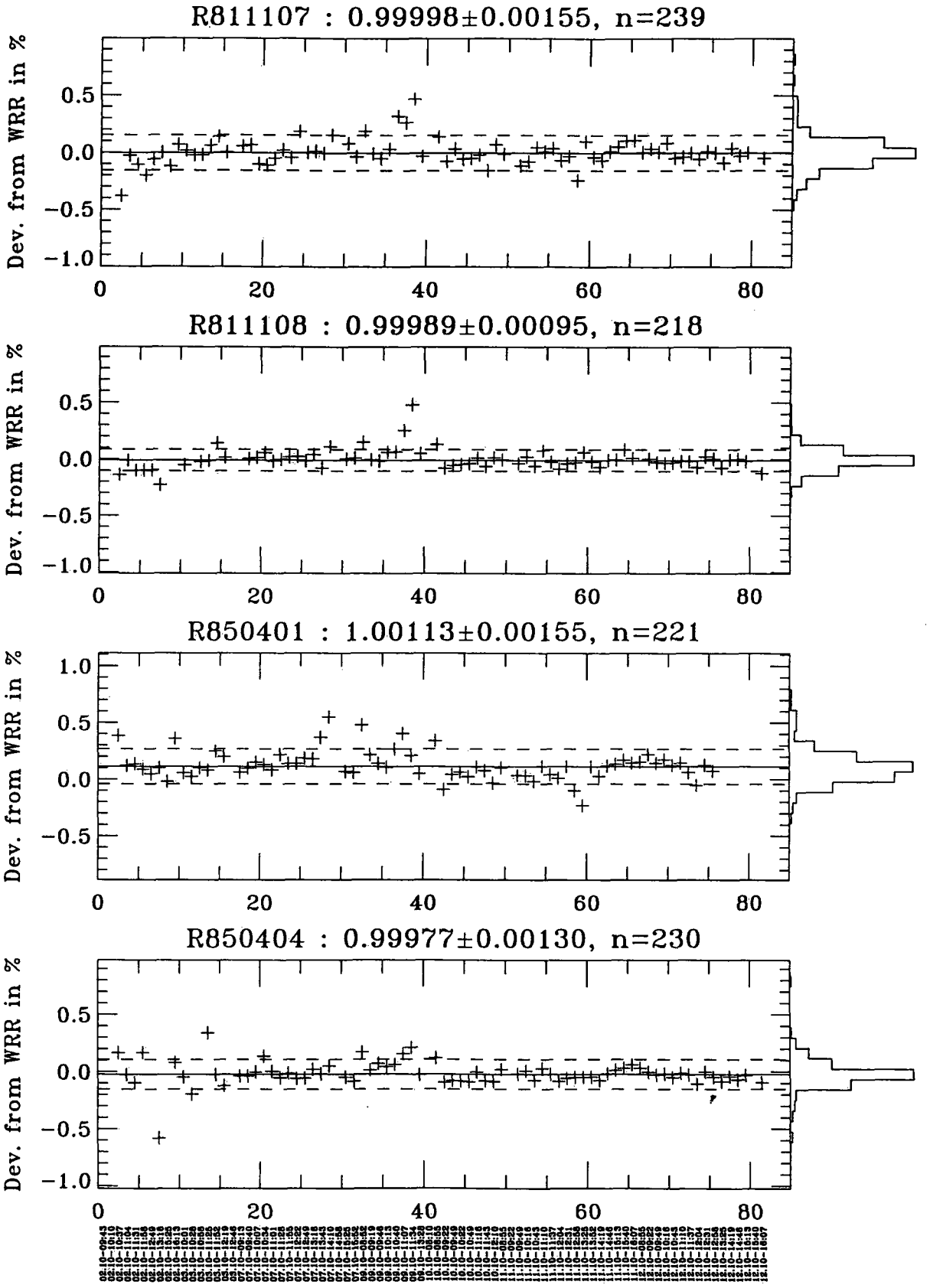

3.6 R850405, R850410, MK67502, MK67604

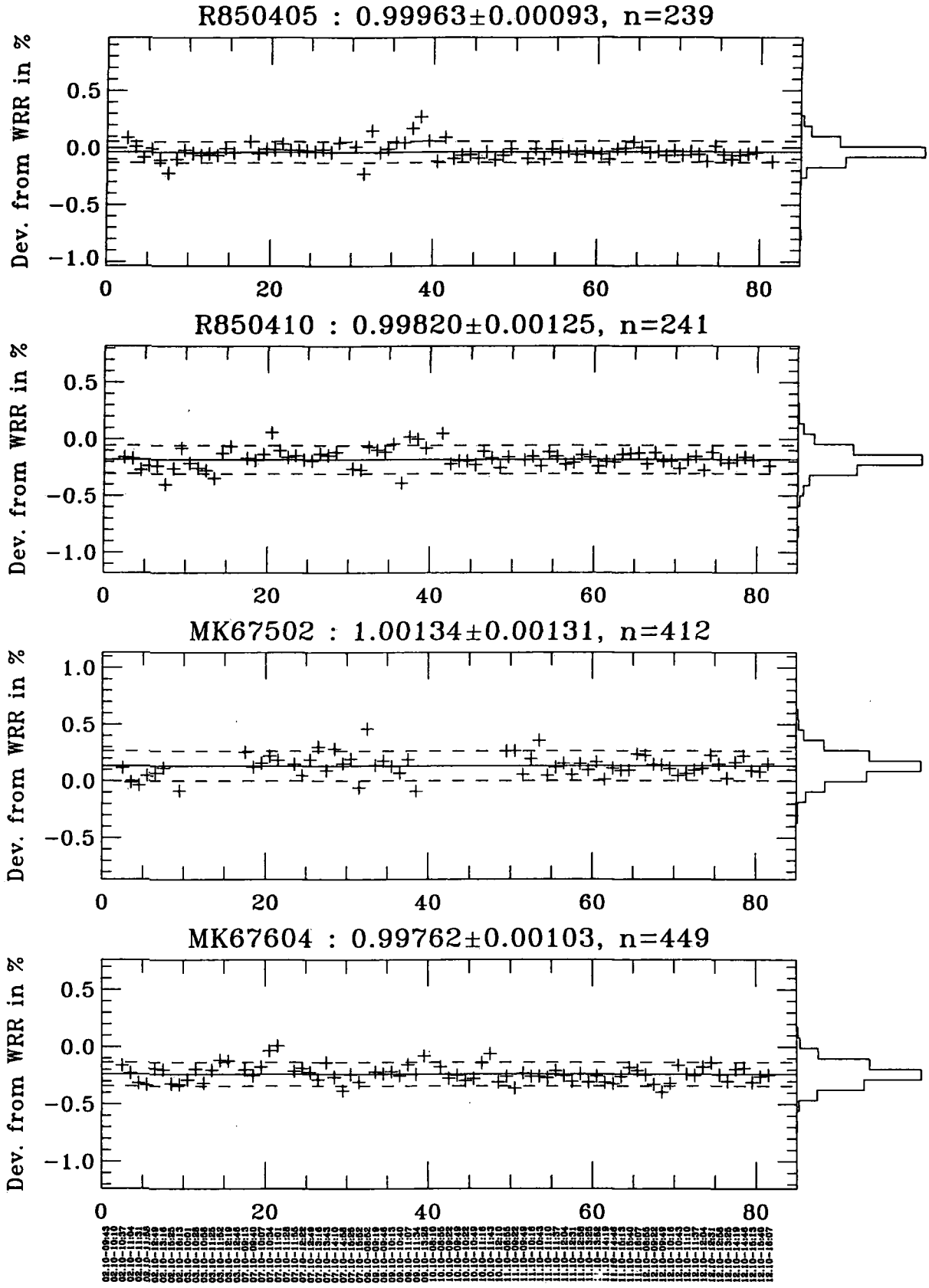

3.7 MK67702, MK67915, MK68016, MK68018

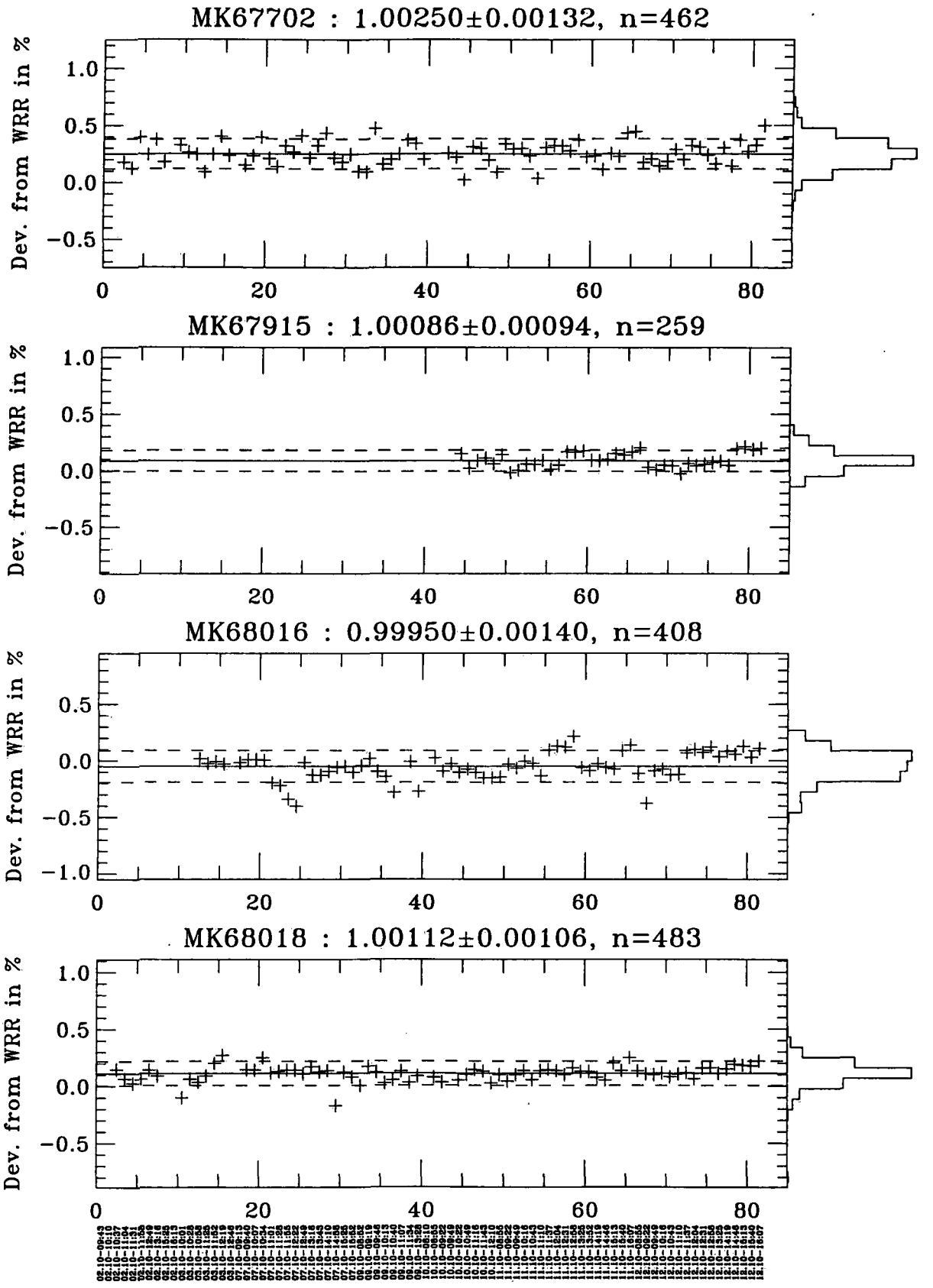

3.8 MK68024, MK68025, MK69137, MAR-1-1

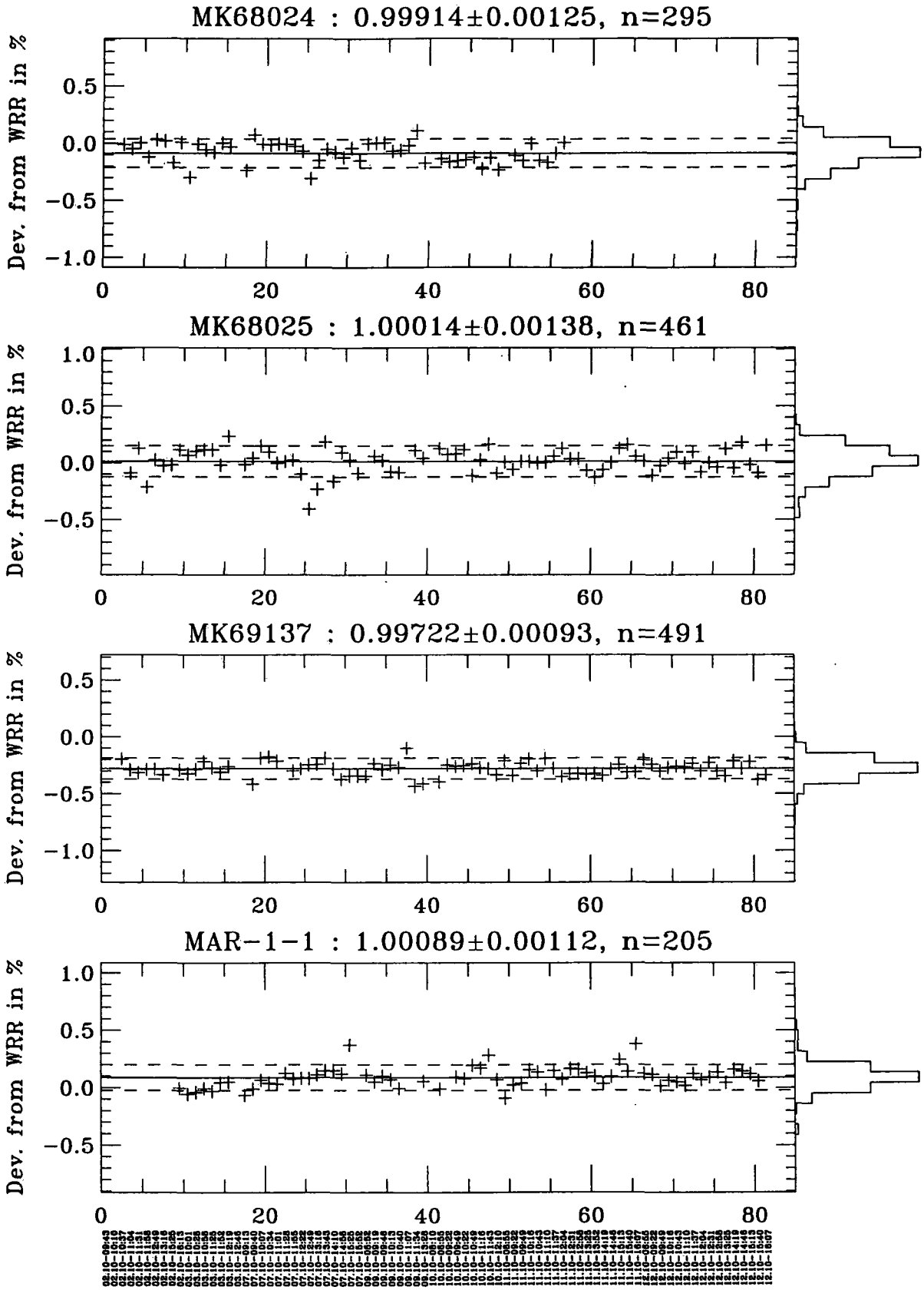

3.9 MAR-1-2, P13219, HF14915, HF15744

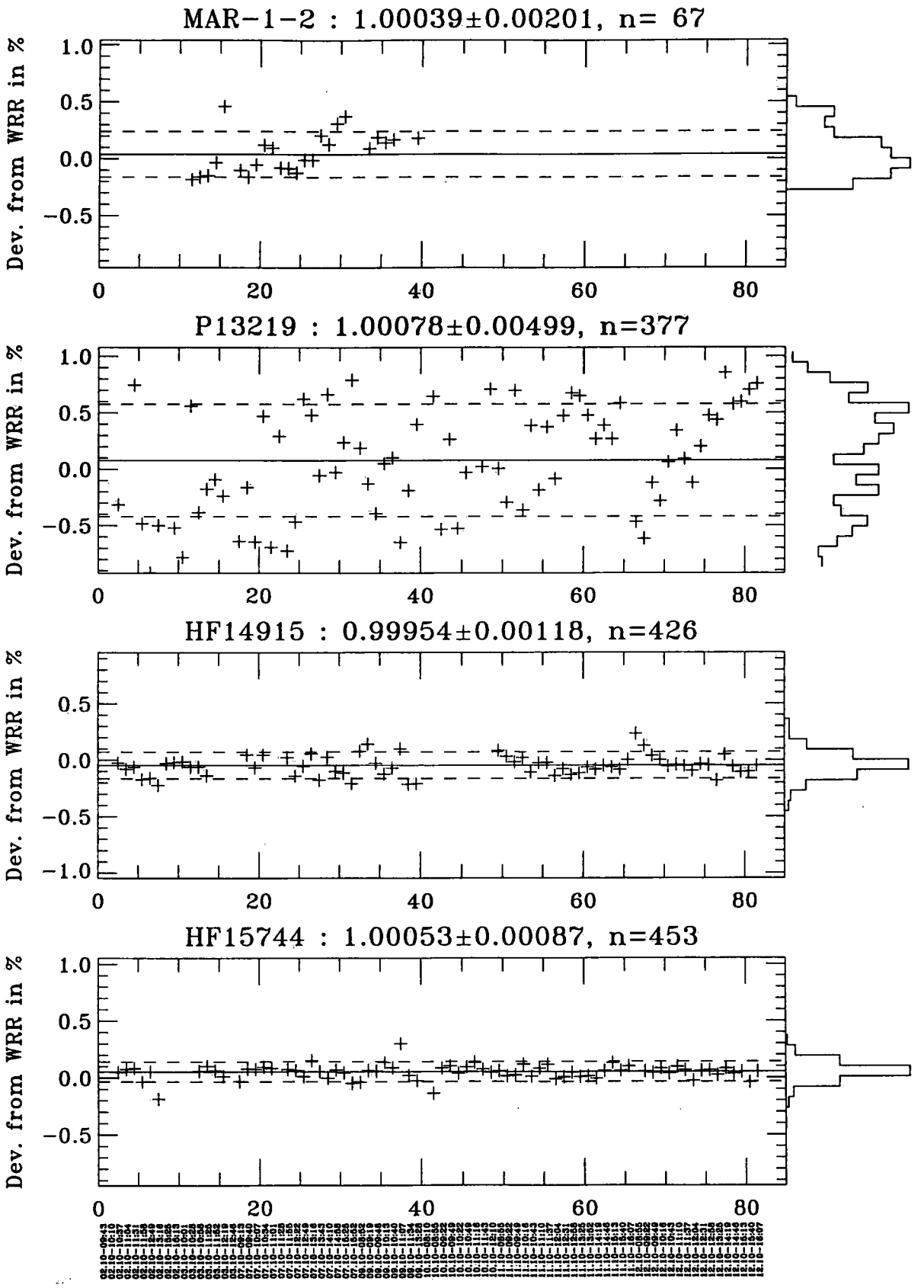

3.10 HF17142, HF18747, HF19746, HF20406

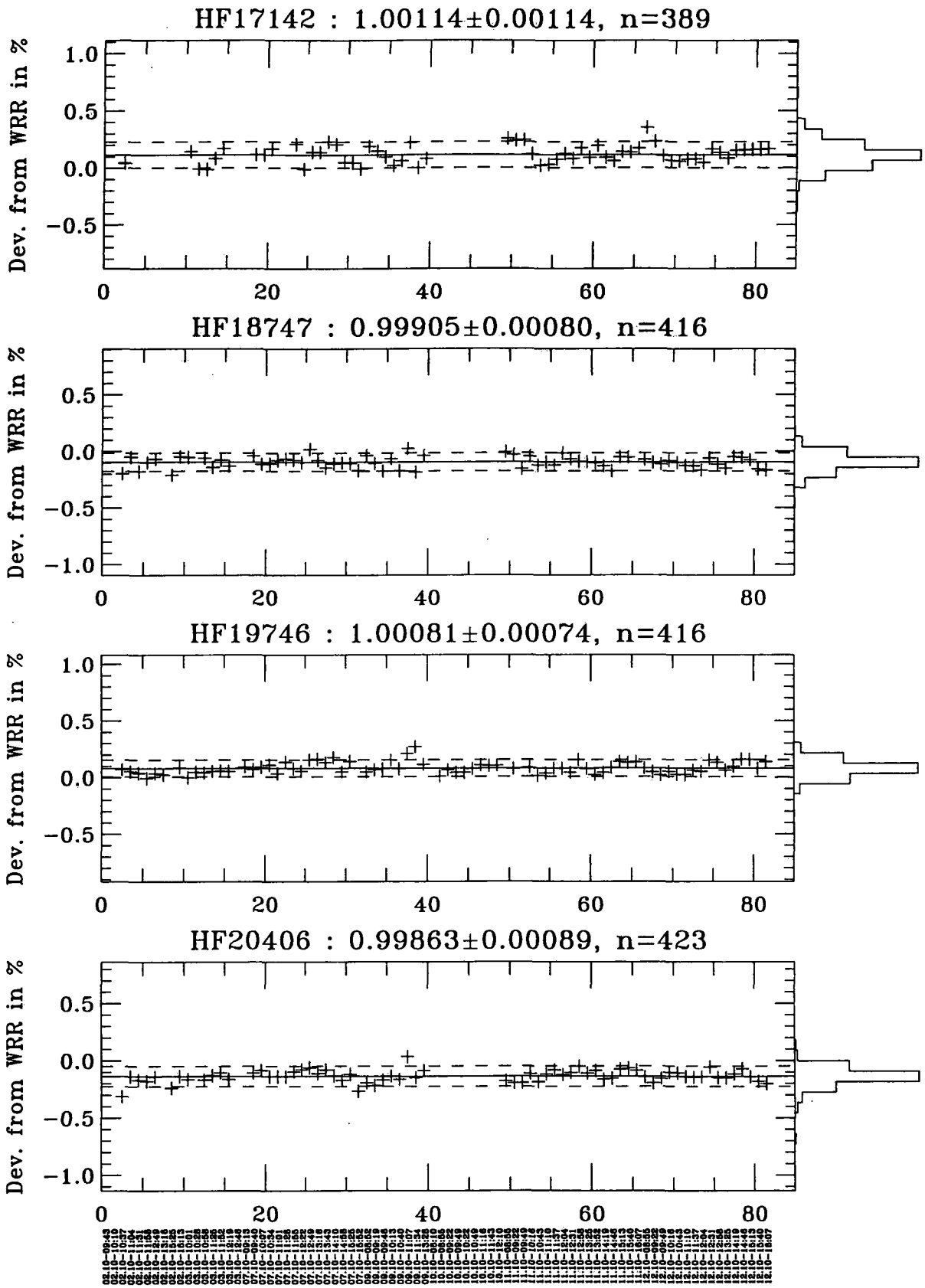

3.11 HF23725, HF27157, HF27159, HF27160

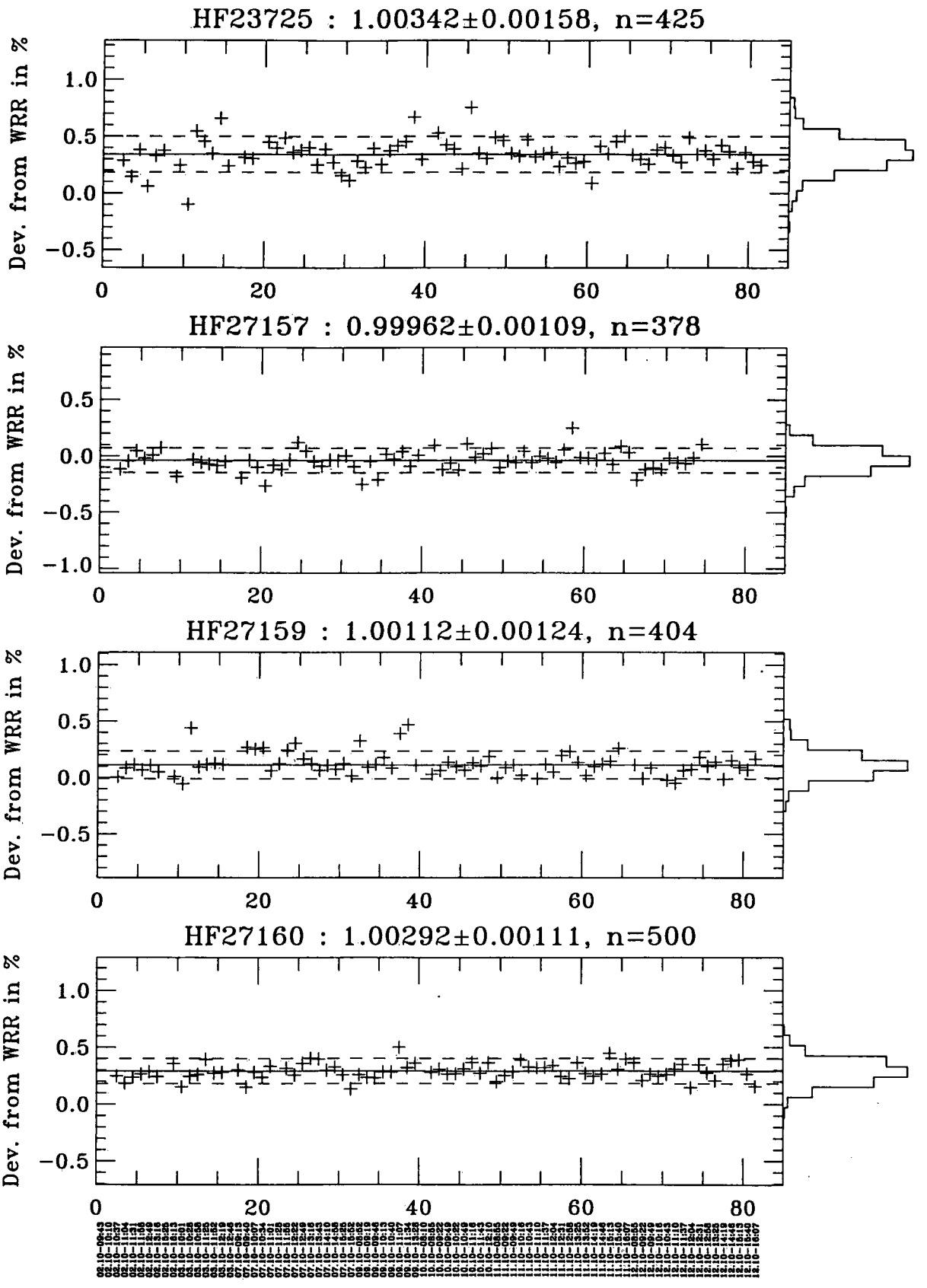

3.12 HF27162, HF27798, HF28553, HF28558

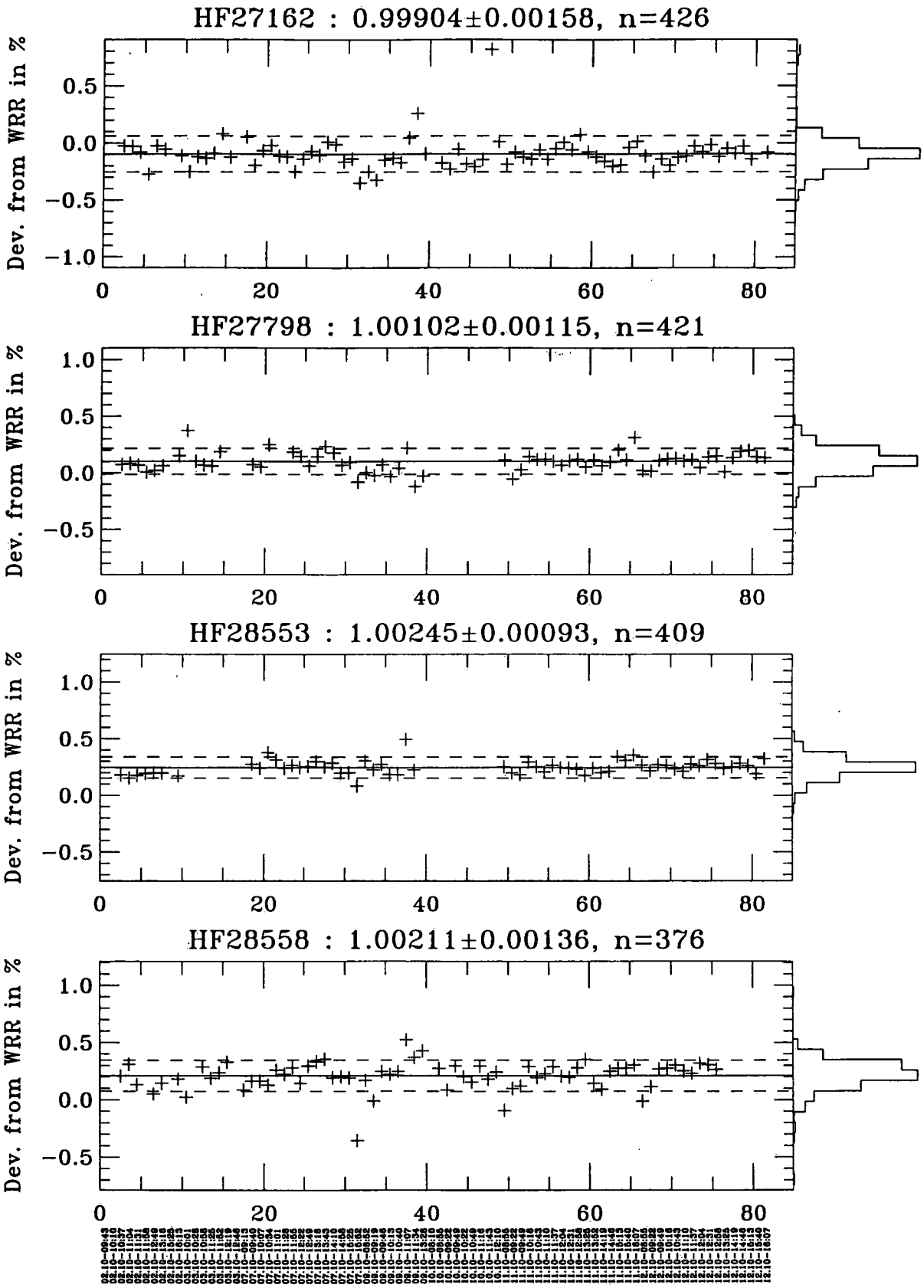

3.13 HF28965, HF28968, HF29220, HF29223

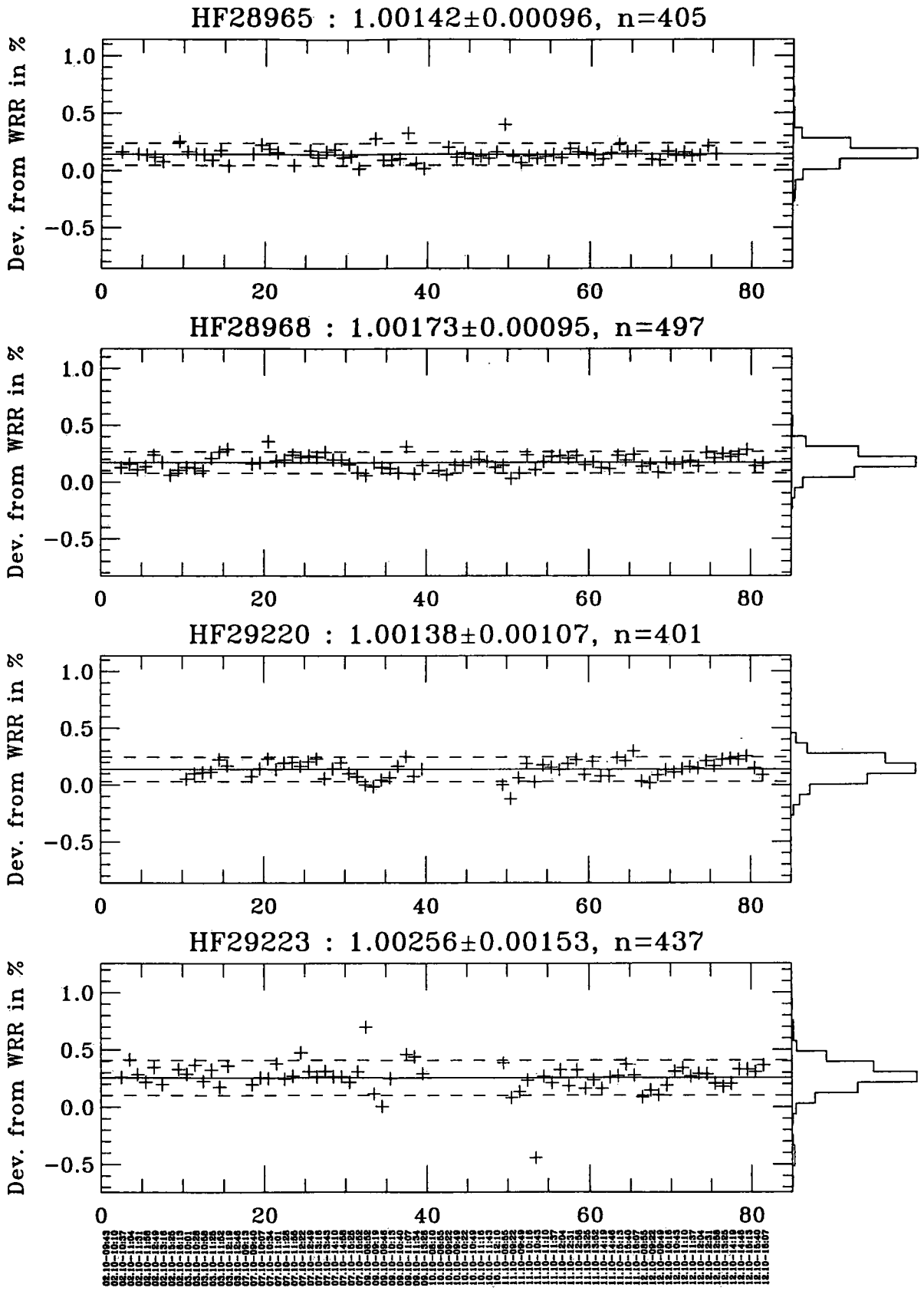

3.14 HF30110, HF30710, N-18649, N-20110

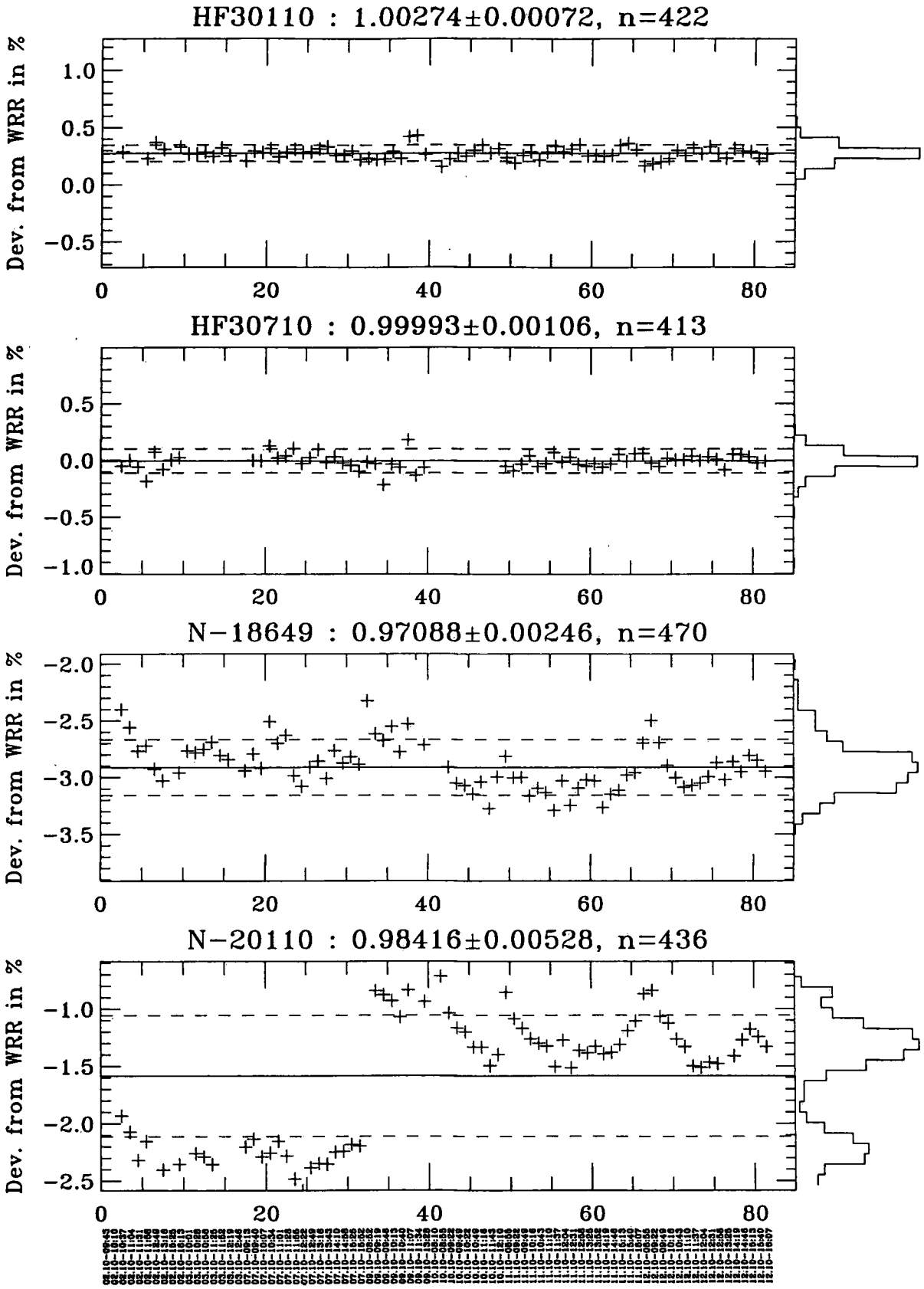

3.15 N-28335, A7, A171, A212

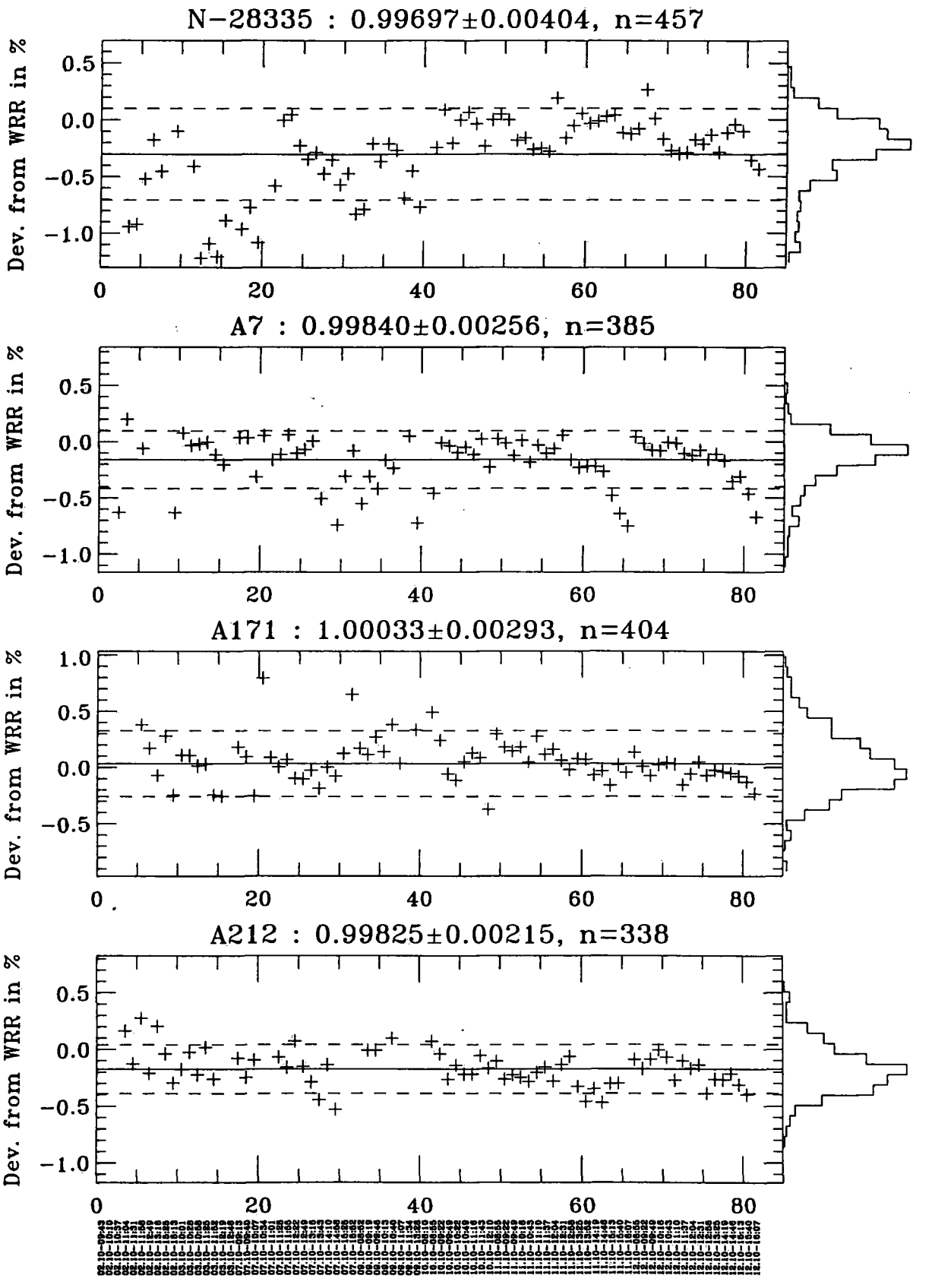

3.16 A238, A556, A564, A576

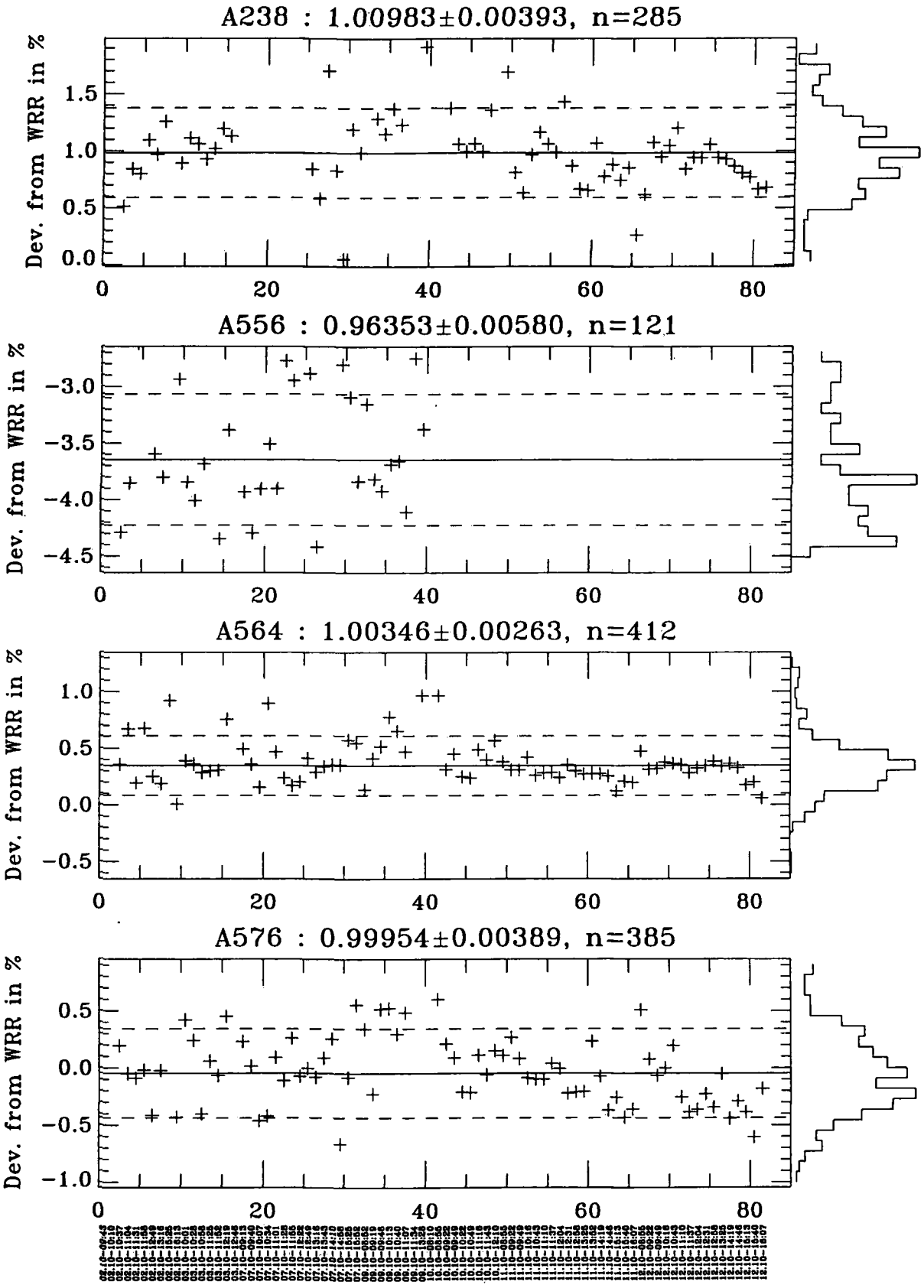

3.17 A578, A585, A702, A7190

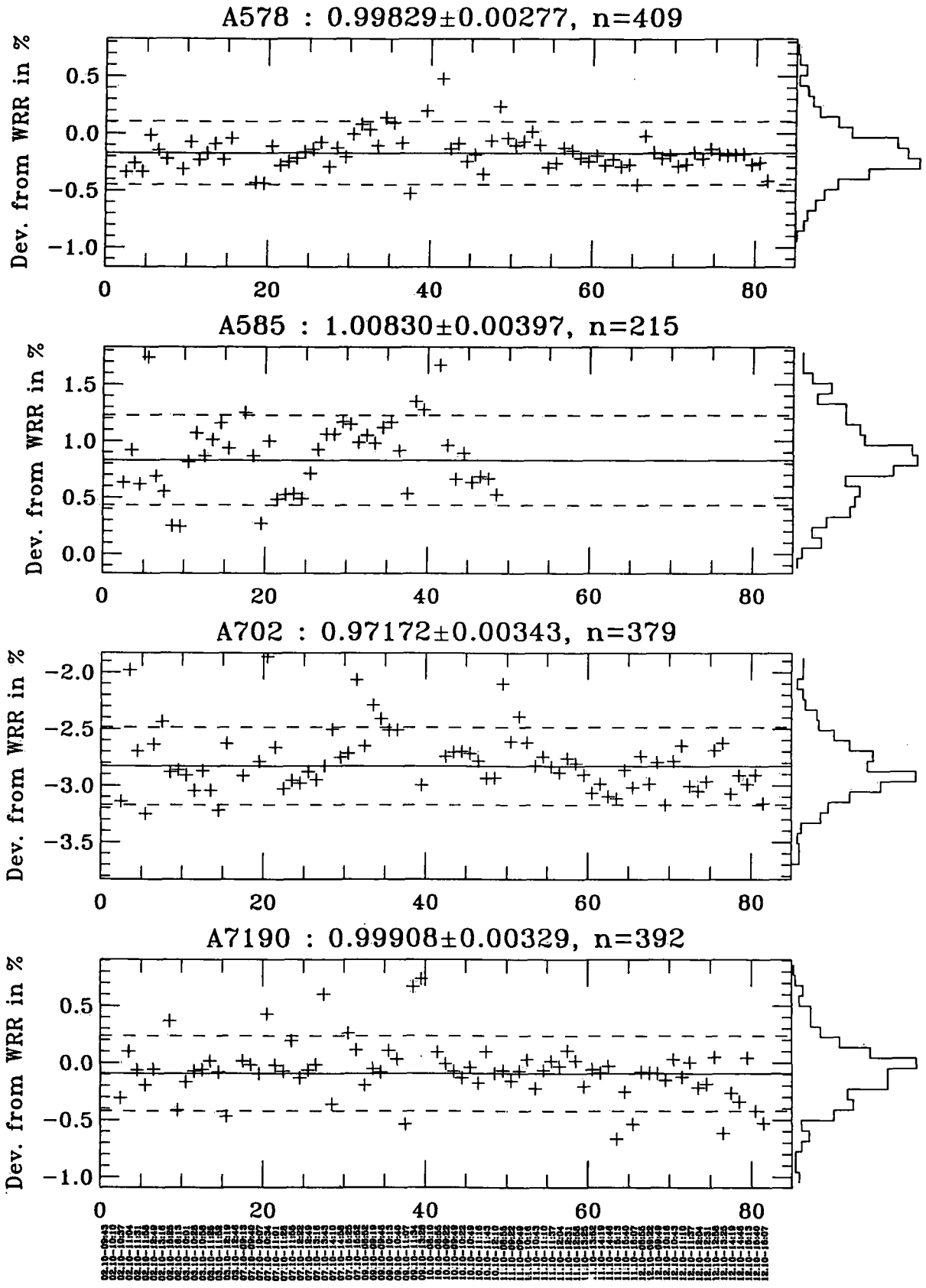

3.18 A7636, A12578, A12579, A13439

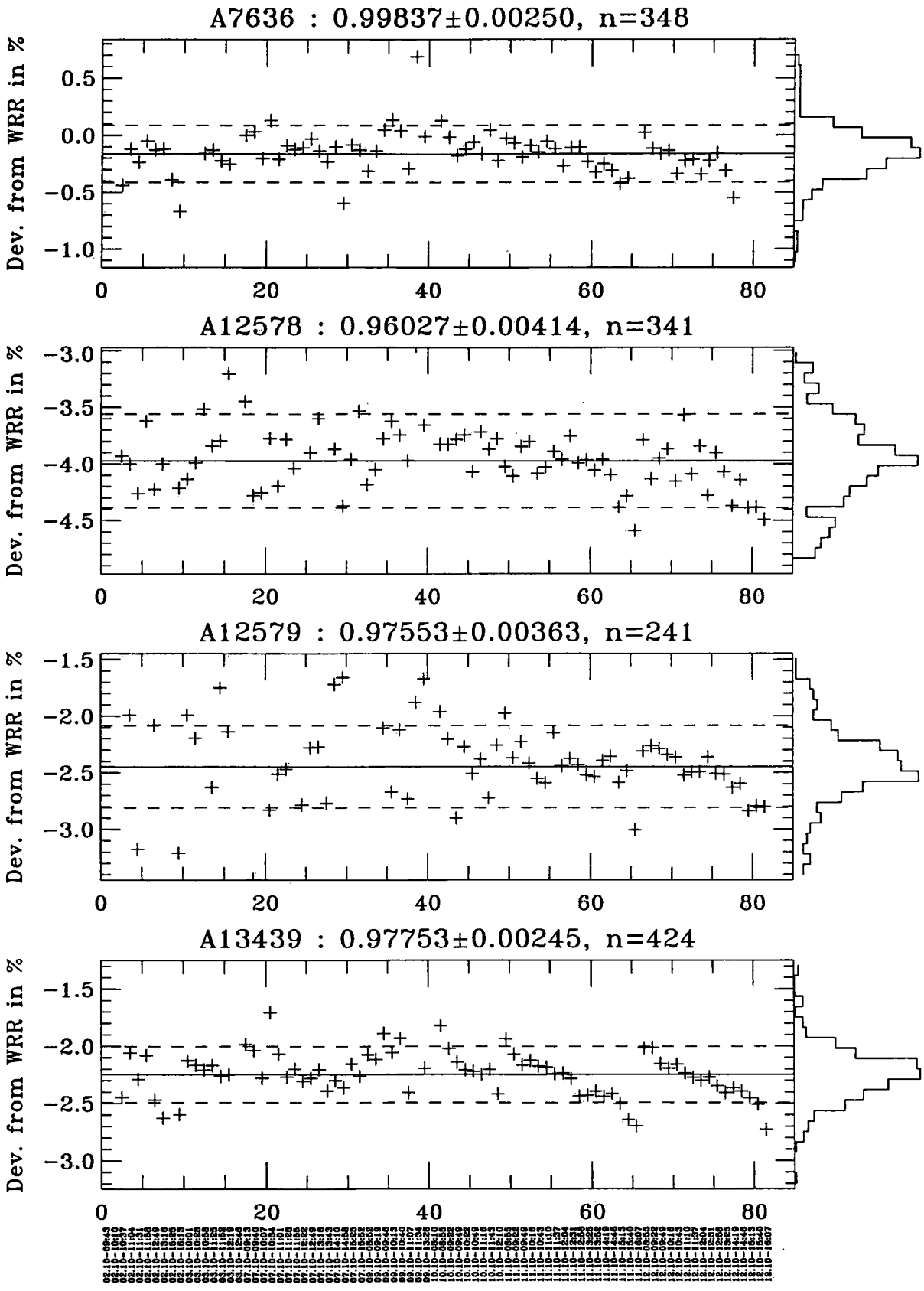

3.19 A15192, A16491, A18587, A25783

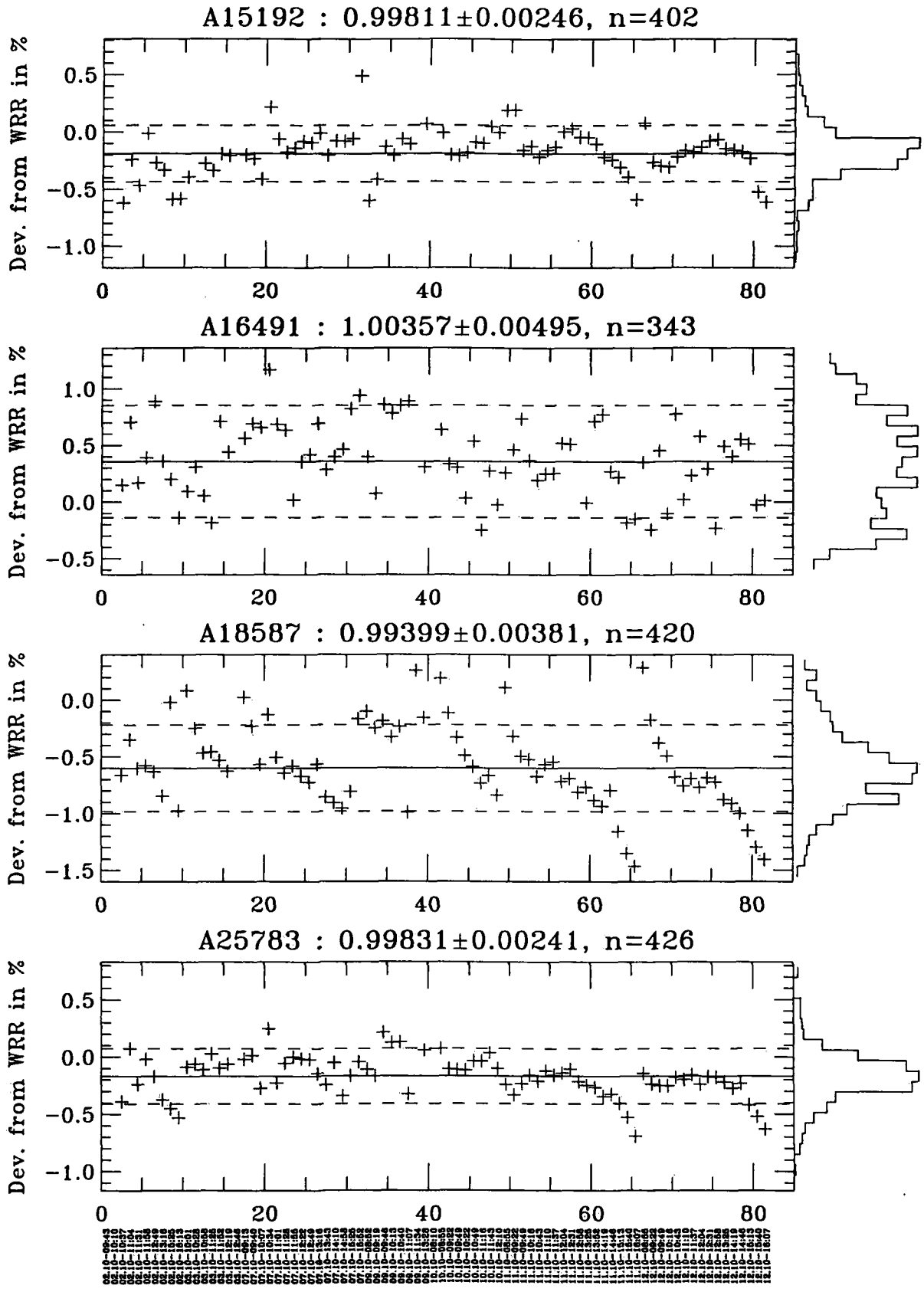

3.20 M-59-8

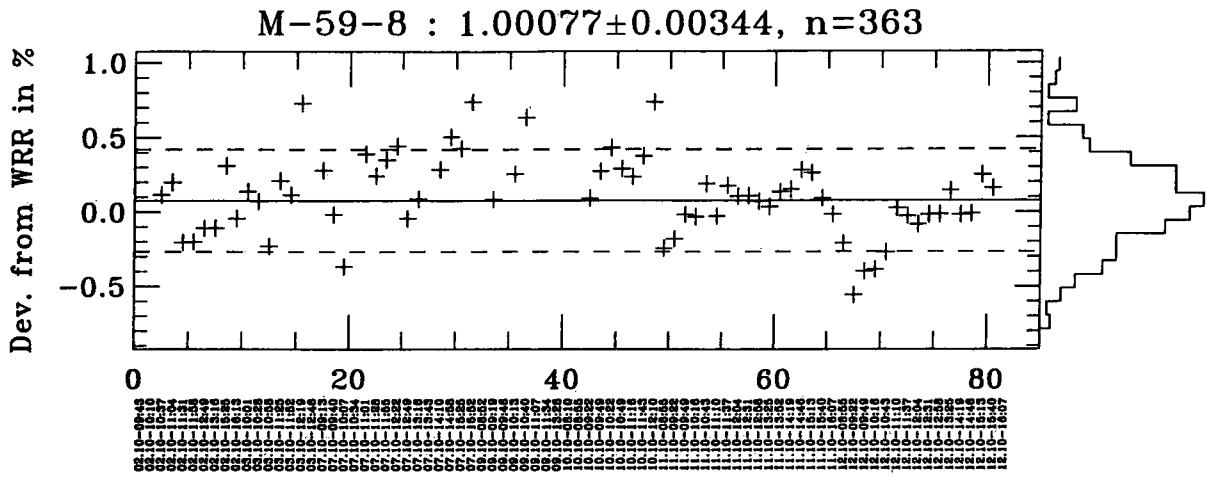

3.21 Total (WRR and RASTA), Global and Sky Irradiance

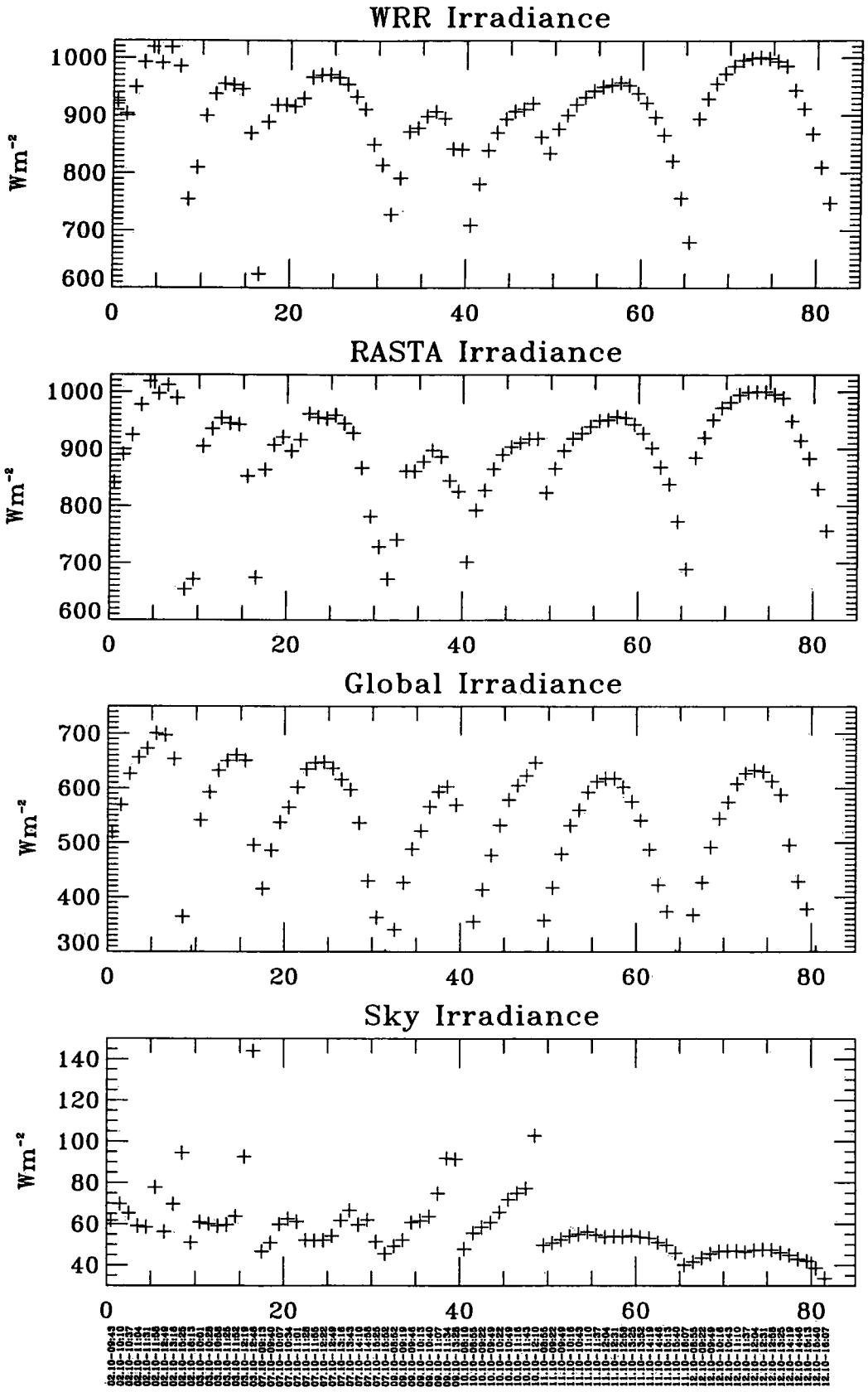

3.22 Airmass and Aerosol Optical Depth at 778, 500 and 368 nm

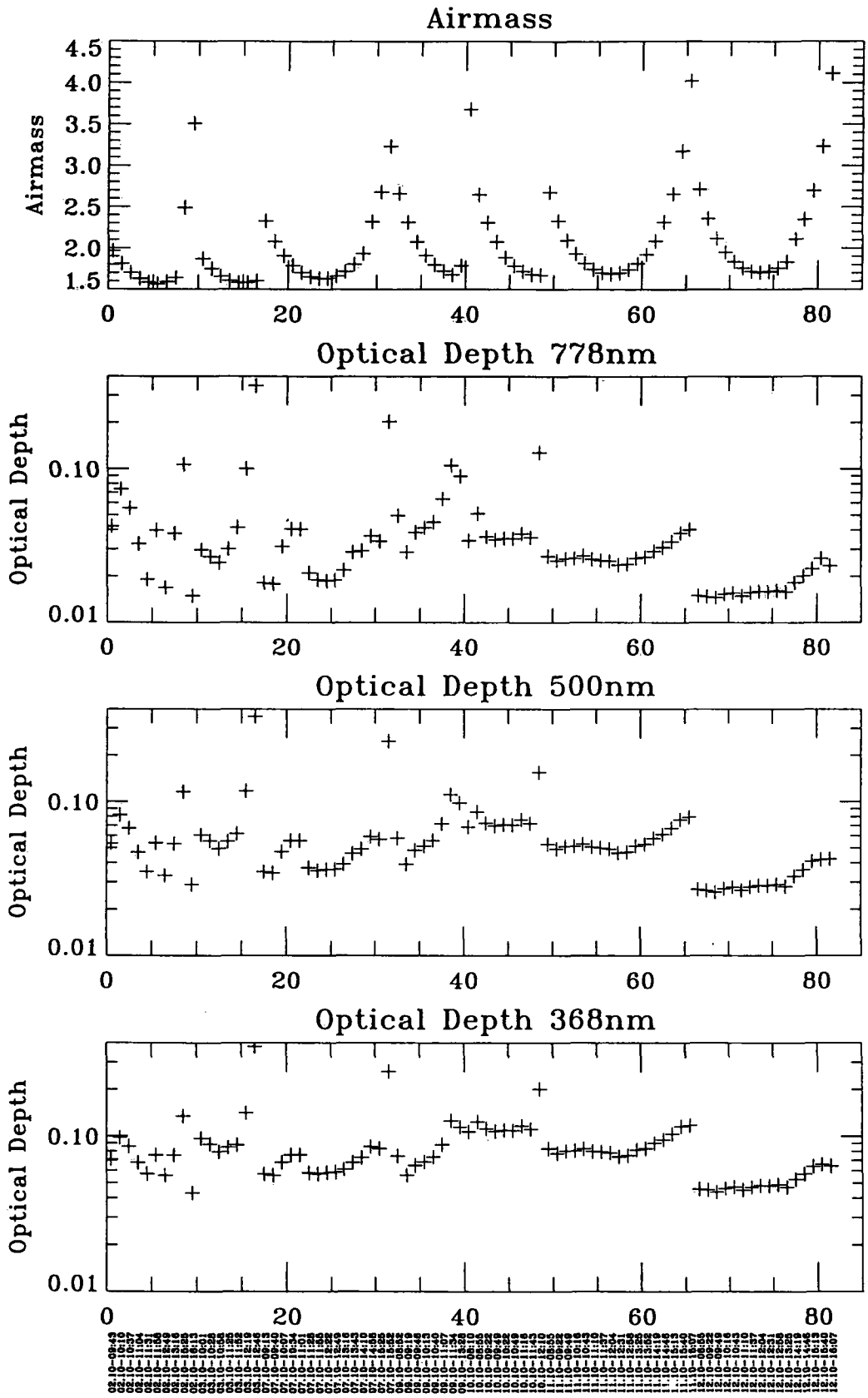

3.23 Meteorological Data

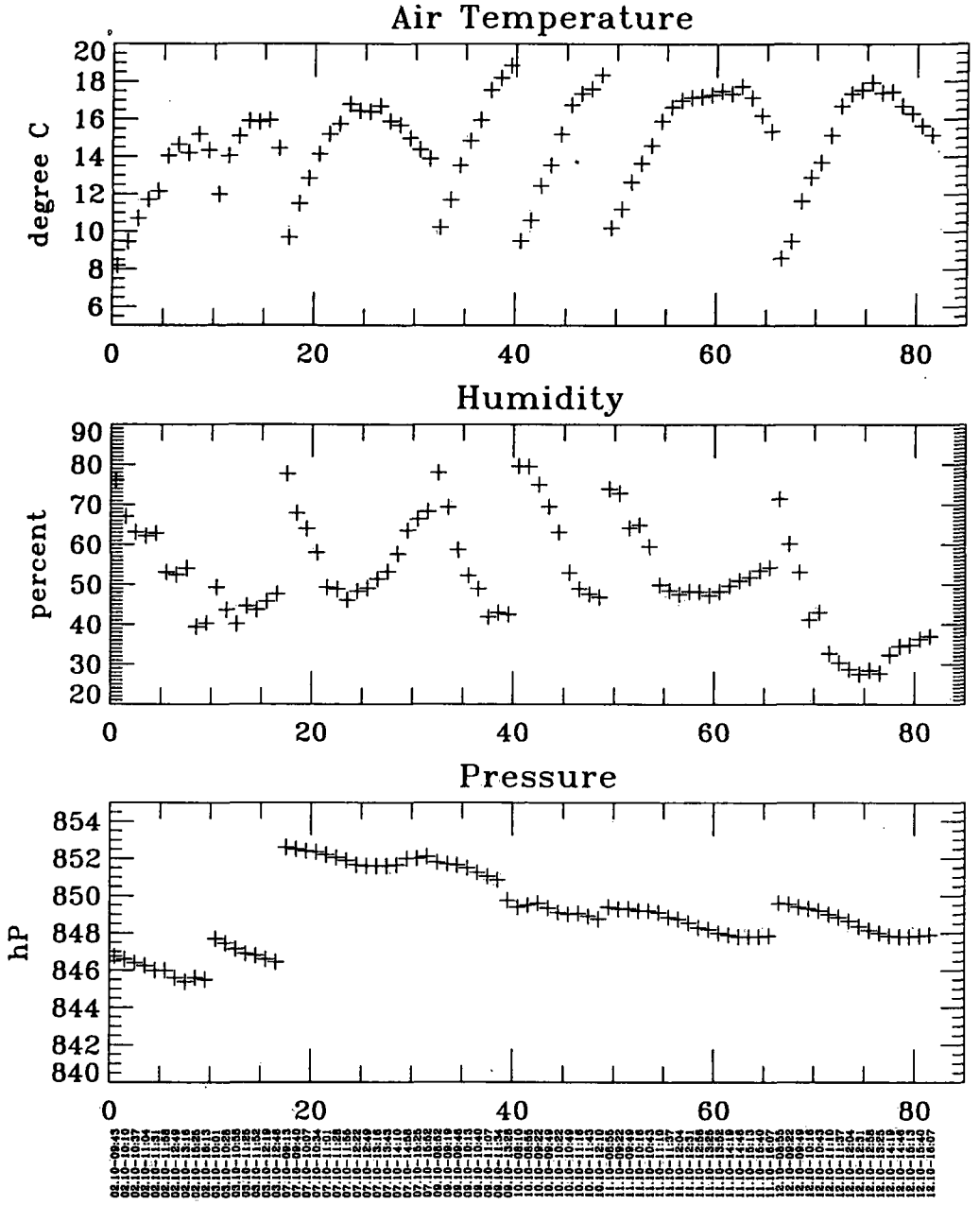

4 Supplementary Information

4.1 View Limiting Geometry

Table 4.1. View limiting geometries of absolute radiometers (R : radius of front aperture, r : radius of receiver aperture, l : distance between apertures)

Radiometer Type	R	r	l
PMO2	3.6	2.5	85
PMO5	3.7	2.5	95.4
CROM 2L	6.29	4.999	144.05
CROM 3L	6.25	5	144
PAC 3	8.18	5.64	190.5
HF 18748	5.81	3.99	134.7
MKVI 67814	8.2	5.65	187.6
PMO6 generic	4.1	2.5	94
PMO6-5	3.6	2.5	84.2
PMO6-10	4.25	2.5	95.4
EPAC generic	8.32	5.64	190.5
HF generic	5.81	3.99	134.7
MKVI generic	8.2	5.65	187.6
MKVI-67401	8.2	5.64	190.5
PCC3-005	10	5	114.5
NIP generic	10.3	4	203

Table 4.2. View limiting geometries of Ångström Pyrheliometers (v : vertical dimension, w : horizontal dimension, l : distance between apertures)

Ångström Type	l	v	w
Å-7	150	9.5	7.5
Å-171	72.2	10.25	2.4
Å-212	50	11.8	2.5
Å-559	70	10	8
Å-564	75.1	10.3	2.5
Å-568	55.5	10.6	4.0
Å-576	82	10	2.5
Å-578	70.5	10.3	2.5
Å-Eppley	111	10.3	4.

4.2 Addresses of Particpants

Haroun Abdalla
Meteorological Department
P.O. Box 574
Khartoum
Sudan
Tel: +249 11 778 836
Fax: +249 11 771 693

M. Al-Muhaisni
King Abdulaziz City for Science
P.O. Box 6086
Riyadh 11441
Saudi Arabia
Tel: +966 1 488 3555
Fax: +966 1 488 3683

Calvin Archer
Dept. Environment Affairs and Tourism
The Weather Bureau Pretoria
Forum Building, Struben Street, Pretoria
Private Bag X097
Pretoria 0001
South Africa
Tel: +2712 290 3006
Fax:+2712 290 3031
email: carcher@cirrus.sawb.gov

Gustavo Atienza
Red Solarimetrica
Servicio Meteorologico Nacional
Av. Mitre 3100
1663 San Miguel, Buenos Aires
Argentinien
Tel: +541 455 6762
Fax: +541 455 6762

Dipl.-Met. Klaus Behrens
Deutscher Wetterdienst
Met. Observatorium Potsdam
Telegrafenberg
Postfach 600552
D-14405 Potsdam
Tel: +49 331 316 530
Fax: +49 331 316 531

Eshetu Bekele
National Meteorl. Services Agency
P.O. Box 1090
Addis Ababa
Ethiopia
Tel: +251 1 512 299
Fax: +251 1 517 066

Semir Ben Abdallah
I.N. Météo
Inst. National de la Météorologie
B.P. 156
2035 Tunis Carthage
Tunisia
Tel: +21 61 782 400
Fax: +21 61 784 608

Mohammed Yeslam Bin Mihfood
Solar Radiation Resource Ass.
King Abdulaziz City for Science+Techn.
P.O. Box 6086
Riyadh 11441
Saudi Arabia
Tel: +966 1 488 3555
Fax: +966 1 488 3683

José Luis Bravo-Cabrera
Instituto de Geofísica
Cd. Universitaria
Coyoacan
04510 México
México
Tel: +52 5 622 4139
Fax: +52 5 550 2486

Vilma Castro
Escuela de Fisica
Universidad de Costa Rica
San José
Costa Rica
Tel: +506 207 5394
Fax: +506 223 1837
emal: vcastro@cariari.ucr.ac.cr

Miguel Cerezo
Jet Propulison Laboratory
4800 Oak Grove Drive
MS 125-18
Pasadena, CA 91109
U.S.A.
Tel: +1 818 354 3033
Fax: +1 818 354 8153
standlab@inst-sun1.jpl.nasa.gov

Aissa Chabane
O.N.M DMRO
Seololikia
B.P. 7022
A Oran
Algerien
Tel: +213 645 1136
Fax: +213 635 5424

Michael Collins
Observation Provision
Meteorological Office
London Road, Bracknell
UK-Berkshire RG12 2SZ
Tel: +44 344 856 430
Fax: +44 344 856 412
email: mcollins@meteo.govr.uk

Dr. Lars Dahlgren
S M H I
S-60176 Norrköping
Tel: +46 11 158 186
Fax: +46 11 170 207
email: ldahlgren@smhi.se

M. Darwisch
Egyptian Meteorological Authority
P.O. Box 11784
Koubry El-Quobba, Kairo
Egypt
Tel: +202 284 9860
Fax: +202 284 9857

Dr. Klaus Dehne
Meteorol. Observatorium
Potsdam
Deutscher Wetterdienst
Postfach 600552
D-14405 Potsdam
Tel: +49 331 316 501
Fax: +49 331 316 591
email: dehne@mop.dwd.d

Dr. Ellsworth Dutton
R/E/CG1
N O A A /CMDL
325 Broadway
Boulder, CO 80303
U.S.A.
Tel. +1 304 397 6660
Fax: +1 303 497 6290
email: dutton@cmdl.noaa.gov

Dr. Bruce Forgan
Sup.Instr.+Lab.Obs.+Eng.Branch
Bureau of Meteorology
150 Lonsdale Street
P.O. Box 1289K
Melbourne, Vic 3001
Australia
Tel: +61 3 9669 4599
Fax: +61 3 9669 4736
email: bwf@bom.gov.au

Director Dr. Ignacio Galindo
Centro Univ. de Inv. en Ciencias
de la Tierra
Universidad de Colima
25 de Julio No. 965 Col Villas
San Sebastián
Apartado Postal No. 380
28045 Colima, Col.
México
Tel: +52 331 31165
Fax: +52 331 30709
email: ciencias@volcan.ucol.mx

Georgina Galindo Rios
Centro Univ. de Inv. en Ciencias
de la Tierra
Universidad de Colima
25 de Julio No. 965 Col Villas
San Sebastián
Apartado Postal No. 380
28045 Colima, Col.
México
Tel: +52 331 31165
Fax: +52 331 30709
email: ciencias@volcan.ucol.mx

S. Ginion
I R M B, Bruxelles
3, Avenue Circulaire
B-1180 Bruxelles
Tel: +32 2 373 0623
Fax: +32 2 374 6788

Stuart Goldstraw
Meteorological Office
London Road
Bracknell
UK-Berkshire RG12 2SZ
Tel: +44 344 854 636
Fax: +44 344 856 412

Sambuu Gonchig
Nat. Hydrometrol. Service of
Mongolia
Hydromet. Instr. Verif. and Cal.
Office
Khudaldaany gudamj - 5
Ulaanbaatar 11
Mongolia
Tel: +976 1 341 816
Fax: +976 1 321 401

Tom Grajnar
Atmosph. Environment Service
4905 Dufferin Street
Downsview, Ontario M3H 5T4
Canada
Tel: +1 416 739 4633
Fax: +1 416 739 4281
email: tgrajnar@dow.ow.doe.ca

Dr. John Hickey
Eppley Laboratory, Inc.
12 Sheffield Avenue
P.O. Box 419
Newport, R.I. 02840
U.S.A.
Tel: +1 491 847 1020
Fax: +1 401 847 1031
email: crks34b@prodigy.com

Yasuo Hirose
Atmos.Environment Division,
Obs. Dept.
Japan Meteorol. Agency (JMA)
1-3-4 Otemachi, Chiyodaku
Tokyo 100
Japan
Tel: +81 3 3287 3439
Fax: +81 3 3211 4640
email: rad-obs@hg.kishou.go.jp

Viera Horecká
Slovak Hydrometeorol. Institute
Jesénova 17
833 15 Bratislava
Slovakia
Tel: +42 7 378 5138
Fax: +42 7 372 034

Amos Israeli
Israel Meteorological Service
P.O. Box 25
50225 Bet Dagan
Israel
Tel: +972 3 968 2171
Fax: +972 3 960 4854

Dr. Alexandre Joukoff
I R M B
3, Avenue Circulaire
B-1180 Bruxelles
Tel: +32 2 373 0623
Fax: +32 2 374 6788
email: alexandre.joukoff@oma.be

PhD Ain Kallis
Estonian Meteorol. & Hydrol.
Institute
Toravere
EE-Tartu County EE2444
Tel: +3727 410 136
Fax: +3727 410 205
email: kallis@aai.ee

Farrakh Khani Moghanaki
Meteorological Organization
IRIMO
Mehrabad Airport
P.O. Box 13185-461
Tehran
Republic of Iran
Tel: +9821 6004 0268
Fax: +9821 6469 044

Kriengkrai Khovadhana
Dept. of Meteorology
Sukumvit Road
Bangkok
Thailand
Tel: +66 2 393 1681
Fax: +66 2 398 9886

Tom Kirk
The Eppley Laboratory Inc.
12 Sheffield Avenue
Newport, R.I. 02840
U.S.A.
Tel: +1 401 847 1020
Fax: +1 401 847 1031

Dr. Victoria Klevantsova
World Radiation Data Center
Main Geophysical Observatory
Karbysheva 7
194018 St. Petersburg
Russia
Tel: +7 812 247 0103
Fax: +7 812 247 0103
email: wrdc@ilca.spb.su

Dr. Foeke Kuik
Research Scientist
Royal NL Meteorological Inst.
Wilhelminalaan 10
P.O. Box 201
NL-3730 AE De Bilt
Tel: +31 30 206 482
Fax: +31 30 210 407
email: kuik@knmi.nl

Leila Laitinen
Observ. Instrumentation Division
Finnish Meteorological Inst.
Vuorikatu 24
P.O. Box 503
Fin-00101 Helsinki
Tel: +35 8 192 9443
Fax: +35 8 192 9537
email: leila.laitinen@mi.fi

Wolfgang Laube
Inst. für Meteorol. und Physik
Universität für Bodenkultur
Türkenschanzstrasse 18
A-1180 Wien
Tel: +43 1 470 582 022
Fax: +43 1 470 582 012

Leif Liedquist
Physics and Electrotechnics
Swedish Nat.Testing + Res.Inst.
Box 857
S-50115 Boras
Tel: +46 33 165 448
Fax: +46 33 138 381
email: leif.liedquist@sp.se

Dr. Alexander Manes
Israel Meteorological Service
(IMS)
P.O.Box 25
50250 Bet Dagan
Israel
Tel: +97 23 968 2187
Fax: +97 23 960 4854

Dr. Bruce McArthur
Atmosph. Environment Service
4905 Dufferin Street
Downsview, Ontario, M3H 5T4
Canada
Tel: +1 416 739 4464
Fax: +1 416 739 4281
bmcarthur@dowsv01.dow.on.doe
.ca

Dr. Svetlana Morozova
Optical and Physical Meas.
All-Russian Research Institute
Ozernaya str. 46
Moscow 119361
Russia
Tel: +7 95 437 2992
Fax: +7 95 437 3147
email: sapritsky@glas.apc.org

Agustín Muhlia Velázquez
Instituto de Geofísica
Univ. Nacional Autónoma de
México
Circ. Ext., Ciudad Universitaria
Deleg. Coyoacan
04510 México, D.F.
México
Tel: +52 5 622 4139
Fax: +52 5 550 2486
amuhlia@tonatiuh.igeofcu.unam.
mx

Zoltan Nagy
Inst. for Atmospheric Physics
P.O. Box 39
H-1675 Budapest
Tel: +36 1 290 0163
Fax: +36 1 290 4174
email: znagy@mat.hu

Shaik Naseeruddin
Instrumet Division
India Met. Department
Megeorological Office
Pune 411005
India
Tel: +91 212 339 015
Fax: +91 212 323 201

Donald Nelson
C M D L R/E/CG1
N O A A
325 Broadway
Boulder, CO 80303
U.S.A.
Tel: +1 303 497 6380
Fax: +1 303 497 6290
email: dnelson@cmdl.noaa.gov

Ifeanyi Nnodu
Headquarters
Meteorological Department
Private Mail Bag 12542
Lagos
Nigeria
Tel: +2341 263 3371
Fax: +2341 263 6097

Dr. Peter Novotny
Bureau of Meteorology
150 Lonsdale Street
G.P.O. Box 1289K
Melbourne, Victoria 3001
Australia
Tel: +61 3 9669 4050
Fax: +61 3 9669 4736
email: p.novotny@bom.gov.au

Ing. Jean Oliviéri
Centre Radiometrique
Météo-France
Chemin de l'Hermitage
F-84200 Carpentras
Tel: +33 9063 6968
Fax: +33 9063 6969
email: jolivieri@magic.fr

Cristian Oprea
Atmosph. Physic Laboratory
Nat.Inst. of Met.and Hydrologie
Sos. Bucurest-Ploiesti 97
RO-71881 Bucaresti
Tel: +40 1 312 9842
Fax: +40 1 312 9843

Juan José Pardo Mainez
Instituto Nacional de
Meteorologia
Centro Radiom. Nacional
(I.N.M.)
Camino de las Moreras S/N
Ciudad Universitaria
E-28070 Madrid
Tel: +341 581 9638
Fax: +341 581 9767

Dr. Maria Pavlovitch
Radiometric and photometric Lab.
All-Russian Research Institute
Ozernaya str. 46
Moscow 119361
Russia
Tel: +7 95 437 2992
Fax: +7 95 437 3147
email: sapritsky@glas.apc.org

Julián Pérez de la Puerta
Centro Met. Territorial de
Canarais Occ.
Observat. Meteorol. Especial de
Izana
c/ San Sebastián, 77
Apartado 38071
E-38080 Santa Cruz de Tenerife
Tel: +34 2237 3878
Fax: +34 2237 3720

Thomas Persson
S M H I
S-60176 Norrköping
Tel: +46 11 158 229
Fax: +46 11 170 207
email: tpersson@smhi.se

Ibrahim Reda
Nat. Renewable Energy Laborat.
1617 Cole Boulevard
Golden, CO 80401-3393
U.S.A.
Tel: +1 303 275 3806
Fax: +1 303 275 4611
email: redaiel@tcplink.nrel.gov

Manuel Rocha
Instituto de Meteorologia
Rua C ao Aeroporto
P-1700 Lisbon
Tel: +351 1 847 2880
Fax: +351 1 802 370

Tom Stoffel
Nat. Renewable Energy Laborat.
1617 Cole Boulevard
Golden, CO 80401-3393
U.S.A.
Tel: +1 303 275 4690
Fax: +1 303 275 4611
email: tstoffel@nrel.nrel.gov

James Treadwell
Nat. Renewable Energy Laborat.
1617 Cole Boulevard
Golden, CO 80401-3393
U.S.A.
Tel: +1 303 275 3806
Fax: +1 303 275 4611

Avrar Umarov
Glavgidromet of the Republ. of
Uzbekistan
Observatorakaya str. 72
7000052 Tashkent
Uzbekistan
Tel: +7 3712 336 180
Fax: +7 3712 332 025

André Van Londen
Head of Calibration Laboratory
K N M I
Wilhelminalaan 10
P.O. Box 201
NL-3730 AE De Bilt
Tel: +31 3020 6425
Fax: +31 3021 8407
email: londenv@knmi.nl

L. Van Wely
Kipp & Zonen
Mercuriusweg 1
P.O. Box 507
NL-2600 AM Delft
Tel. +31 15 561 000
Fax: +31 15 620 351

Manuel Vargas
Direction Meteor. de Chile
Casilla 717
Santiago
Chile
Tel: +56 601 9001
Fax: +56 601 9590

Fernando Vigón del Busto
Instruments and Methods
Instituto de Meteorología
Foma de Casablance s/n, Regla
Habana 17
Cuba
Tel: +53 7 617 500
Fax: +53 7 338 010

Dr. Ernst Wessely
Zentralanstalt für Meteorolgie &
Geodynamik
Hohe Warte 38
A-1190 Wien
Tel: +43 136 4453 2703
Fax: +43 136 4453 2720
email: wes@zatsun1.zamg.ac.at

Jesusito Yunzal
Chief
Solar Radiation Center PAGASA
1424 Quezon Ave.
Quezon City
Philippines
Tel: +632 922 8416
Fax: +632 922 9291

5 Symposium

List of Contributions

J. Ronald Latimer
in memoriam

This past year the meteorology community overall and the radiation community specifically suffered the loss of a premier scientist. In early February 1994, J. Ronald Latimer passed away.

Ron, as he was known by virtually everyone, was a careful, meticulous scientist. He was a true leader in the field of solar radiation measurement; both concerning the science of measurement and in understanding the need to make measurements of solar radiation for the advancement of science. He was one who realized that international cooperation was essential for the field of solar radiation to progress.

Ron's career spanned more than 20 years with the Canadian Atmospheric Environment Service before illness forced him into early retirement. His achievements during that time are a lasting tribute to his scientific ability. During this illustrious career he laid the framework for what is now a 50-station network of routine and research quality radiation monitoring stations across Canada. This network in the late 60's and early 70's was admired throughout the world because of his care and attention to detail. It is not going too far to say that this network, under Ron Latimer's control and guidance, produced the highest quality data of the day.

To do this required not only care in the management of the network, but also the ability to characterize and calibrate the instruments that formed that network. Ron, with his assistants, developed calibration equipment and procedures which were not only advanced for his day, as evidenced by his scientific publications, but remain functional to the present. Canada's continuing successes in solar radiation science are directly attributable to Ron's foresight in building a high quality short and longwave calibration facility.

The Canadian solar radiation community recognized this dedicated effort as early as 1978 when the First Canadian Solar Radiation Data Workshop was dedicated to Ron with these words,

> "John Ronald Latimer who, through meticulous care in ensuring the highest standards in data originating from the Canadian solar radiation monitoring network, has provided a strong foundation for the studies of Canadian solar radiation."

Yet, Ron was much more than a Canadian scientist. He was a global scientist. Throughout his career he maintained both the Ångström scale with Å149 and the Smithsonian scale with T7 and SI 14. In 1973 his published analysis showed that the International Pyrheliometric Scale of 1956 was approximately 2% low. Such results led him onto the group of scientists which established the World Standard Group of instruments in Davos for the realization of the SI scale. He was a supporter of the need for regular International Pyrheliometer Comparisons to maintain these high standards globally. In a more human way Ron was part of these comparisons from 1975 through 1990 as the voice that regularly announced, "Please shade and heat the right-hand strip . . . "

Ron Latimer was one who measured radiation, developed techniques for the calibration of pyranometers, saw the need for networks and last, but not least, saw the need for good operating procedures. During the International Hydrologic Decade, 1965 to 1974, the United States and Canada embarked upon a major field program, the International Field Year for the Great Lakes. Ron was commissioned with the development of the Solar Radiation manual. This manual remains a significant piece of literature to this day. While some photos appear dated, and computer algorithms have replaced the tables, the care and dedication to instrument maintenance found in the publication continues to provide good lessons for us all.

Ron was a quiet man, a dedicated man, a man without professional enemies. Ron was a man who stood up for sound scientific principles. These qualities drew people to Ron and are qualities that remain virtuous today. Good scientists like Ron are hard to find. Although the man is gone, his legacy will live for years to come.

Toronto, November 1995 — Bruce McArthur

Maintenance of the World Radiometric Reference

J. Romero, Ch. Wehrli and C. Fröhlich

Physikalisch-Meteorologisches Observatorium Davos / World Radiation Center
Dorfstrasse 33, CH-7260 Davos Dorf

INTRODUCTION

In order to insure the homogeneity of the radiation measurements in meteorology, the World Meteorological Organization introduced in 1979 the World Radiometric Reference [1], to which all pyrheliometers shall be referenced starting in 1980. The World Radiation Center at Davos was charged with the maintenance of the WSG realizing the WRR. The WSG is presently composed of seven absolute pyrheliometers: PMO2, PMO5, CROM2L, CROM3R, HF18748, PAC3 and MK67814. They are frequently intercompared in order to monitor their stability or detect systematic bias of a family of pyrheliometers. Here we present a record of measurements from October 1990 until October 1995 showing the behavior of the WSG pyrheliometers between the last two International Pyrheliometer Comparisons (IPC VII and VIII).

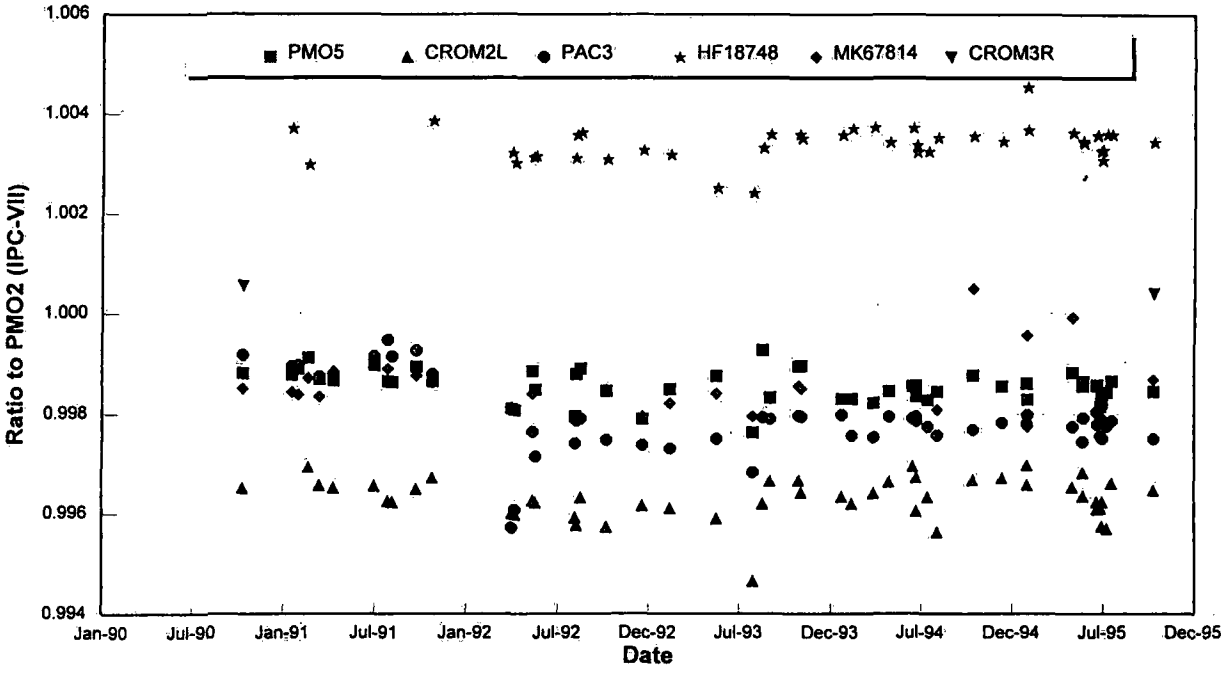

Figure 1: Comparison of WSG instruments from 1990 - 1995 given as ratios to PMO2. The original calibration factors are used for each instrument.

RESULTS OF THE COMPARISONS

The results of the WSG comparisons since IPC VII are plotted in Fig.1 as daily average ratios to the working reference instrument PMO2. All WSG radiometers are evaluated with the original WRR constants. The averages and standard deviations over the period 1990-1995 are summarized in Table 1. The standard deviations are all below 0.1% indicating that the instru-

ments remained stable, although some of them have experienced some troubles. Flies have entered the cavities of HF18748 and PAC-3 causing changes in sensitivity. In the case of HF 18748 an insect was removed and the cavity cleaned in April 1990 leaving an increased sensitivity of +0.25%. For PAC-3 the fly was just removed, but no cleaning could be performed without jeopardizing the unique instrument. Its sensitivity was lowered by about -0.2% since April 1992. In October 1994, the electronics box of MK67814 developed problems and failed completely in September 1995, just before IPC-VIII, during which the radiometer was operated like PAC3 using laboratory equipment. A new electronics box is now under construction. CROM3L was retained at IRMB since the end of IPC-VII and no comparisons are available for this instrument until its participation in IPC-VIII. The scatter of these daily average ratios is of the order of 0.1%. The first and last column of values in Fig.1 represents the ratios to WRR obtained during IPC-VII and IPC VIII respectively. As an independent verification of the stability, the mean ratio of all (39 including the WSG) instruments having participated in IPC VII to the WRR as realized for IPC VIII was determined to be 0.99971 ±0.00133.

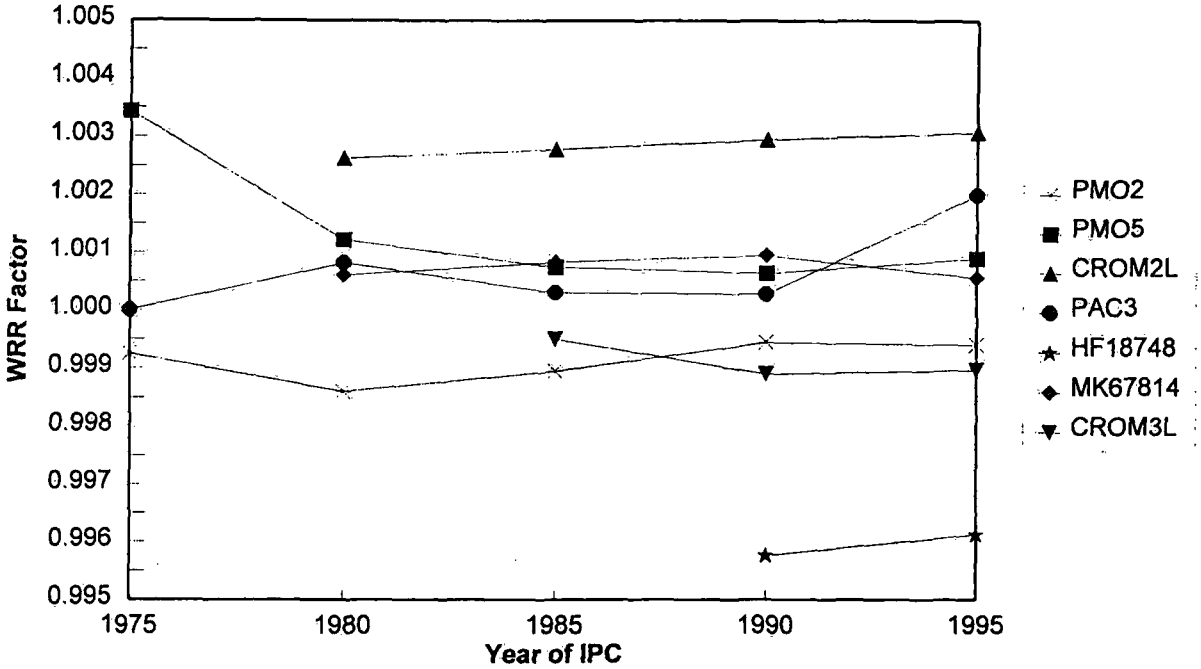

Figure 2: WRR factors of the different WSG pyrheliometers as determined since IPC IV.

Table 1: Summary of the comparison of the WSG instruments for the period of 1990-1995.

	Ratio to PMO2				
Instrument	PMO5	CROM2L	PAC3	HF18748	MK67814
Average	0.99855	0.9963	0.9979	1.00332	0.99858
Stdev	0.00032	0.00041	0.00073	0.00059	0.00059

Figure 2 shows the WRR reduction factors of the WSG radiometers since the last twenty years. It demonstrates, that the WSG instruments have indeed remained stable within 0.1% since the WRR was established in 1980. The larger deviation of PAC3 is explained by intrusion of an insect.

CONCLUSIONS

The frequent comparison of the WSG pyrheliometers (except for CROM3L) are needed to establish their relations between the International Comparisons IPC VII and IPC VIII in order to reliably transfer the WRR from one IPC to the next. The instrument problems during the period between the IPC show that lack of comparison would have jeopardized the judgment of the stability or change of the different WSG instruments.

REFERENCES

WMO, Technical Regulations, World Meteorological Organization, WMO No. 49, Geneva, 1979

IPC VI, 1985, International Pyrheliometer Comparisons 1985, Working Report No. 137, Swiss Meteorological Institute, Zürich and PMOD/WRC Davos, December 1985

IPC VII, 1990, International Pyrheliometer Comparisons 1990, Working Report No. 162, Swiss Meteorological Institute, Zürich and PMOD/WRC Davos, March 1991

Fröhlich C., 1984, Maintenance of the World Radiometric Reference 1978 to 1984, PMOD/WRC Davos, No. 607

FITTING OF WEIBULL FUNCTIONS TO TOTAL SOLAR RADIATION IN MEXICO CITY

by
José Luis Bravo and Agustín Muhlia
Instituto de Geofisica UNAM, México DF.

INTRODUCTION

Usually, evaluation of the total solar radiation is made with models like Ångström (1924, 1958) and similar, recently Estrada (1990, 1992) made a revision of more elaborated models. The most of these use sunshine as a parameter and makes estimations of daily totals of global radiation. In this work, a statistical point of view is given to the description of solar radiation at Mexico Valley, some common statistical distributions (normal, lognormal, beta and Weibull) were adjusted to empirical distributions of hourly integrals of global radiation for hours with intensities that was sufficient to burn a heliographic strip (100% of sunshine). It was found that Weibull distribution (Johnson and Kotz, 1970) offers satisfactory results.

CONDITIONS OF THE OBSERVATION

The data used in this work were hourly integrals of global radiation fluxes (megajoules/m^2) and hourly values of sunshine obtained in the Solar Radiation Observatory of the Institute of Geophysics in the campus of Mexico City National University. The site of observations is at southwest part of Mexico Valley (19° 20'N, 99° 11'W and 2268 m asl). Observing period was from January 1983 to December 1987. Global radiation measurements were made with a piranometer and radiation intensity was hourly integrated with a printer integrator both made by Kipp & Zonen. The used piranometer had been periodically compared with the Eppley pirheliometer of electrical compensation N° 18587 which participates in the international intercomparisons in the World Radiation Center at Davos, Swiss.

Measurements of sunshine were made with a Campbell Stokes Heliograph placed near the piranometer.

Integration and readings of global radiation and sunshine are made in true solar time (tst). It has been used only the period between 8 and 17 hrs tst because it is the energetically important time for the latitude of the point of observation. It was selected all the hourly that in the heliographic strip have 100% of sunshine. The selected integrals were classified according to the hour (in tst) and the month in 108 groups (12 months and 9 hours). Each of these groups are treated as an independent sample of the global radiation. Notice that days with thin clouds are included in the sample because it is impossible to distinguish, with a heliographic strip, between a clear day and a day with thin clouds.

CHARACTERISTICS OF THE GLOBAL RADIATION HISTOGRAMS

Using the 108 groups of data it was constructed 108 histograms that have the following remarkable characteristics:

a) Solar radiation always has values greater than zero.

b) Values with high solar radiation are rarely presented because days with high transparency and/or with low white clouds in the atmosphere of Mexico City have low frequencies, then the right hand tail of the histograms (empirical probability density functions) go down fast.

c)In the low radiation side, the case is distinct because in Mexico Valley days with high atmospheric turbidity are frequent, then the histograms go to zero slowly. As a consequence of, this histograms are skewed to left.

ADJUST OF WEIBULL DISTRIBUTIONS TO GLOBAL RADIATION

The empirical distribution functions for global radiation (Bravo J.L. et al.,1991) are useful because they permit approximate estimations of probabilities. However, to obtain a parsimonious model (with few parameters) and make easier the calculus of some characteristics of the distributions, such as modes or confidence intervals, several analytical distributions, with shape compatible with the remarkable characteristics mentioned earlier, were adjusted (normal, lognormal, beta and Weibull) and Weibull was the best adjusted distribution, analytic form of their probability density function is as follows:

$$P_X(x) = c\alpha^{-1}\{x/\alpha\}^{c-1} \exp[-\{x/\alpha\}^c] \qquad (1)$$

where α and c are parameters of scale and shape respectively. Table I shows the parameters of the adjustement. Chi square and Kolmogorov-Smirnov (Conover, 1980)) test were made for the goodness of fit. Chi square test reject the hypothesis for 8 of 87 cases in which there were sufficient points to perform the them. Kolmogorov - Smirnov test did not reject any case. Empty places in the table means that there was not enough observations for the fitting and/or for the goodness of fit test.

GLOBAL RADIATION ESTIMATION

Using adjusted distributions it is possible to calculate values of P_1 probability from left and P_2 from right tails, and calculate interval for 1- (P_1 + P_2) confidence for the global radiation for the desired day and hour.

Modal values for each distribution can be calculated derivatting equation (1) and can be considered as a representatives for the distributions. Results are shown in table I and modal values are graphed in figure 1. It is easy to see maximum values for 12 -13 hrs during March to August and the low values in the afternoon during May to September reflecting a reduction in the air transmissibility caused by the rainy season.

TABLE I. Shape (c) and scale (α) parameters for the Weibull fitting to hourly integrals of global radiation and value of maximum probability of occurrence (mode) derived from the fitting. global radiation in megajoules/m^2 and hours in true solar time.

MONTHS		HOURS 8-9	9-10	10-11	11-12	12-13	13-14	14-15	15-16	16-17
I	c	10.5	11.5	12.3	10.6	10.3	8.8	7.0	6.4	12.4
	α	147.9	119.2	263.6	280.1	279.4	254.1	202.5	145.8	75.9
	mode	146	218	262	277	277	251	198	142	75
II	c	10.9	14.4	15.1	13.2	11.2	11.1	10.6	9.6	11.4
	α	177.0	250.6	300.7	322.8	320.2	296.7	248.4	178.2	94.8
	mode	175	249	299	321	318	294	246	176	94
III	c	13.8	17.0	16.9	16.9	12.4	12.1	10.3	7.9	11.2
	α	211.9	284.8	332.1	357.4	349.4	319.4	269.8	203.4	119.4
	mode	211	284	331	356	347	317	267	200	118
IV	c	14.1	15.0	14.8	16.1	13.5	9.1	11.3	11.1	10.5
	α	217.8	287.3	333.8	354.3	348.5	309.9	269.9	199.0	124.0
	mode	217	286	332	353	347	306	268	197	123
V	c	11.6	14.2	13.5	12.6	11.2	11.0	12.5	11.4	8.7
	α	214.0	278.0	321.0	339.0	344.2	325.0	290.0	223.0	143.0
	mode	212	277	319	337	341	322	288	221	141
VI	c	19.6	16.7	13.0	15.3	17.5	15.6	17.2	—	—
	α	221.8	293.4	323.7	342.5	349.5	327.5	277.1	—	—
	mode	221	292	322	341	348	326	276	—	—
VII	c	11.6	14.7	15.0	13.4	9.2	9.3	—	—	—
	α	19.5	288.4	333.4	347.4	347.0	324.2	—	—	—
	mode	218	287	332	345	343	320	—	—	—
VIII	c	17.8	13.7	15.0	12.3	13.3	9.9	11.1	—	—
	α	215.8	279.6	324.0	344.6	346.5	322.1	264.5	—	—
	mode	215	278	323	342	344	319	262	—	—
IX	c	14.6	15.1	13.5	13.9	11.5	9.4	8.2	9.8	—
	α	205.9	271.7	319.7	342.0	338.7	312.2	267.2	196.1	—
	mode	205	270	318	340	336	308	263	194	—
X	c	13.1	13.4	13.3	11.9	13.7	11.0	10.5	9.1	8.3
	α	177.4	248.3	294.4	314.3	311.7	284.8	236.0	170.1	93.7
	mode	176	247	293	312	310	282	234	168	—
XI	c	12.8	13.5	13.3	12.1	11.4	9.5	8.4	7.2	7.3
	α	152.5	219.5	264.2	285.0	277.7	253.0	211.0	146.0	77.8
	mode	152	218	263	283	275	250	208	143	76
XII	c	10.9	9.3	12.4	12.3	10.6	8.9	5.2	5.1	—
	α	135.7	201.4	246.4	265.0	260.3	239.4	192.3	129.5	—
	mode	135	199	245	263	258	236	185	124	—

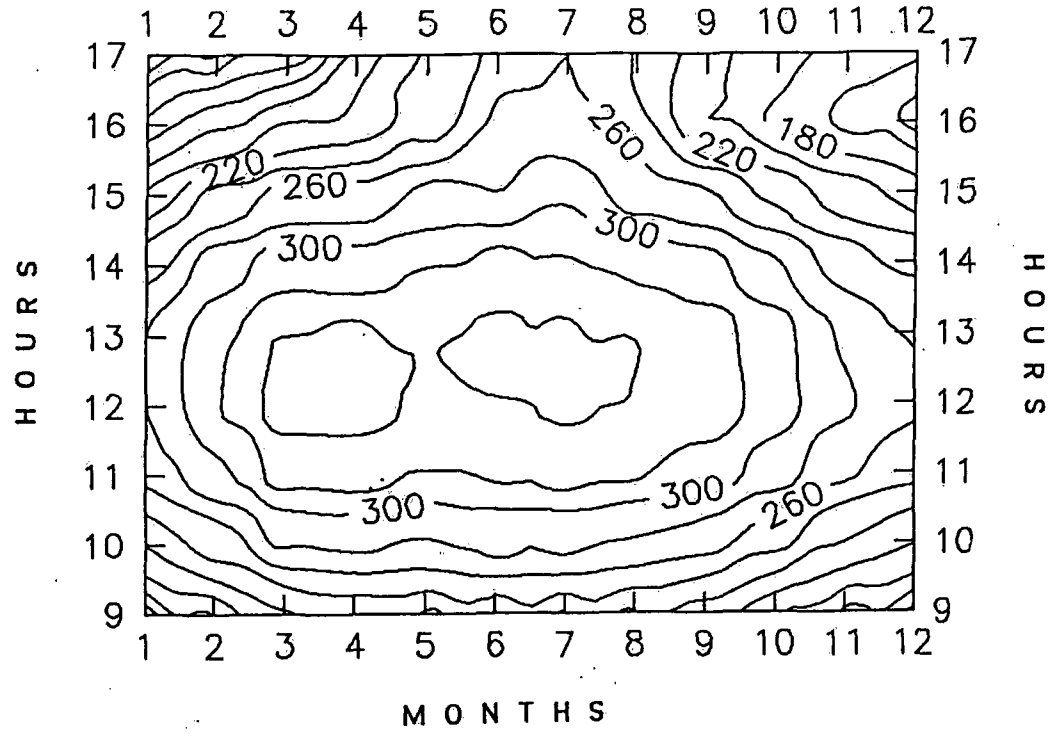

Fig 1. Level curves for modes of Weibull adjusted distributions (megajoules/m^2 x 10^2).

REFERENCES

Ångström, A. 1924 Solar and Terrestrial Radiation. Quart. Jour. Roy. Met. Soc. 50, p. 121-126.

Ångström, A. 1956 On Computation of Global Radiation From Records of Sunshine. Arkiv. Geophysik. 3.

Bravo, J.L., Muhlia, A., Leyva, A., Mota, A., 1990, A Statistical Model that describes the Sunshine at the Southern Metropolitan Area of the México Valley. Geogísica Internacional, Vol. 29-1.

Conover, W. J., 1980. Practical Nonparametric Statistics. John Wiley & Sons, 2ed. p. 69-70, 189-199.199.

Estrada, V., 1990, Métodos de Cálculo de la Radiación Solar. Notes from Actualization course of Solar Energy. Instituto de Investigación en Materiales. Universidad Nacional Autónoma de México

Estrada, V., 1992, Datos de Radiación Solar en la República Mexicana, alcances y limitaciones. La Revista Solar No 21 Asociación Nacional de Energía Solar. México.

Johnson, N., S. Kotz, 1970. Continuous Univariate Distributions 1. Houghton Mifflin Company. Boston pp. 251-271.

RESULTS OF THE ACTINOMETRIC AND SPECTROPHOTOMETRIC MEASUREMENTS IN MEXICO CITY

Agustin Muhlia-Velazquez, Amando Leyva-Contreras.

Observatorio de radiación Solar, Instituto de Geofisica,
Universidad Nacional Autónoma de México.

INTRODUCTION

The main objective of this investigation has been to determine the levels of pollution present in the Mexico City atmosphere and then to compare these levels with those found in rural, unpolluted regions (Mauna Loa Observatory in Hawaii, at the DOE ARM Program site in Oklahoma and in Rapid City, SD) and to use the actinometric (broadband) series of measurements to examine the temporal variations of the processes under investigation.

In recent years air quality has become a serious issue for many urban regions. For example, measurements of aerosol concentration both at ground level and in the entire atmospheric column in Mexico City exceed values in rural regions by an order of magnitude. It is possible to monitor aerosol pollution using ground-based sunphotometers, since aerosol particles attenuate the solar radiation propagating through the atmosphere. Measurements of the atmospheric integral and spectral transparency are widely used for this purpose. Using a model of the aerosol optical properties, the "inverse method" endeavors to estimate the aerosol concentration. In particular, spectral optical depth (SOD) measurements allow conclusions to be made about the size distribution of aerosol ensembles present in the air.

INSTRUMENTS, SITES AND METHODS OF MEASUREMENTS

The actinometric measurements in the shortwave spectral region (0.3-4.0 mm) were made at the Observatory of Solar Radiation of the Institute of Geophysics (ORS IGf) of the National Autonomous University of Mexico (UNAM), using an actinometer of the Linke and Feussner type, which was systematically calibrated against the Ångström national standard pyrheliometer. Well-known methods of calculations were used to obtain atmospheric transparency (Kondratyev, 1969; Iqbal, 1983). The Ångström turbidity coefficient (β) was used to characterize the atmospheric turbidity levels of aerosol pollution. A numerical algorithm was used; it was assumsed, that in the spectral dependence of the optical depth $\tau(\lambda) = \beta/\lambda^{\alpha}$, the power α is equal to an average value of 1.3 (Ångström, 1961). Then, using the method, described by Muhlia *et al.* (1989), the columnar concentration of aerosol particles may be estimated. The series of measurements comprising three periods are described: 1911-1928, 1957-1962 (Galindo and Muhlia, 1970), and 1967-1991 (Muhlia, 1995).

SOD measurements in Mexico were made using the Russian-built K-2 and K-3 Spectrophotometers in the spectral range of 355-950 nm, with a spectral resolution of about 2 nm. Measurements in the US were made using the Russian-built Spectroradiometer based upon Wedge Interference Filters (SWIF) in 200 channels in the spectral range of 350-1150 nm, with a spectral resolution of about 15 nm. The description of these instruments is given in (Vasilyev *et al.*, 1994a,b).

Spectral measurements were made in Mexico City during April-June 1992 at ORS IGf. A total of about 30 series were taken, and half of them were used for further processing. In Hawaii, measurements were made in May-June 1993 (4 series); at the ARM Program site in Oklahoma, 5 series were taken in August 1993; and 11 series were taken in Rapid City,SD, during August- September 1993.

The "long method" was used for the calculations of SOD values (Liou, 1980), in which "Langley plots" or "Bouguer lines" are plotted. These are regression lines of the logarithm of measured intensity plotted against the optical path length (*i.e.* "air mass").

RESULTS

Results of determination of the optical depths (τ) and of the calculations of Ångström turbidity coefficient (β) and of the columnar particle concentration (N,cm^{-2}) on the basis of the measurements of broadband (0.3-4.0 mm) direct solar radiation fluxes (Muhlia et al., 1989) are presented in Fig. 1, and the average values of these parameters for the tree periods are presented in Table 1. During recent years the columnar concentration of aerosol particles on some days was found to be as large as $1.5*10^9$ cm^{-2} - greater by one order of magnitude than those in rural areas.

Fig. 1.

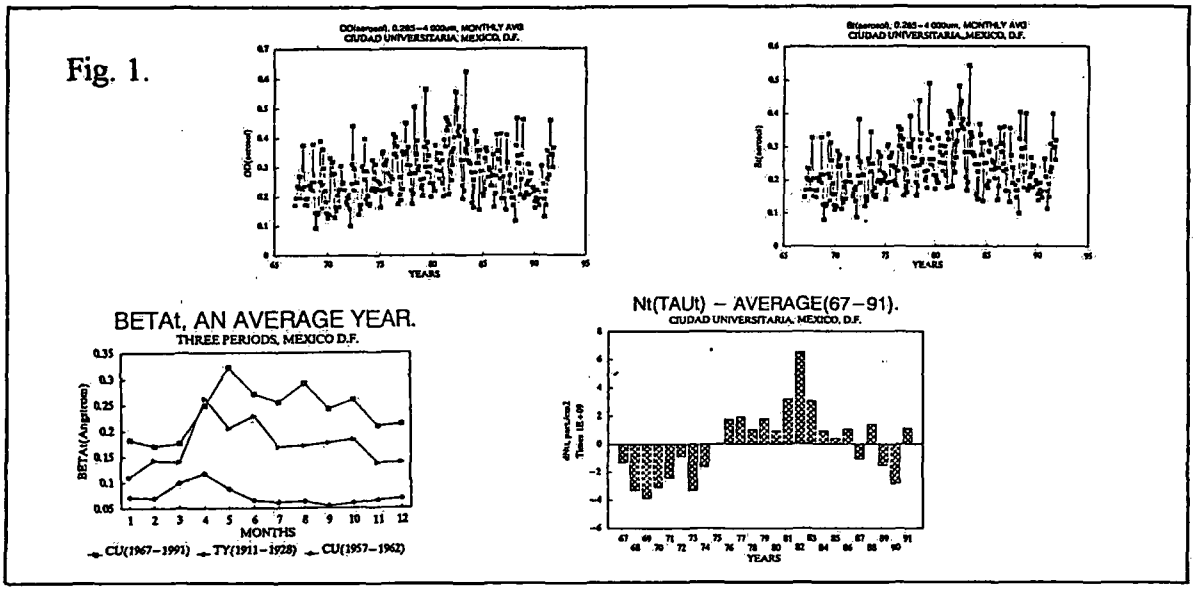

Table 1. Results of the actinometric measurements in Mexico City, average values.

Period	τ	β	$N*10^{-9}$
1911-1928	0.084	0.071	0.63
1957-1962	0.173	0.147	1.30
1967-1991	0.286	0.246	12.5

Measured values of SOD in Mexico City on some days reached as high as 1.2 in the UV, 0.8 in the visible and 0.5 in the near-IR spectral regions. Ångström turbidity coefficient in Mexico City atmosphere taken in 1992 from SOD data was equal to 0.34, *i.e.* according to Ångström's classification (Ångström, 1961) the atmosphere has to be labeled only as "very turbid".

The values of SOD measured at MLO in Hawaii vary approximately from 0.1 in UV to about 0.05 in the visible and near-IR spectral

regions (free of water vapor absorption bands). The coefficient β was found to be equal to 0.033, and this site is labeled as "clean". However, these values were higher than typical background values due to the continuing influence of the Mt. Pinatubo eruption.

The values of SOD measured in Rapid City, SD, and at ARM Program site in Oklahoma were about 0.05 and 0.1, respectively larger than in Hawaii. The coefficients β were found to be equal to 0.047 and 0.086, and the atmospheres were labeled as "clean" and "clear", respectively.

In Fig.2 the average curves for all the series of measurements at all sites of the observations and the results of the calculations of SOD according the WMO Standard Atmosphere (WMO,1986) and according to Elterman model of the atmosphere of moderate pollution (Elterman, 1968) are presented. The difference in the optical state of the polluted urban and unpolluted rural atmospheres is well recognized.

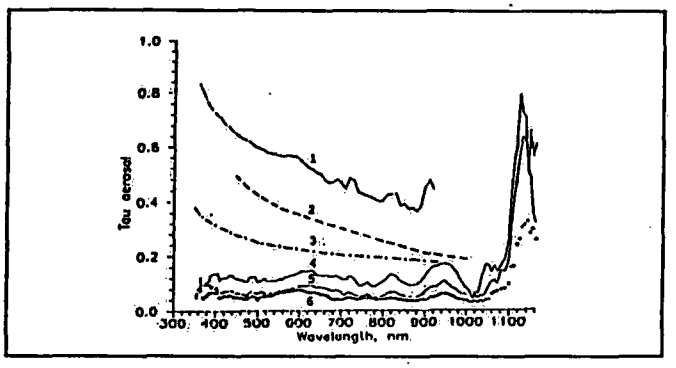

Fig.2. Comparison of average SODcurves,measured: 1 - in Mexico City, 4 - at ARM Program site in Oklahoma, 5 - in Rapid City, SD, and 6 - at MLO in Hawaii; with calculated values of SOD: 2 - according to WMO Standard Atmosphere and 3- according to Elterman model of the atmosphere of moderate pollution.

DISCUSSION

Table 1 shows a tendency for an increase in the turbidity of the Mexico City atmosphere in the period of observations approximately by 2 % per year (or $1.72*10^9$ part./cm^2 per year). The tendency of the direct solar radiation, at an air mass equal to 2, to decrease is also well recognized, coinciding with that obtained for highly polluted industrial areas in the ex-USSR. This indicates that the atmosphere above Mexico City is tremendously polluted and is becoming more so with time. Serious government efforts are needed in order to stop this process. Figure 1 shows among another influences the effect of El Chichon, 1982, the increase of the columnar concentration of aerosol particles was around 50% above the 1967-1991 period average.

The highly polluted atmosphere in Mexico City has SOD more than twice that of the clear atmosphere. The solar radiation scattered by aerosol particles in this polluted atmosphere is of the same order as the radiation scattered by all air molecules. In situations of strong pollution, the absorption of aerosols in atmosphere also can reach the order of the molecular absorption in atmospheric gases (Kondratyev *et al.*, 1974). Hence, the SOD of molecular (Rayleigh) scattering, the SOD of molecular absorption, the SOD of aerosol scattering and the SOD of aerosol absorption of light in the strongly polluted terrestrial atmosphere are all of comparable size. The presence of a big amount of aerosol particles in the atmosphere changes significantly the spectral signature of aerosol SOD: it becomes strongly dependent against wavelength, and resembles the curves of typical Mie scattering.

Assuming the correctness of an "Ångström law" (Ångström, 1961) and using the spectral dependence of $\tau(\lambda)$ measured, *e.g.* in Mexico City, the slope of the model, Junge type, size distribution of the aerosol particles in the entire atmospheric column can be estimated: $N(r) \cong 3*10^9 / r^{3.5} * H$ (cm^{-3}), where H (in cm) is the height of the so called

"homogeneous" aerosol layer (its estimates using actinometric measurements give in Mexico City values equal to 0.6 - 1.0 km). Size distributions, measured *in situ* near the ground level, using the particle counters were found to be, as a rule, strongly multimodal.

ACKNOWLEDGEMENTS

The authors express for the excellent technical support their gratitude to personnel of the ORS IGf at UNAM, of the Laboratory of Experimental Atmospheric Optics of the Institute of Physics at Saint-Petersburg State University and of the Remote Sensing Group of the Institute of Atmospheric Sciences at South Dakota School of Mines and Technology.

REFERENCES

Ångström, A., 1961: Techniques of Determining Turbidity of the Atmosphere. *Tellus*, 13, 214 p.

Galindo, I.G., and A. Muhlia, 1970: Contribution to the Turbidity Problem in Mexico City. *Arch. Met. Geoph. Biokl., Ser. B*, 18, 169-186 pp.

Elterman, L., 1968: Ultraviolet, visible and infrared attenuation for altitudes to 50 km, 1968. Environmental Research Papers, No. 285, April 1968.

Iqbal, M., 1983: An Introduction to Solar Radiation. Academic Press, Toronto, NY, London, Paris, San Diego, San Francisco, São Paulo, Sidney, Tokyo, 390 pp.

Kondratyev, K.Ya., 1969: Radiation in the Atmosphere. Academic Press, NY, 912 pp.

Kondratyev, K.Ya., O.B. Vasilyev, V.S. Grishechkin, L.S. Ivlev, 1974: Spectral Radiative Flux Divergence and its Variability in the Troposphere in the 0.4-2.4 mm Region. *Applied Optics*, 13, 3, 478-486 pp.

Liou, Kuo-Nan, 1980: An Introduction to Atmospheric Radiation (International Geophysics Series, Vol. 26). Academic Press, NY, London, Toronto, Sydney, San Francisco, 392 pp.

Muhlia, A., A. Leyva, J.-L. Bravo, 1989: Actinometric Method for the Determination of the Total Number of Aerosol Particles in the Vertical Atmospheric Column. *Geof. Intern.*, 28-1, 47-71 pp.

Muhlia, A, 1995: Estudios Actinométricos y Espectrofotométricos en la Atmósfera de la Ciudad de México, Tesis doctoral (PhD), Universidad Estatal de San Peterburgo (en ruso), 188 pp .

Vasilyev, O.B, A. Leyva Contreras, A. Muhlia Velazquez, A. P. Kovalenko, A.V. Vasilyev, L.S. Ivlev, V.M. Jukov, R. Peralta y Fabi, Ronald M. Welch, 1994a: Report on the Optical Properties of the Polluted Atmosphere of Mexico City (Spring - Summer 1992). *Reportes Internos 94-3, Instituto de Geofisica UNAM*, Mexico, 90 pp.

Vasilyev, O.B, R.M. Welch, A. Leyva, A. Muhlia and R. Peralta, 1994b: Spectroradiometer based on wedge interference filters (SWIF) for applications in atmospheric optics. In: Optical Spectroscopic Techniques and Instrumentation for Atmospheric and Space Research (Proceedings of SPIE, v. 2266), 578-587 pp.

WMO, 1986: A preliminary cloudless standard atmosphere for radiative computation. WCRP, IAMAP Radiation Commission. WCP - 112 WMO/TD No. 24.

Solar Radiation Measurement, Modeling, and Dissemination Projects at NREL

Tom Stoffel
National Renewable Energy Laboratory
1617 Cole Boulevard
Golden, Colorado 80401-3393

Abstract

Measurement, modeling, and dissemination of solar radiation resources are key elements within the Resource Assessment Program at the National Renewable Energy Laboratory. This paper provides an overview of these various activities completed recently or in progress during 1995.

Introduction

The Resource Assessment Program (RAP) at the National Renewable Energy Laboratory (NREL) is funded by the United States Department of Energy to provide resource information for a variety of renewable energy conversion technologies (e.g., biomass, photovoltaics, solar thermal, and wind energy). This effort involves the measurement, modeling, and dissemination of solar radiation resources. The following research activities have been recently completed or are in progress.

Measurements

The *Solar Radiation Research Laboratory* (SRRL) is located on South Table Mountain in Golden, Colorado. The mesa-top location provides the outdoor measurements laboratory with excellent solar access. The SRRL objectives are to develop a solar radiation resource climatology for NREL and conduct resource measurement research and development in support of renewable energy conversion technologies at NREL. The Baseline Measurement System at SRRL collects 5-minute averaged data from 10-second samples of 18 instruments, including pyranometers, pyrheliometers, photometers, and meteorological monitoring instruments. Standard procedures for the maintenance and operation of this data collection system have been developed to provide an adequate level of quality control. Quality-assessed data are available for the period 1981 to 1991 (Marion, 1993). Access to more recent data is now available from the Renewable Resource Data Center on the Internet: http://rredc.nrel.gov. The SRRL also provides for the comparison of absolute cavity radiometers traceable to the World Radiometric Reference, development of improved methods for outdoor radiometer calibration and characterization, outdoor characterization of photovoltaic devices, and facilities to meet the general demands for outdoor measurement research and development activities at NREL.

In conjunction with the *King Abdulaziz City for Science and Technology of Saudi Arabia* (KACST), NREL is working on a 48-month project to improve the assessment of solar radiation resources in Saudi Arabia by upgrading surface measurements and by developing correlations between surface and satellite data. A 12-station solar radiation network is now providing direct normal, diffuse horizontal and global horizontal irradiances measured with thermopile radiometers. Diffuse irradiance measurements are made with a tracking disk system mounted on a radiometer mounting fixture designed for this application as shown in Figure 1. Telephone access to the data acquisition system allows for daily processing of the data. The network is supported by an upgraded calibration facility which includes a reference absolute cavity radiometer that participated in the Eighth International Pyrheliometer Comparisons.

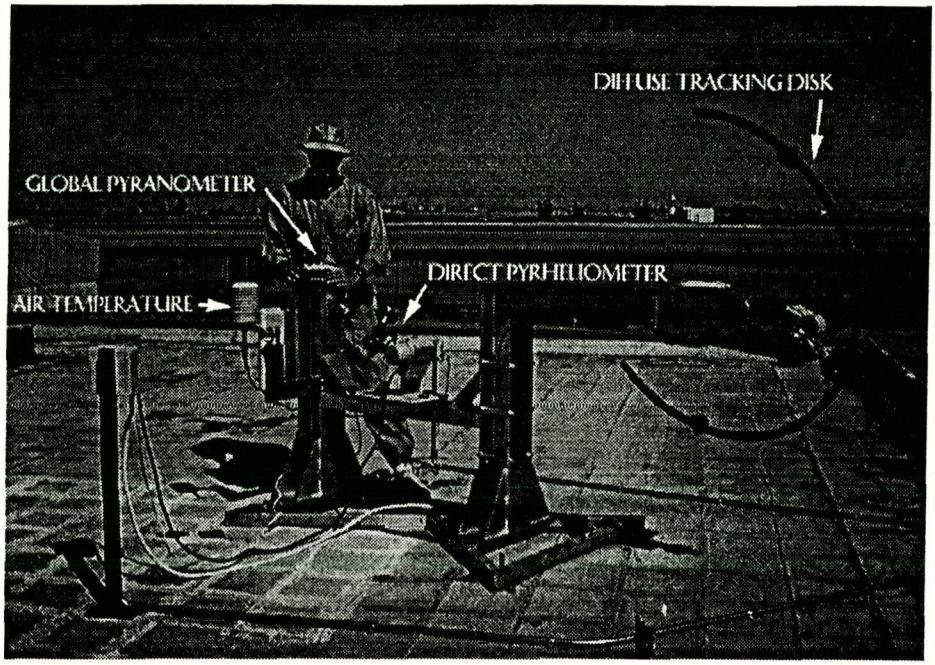

Figure 1. Radiometer mounting platform for Saudi Arabian Network

As part of the joint KACST-NREL effort to establish and operate a solar measurements network and to improve our understanding of pyranometer measurement performance, we are developing the *Radiometer Calibration and Characterization* (RCC) system. An extension of our existing method of radiometer calibration (Myers and Stoffel, 1989), RCC is a data acquisition and processing system used to determine the typical single-value calibration factor ($\mu V/Wm^{-2}$) and a more detailed description of the pyranometer's angular response characteristics by providing a calibration vector. This calibration vector provides the instrument sensitivity as a function of solar zenith angle. The data acquisition system includes a nearly real-time analysis of the atmospheric stability to control the collection of irradiance data used for the calibration and characterization analyses. The goal of RCC is to produce characterization information for use in post-measurement processing of pyranometer data to improve the representativeness of the irradiance measurements.

The *Historically Black Colleges and Universities (HBCU) Solar Measurements Network* was implemented in 1985 and continues to provide high-quality measurements of global, diffuse, and direct solar irradiance (Marion, 1994). Comprised of six stations in the southeastern United States, the HBCU network continues to provide 5-minute solar radiation measurements from the locations found in Table 1.

In a effort to establish a national network of solar radiation and wind resource measurement stations, NREL is in the process of developing the *Cooperative Networks for Renewable Resource Measurements* (CONFRRM). Under this concept, regional centers would operate and maintain a collection of solar measurement stations each acquiring data for global horizontal, diffuse horizontal, direct normal, and irradiance on a south-facing tilted surface. Two categories of standard instrument configurations have been specified based on the radiometer measurement performance. Additionally, benchmark wind measurement stations are planned to provide research-quality wind resource data from instrumentation mounted on three levels of a standard, 40 meter meteorological tower. The number of measurement stations to be implemented under the

CONFRRM project, depends on the level of funding from the U.S. Department of Energy. We hope to collect at least three years of resource data from this new resource measurement network initiative.

Table 1. HBCU Solar Measurements Network Station Summary

College or University	Location	Latitude (°N)	Longitude (°W)	Elevation (meters)
Bethune-Cookman College	Daytona Beach, Florida	29.18	81.02	20
Bluefield State College	Bluefield, West Virginia	37.26	81.24	803
Elizabeth City State University	Elizabeth City, North Carolina	36.30	76.25	4
Mississippi Valley State University	Itta Bena, Mississippi	33.50	90.33	52
South Carolina State University	Orangeburg, South Carolina	33.45	80.85	96
Savannah State College	Savannah, Georgia	32.03	81.07	11

Members of the RAP also are involved with the *Atmospheric Radiation Measurement (ARM) Program* supported by the U.S. Department of Energy. Designed to improve the understanding of processes that affect atmospheric radiation and the description of these processes in climate models, ARM includes several radiometric measurement activities (Stokes and Schwartz, 1994). Our current involvements are with the design and deployment of a radiometer calibration facility at the Cloud and Radiation Testbed site in the southern Great Plains and the solar radiation measurement platforms for the Tropical Western Pacific. The goal for these and other measurement sites is to collect seven to ten years of extensive atmospheric and solar radiation measurements representative of the area now used in global circulation models, about 350 kilometers on a side.

The RAP also continues to work in cooperation with the World Radiation Data Center in St. Petersburg, Russia to acquire, assess, archive, and distribute solar radiation and radiation balance data from international sources. Improvements are being made to the data processing systems to allow for more efficient collection, inspection, archival, and dissemination of solar measurements.

Although not a formal contributing member of the *Baseline Surface Radiation Network* (BSRN), we have shared our experiences with measurement quality control and data quality assessment practices with BSRN participants. If funding and staffing resources permit, we hope to provide the World Radiation Monitoring Center with future SRRL data in BSRN format (Gilgen, et al., 1995).

Modeling

Because the need for site-specific solar radiation data often exceeds the availability of historical ground-based irradiance measurements, techniques have been developed for estimating solar irradiance from available meteorological data (Hulstrom, 1989; Iqbal, 1983). Additionally, methods of assessing the quality of measured shortwave solar irradiance can be considered a modeling effort.

The development of the *National Solar Radiation Data Base* (NSRDB) involved both of the above modeling concepts (NREL, 1992; NREL, 1995). The NSRDB is a collection of hourly solar radiation and meteorological data for 239 cities in the United States for the period 1961 through

1990. An important element of the NSRDB production was the development of a meteorological-statistical solar radiation model, *METSTAT* (Maxwell, 1995) In this model, hourly calculations of solar irradiance are made using hourly total and opaque cloud observations, hourly precipitable water vapor, daily aerosol optical depth, and daily albedo input data. The model produced representative diurnal and seasonal patterns, daily autocorrelations, and persistence of direct normal, diffuse horizontal, and global horizontal solar irradiance elements. The METSTAT model will be made available for use on personal computers (IBM-compatible and Macintosh) and DEC/VAX computer systems. The software and user's manual will be available in 1996.

SERI QC is a mathematical software package that assesses the quality of solar radiation data (NREL, 1993). This software was developed by the National Renewable Energy Laboratory when the Laboratory was called the Solar Energy Research Institute (SERI), hence the name *SERI QC*. The basis for this empirical approach to quality assessment is the combined application of physical limits, internal consistency (i.e., global irradiance is the sum of the diffuse irradiance and the vertical component of the direct normal irradiance elements), and the transformation of the irradiance elements into K-space, a normalization technique based on the extraterrestrial radiation value[1]. Each hourly data value in the NSRDB has been assigned a *SERI QC* flag indicating the degree of certainty.

The objectives of the *Solar Radiation Data Grid* project, initiated in 1995, are to produce a uniform, high-resolution grid (40 kilometers x 40 kilometers) of climatological solar radiation, develop the methodology to model solar resources in remote areas with insufficient conventional surface meteorological observations, and develop the Geographic Information System (GIS) capabilities for efficient processing of both input data and model results. Presently under development at NREL, the project uses detailed cloud information available from the Real Time Nephanalysis data base (40 km x 40 km) produced by the U.S. Air Force (Kiess and Cox, 1988). Current output products are monthly mean daily total direct, diffuse and global irradiation estimates.

The *Typical Meteorological Year Version 2* (TMY2) data files were derived from the thirty years of hourly data in the NSRDB (Marion and Urban, 1995). Except for a few changes to the weighting criteria, which accounts for the relative importance of the solar radiation and meteorological elements in the selection process, the TMY2s were created using procedures similar to those developed by Sandia National Laboratories to create the original Typical Meteorological Year from the 1952-1975 SOLMET data base (Hall et al., 1978). The Sandia method is an empirical approach that selects individual months from different years from the long-term data base. In the case of the NSRDB, data from a station for all 30 Januarys are examined and the one judged most typical is selected to be included in the TMY. Continuing with the remaining months, the 12 selected typical months are concatenated to form a complete year of hourly data. The data elements include extraterrestrial, global, direct normal, and diffuse irradiance; global, direct normal, and diffuse illuminance; zenith luminance; and basic surface meteorological observations.

Dissemination

Measurements, model estimates, and assessments of solar radiation resources are of little value unless the information reaches those in need and can be efficiently applied. The *Renewable Resource Data Center* (RReDC) has been established to make NREL's public domain renewable resource data, including solar radiation, available via Internet and other media (Gardner, Rymes, 1995). Development of the RReDC will continue to build upon the existing data and information: NSRDB statistics files, TMY2, spectral radiation data sets, circumsolar data sets, 1-minute Solar

[1] For a more detailed description of SERI QC method, see companion paper in this publication: *Solar Data Processing Techniques.*

Energy and Meteorological Training Sites (SEMRTS) data sets, and others. The RReDC World Wide Web home page is accessible as "http://rredc.nrel.gov" and provides connections to the World Radiation Data Center, the National Climatic Data Center, Oak Ridge National Laboratory, the U.S. Department of Agriculture, the U.S. Department of Energy, and other NREL home pages. Formalized review and editing procedures are in place for adding information to the RReDC. There are also provisions for user feedback for use in improving the data center.

Conclusion

The United States Department of Energy funds the Resource Assessment Program at the National Renewable Energy Laboratory to perform research and development in solar radiation measurement, modeling, and information dissemination. Several key projects have been introduced.

References

Gardner, T.; Rymes, R. (1995). "Products Available From NREL's Renewable Resource Data Center," *Proc. of the 1995 American Solar Energy Society Annual Conference, SOLAR '95, July 15-20, 1995, Minneapolis,*. R. Campbell-Howe and B. Wilkins-Crowder (ed). pp. 210-215. Boulder, CO: American Solar Energy Society.

Gilgen, H.; Whitlock, C.H.; Koch, F.; Müller, G.; Ohmura, A.; Steiger, D.; Wheeler, R. (1995). *Baseline Surface Radiation Network (BSRN) Technical Plan for BSRN Data Management (Version 2.1 - Final).* WMO/TD-No. 443. International Council of Scientific Unions, Intergovernmental Oceanographic Commission, and World Meteorological Organization. World Climate Research Program. Geneva: World Meteorological Organization.

Hall, F.; Prairie, r.; Anderson, H.; Boes, E. (1978). *Generation of Typical Meteorological Years for 26 SOLMET Stations.* SAND78-1601. Albuquerque, NM: Sandia National Laboratories.

Hulstrom, R. L. (1989). *Solar Resources*, The MIT Press, Cambridge, Massachusetts. ISBN 0-262-08184-9. 408 pp.

Iqbal, M. (1983). *An Introduction to Solar Radiation*, Academic Press, New York, New York. ISBN 0-12-373750-8 (ISBN 0-12-373752-4 for paperback). 390pp.

Kiess, R.; Cox, W. (1988). *The AFGWC Automated Real-Time Cloud Analysis Model*, AFGWC/TN-88/001. Offutt AFB, NE: United States Air force, Air Weather Service, Air Force Global Weather Central. For more information contact the National Climatic Data Center, Asheville, NC 28801.

Marion, W. (1993). *Summary Information and Data Sets for NREL's Solar Radiation Research Laboratory, 1981-1991.* NREL/TP-463-5217. Golden, CO: National Renewable Energy Laboratory.

Marion, W. (1994). *Summary Information and Data Sets for the HBCU Solar Measurements Network.* NREL/TP-463-7090. Golden, CO: National Renewable Energy Laboratory.

Marion, W.; Urban, K. (1995). *User's Manual for TMY2s, Typical Meteorological Years Derived from the 1961-1990 National Solar Radiation Data Base.* NREL/SP-463-7668, DE95004064. Golden, CO: National Renewable Energy Laboratory.

Maxwell, E. (1995). "METSTAT - A Meteorological/Statistical Solar Radiation Model," Chapter 3, *National Solar Radiation Data Base (1961-1990), Final Technical Report, NSRDB-Volume 2.* Golden, CO: National Renewable Energy Laboratory. Available from the National Climatic Data Center, Asheville, NC 28801.

Myers, D.; Stoffel, T. (1989). "Uncertainty Estimates for Global Solar Irradiance Measurements Used to Evaluate PV Device Performance." *Solar Cells.* Vol. 27, pp. 455-465.

NREL (1992). *National Solar Radiation Data Base (1961-1990), User's Manual, NSRDB-Volume 1.* Golden, CO: National Renewable Energy Laboratory. Available from the National Climatic Data Center, Asheville, NC 28801.

NREL (1993). *Users Manual for SERI QC Software, Assessing the Quality of Solar Radiation Data.* NREL/TP-463-5608, DE93018210. Golden, CO: National Renewable Energy Laboratory.

NREL (1995). *National Solar Radiation Data Base (1961-1990), Final Technical Report, NSRDB-Volume 2.* Golden, CO: National Renewable Energy Laboratory. Available from the National Climatic Data Center, Asheville, NC 28801.

Stokes, G. M. and Schwartz, S.E. (1994). "The Atmospheric Radiation Measurement (ARM) Program: Programmatic Background and Design of the Cloud and Radiation Test Bed." *Bulletin of the American Meteorological Society* 75 (7); pp. 1201-1221.

Solar Data Processing Techniques

Tom Stoffel
National Renewable Energy Laboratory
1617 Cole Boulevard
Golden, Colorado 80401-3393

Abstract

The successful application of information available from a collection of solar radiation data is based equally on the efforts to operate and maintain a measurement station and to process the data. Solar radiation measurements must be obtained using adequate quality control methods as part of the routine operation and maintenance procedures. The resulting measured data must be processed to accomplish the necessary data quality assessment, archival, and reporting tasks. The focus of my paper is to introduce the solar data processing techniques used at the National Renewable Energy Laboratory (NREL). More detailed information is available from the references.

Introduction

Adequate processing of solar radiation data is as important as the efforts needed to collect the measurements. In this brief overview, I will describe the practices used at NREL to assess the quality, archive, report, and disseminate solar radiation data. Additionally, I will introduce a relatively new concept of using a relational database software system to help manage the operation of a network of solar measurement stations, including data processing methods.

Quality Control versus Quality Assessment

It is important to distinguish the conceptual differences between data quality *control* and data quality *assessment.* Quality control of solar radiation data involves those operational aspects leading to the recording of each measurement:

- Equipment selection criteria including the number and type(s) of measuring instruments, the measurement performance characteristics of the instruments and data acquisition system, and the ease of equipment installation.
- Equipment installation methods providing stable instrument mounting and proper alignments, unobstructed instrumentation fields of view, sufficient grounding and shielding practices, ease of access for maintenance, adequate security, and provisions for reliable and adequate electrical power and communication systems.
- Operation and maintenance practices documenting the frequency and manner of equipment maintenance, including regular recalibration of the radiometers and data acquisition system, recording of all maintenance activities, and reporting of same on a timely and regular basis.

Quality assessment of solar radiation data involves those efforts to evaluate the accuracy of the information after the measurement has been recorded:

- Manual inspections of the data such as graphical displays of time-series summaries and visual inspections of available station maintenance records.
- Automated tests and analyses based on a variety of computing methods.

The focus of my paper is on the post-measurement, quality assessment practices used at NREL for

processing solar radiation data.

Manual Methods of Data Quality Assessment

The timeliness of inspecting solar radiation data and reporting the findings to the measurement station operator(s) can be considered part of data quality control. The proper operation and maintenance of a solar measurement station is dependant on the early detection of suspect data and taking rapid corrective actions. At NREL, we rely on the ability to directly communicate with the data acquisition system on demand and the daily transmittal of measured data to a central computer system. We deploy data acquisition systems providing automatic data retrieval and storage diagnostic information. This allows us to inspect the station measurements nearly real-time, manually inspect daily time-series graphs of the component data, and review available diagnostic messages regarding the transmittal of measured data.

We are able to detect communication problems such as inoperable modems, telephone lines out of service, or computer system failures due to electrical power interruptions. Using the daily time-series graphs (see Figure 1), a trained inspector can identify improperly tracking pyrheliometers, misaligned shadowbands, or contaminated optical surfaces of the radiometers. This method is efficient for detailed inspections of data collected over a short (less than 1 week) period. Automated assessment techniques are more efficient for larger quantities of data.

Automated Method of Data Quality Assessment

SERI QC is a mathematical software package that assesses the quality of solar radiation data (NREL, 1993; Maxwell et al., 1995). This software was developed by the National Renewable Energy Laboratory when the Laboratory was called the Solar Energy Research Institute (SERI), hence the name *SERI QC*. The basis for this empirical approach to quality assessment is the combined application of physical limits, internal consistency (i.e., global irradiance is the sum of the diffuse irradiance and the vertical component of the direct normal irradiance elements), and the transformation of the irradiance elements into K-space, a normalization technique based on the extraterrestrial radiation value.

The transformation of irradiance data from power densities (eg. Watts per square meter) to K-space results in the normalization with respect to the corresponding extraterrestrial radiation (ETR). The following expressions are used to complete the transformation into K-space:

Kn	=	I_n / I_0	(direct beam transmittance)
Kt	=	$I_t / (I_0 \cos Z)$	(global horizontal transmittance)
Kd	=	$I_d / (I_0 \cos Z)$	(effective diffuse horizontal transmittance)
Kt	=	Kn + Kd	(physical consistency of the three elements)

where,

I_n	=	direct normal irradiance at the earth's surface
I_0	=	extraterrestrial direct normal irradiance
I_t	=	global (total) horizontal irradiance at the earth's surface
Z	=	solar zenith angle.

Hourly values of global and direct data collected for solar zenith angles less than 80° at Tallahassee, Florida from 1977 through 1980 are presented in K-space as Figure 2. Assuming the four years of data are representative of average conditions at Tallahassee, the dashed lines provide quality assessment boundaries. This represents almost a 50% reduction in the area of acceptability when using the usual physical limits of zero and the computed extraterrestrial irradiance (ETR). In

K-space, ETR equals 1.0. To refine the assessment, we use boundaries established for monthly data sets and for three air mass zones as shown in Table 1.

Table 1. Air Mass and Solar Zenith Angle Ranges for SERI QC

Range	Air Mass	Solar Zenith Angle
Low	1.00 - 1.25	0° - 36.96°
Medium	1.25 - 2.50	36.96° - 66.57°
High	2.50 - 5.76	66.57° - 80.00°

Mathematically, the boundaries of the data presented in K-space can be computed using the double exponential Gompertz Function:

$$Kn = AB^{CB^{DKt}}$$

where,

A = Kn asymptote
B = Kn inflection
C = Kt inflection
D = slope at the inflection point.

Coefficients are determined separately for the left and right boundaries of the data in K-space.

It is possible to correlate atmospheric conditions and/or equipment performance with the location of a measured data set presented in K-space. Data in regions A through E identified in Figure 3 can be associated with:

A - Clear-sky direct normal and global enhanced by cloud reflection/scattering
B - Clear-sky direct normal and global enhanced by cumuloform clouds
C - Upper portion indicates clear to low cloud amounts; middle portion is partly cloudy sky; and lower portion moderate cloud amounts
D - Moderate cloud amounts
E - Increasing clouds and possible high surface albedo.

Data in regions A and B correspond to relatively short-lived phenomena. Hourly data are rarely observed in these regions. Data collected from a pyrheliometer mounted in a misaligned solar tracker misalignment and/or obscured optics lie to the left of region E (high global, low direct). Contaminated optics or other pyranometer measurement problems result in data above region C but below the 1:1 line (high direct, low global).

SERI QC establishes the site-specific Gompertz coefficients and computes a data quality "flag" value for each measurement. A 2-digit flag indicates the direction and amount of departure from the expected region of data.

Data Archival

Proper storage of measured data significantly enhances the opportunities for its future application. Archival should include the raw measurements, the results of standardized quality-assessment evaluation(s), and pertinent information about how and where the data were acquired. The information should be stored on digital, rather than analog, media to reduce the labor needed to

evaluate large data sets now possible with modern data acquisition systems.

The *Standard Broadband Format* (NREL, 1988) provides the following benefits:

1. Easily readable to computers - fixed record length of 80 characters, adjustable blocking factors based on the number of instruments and data frequency.
2. Easily readable to users - display fits on monitor screen, descriptive text in header records, and logical time spacing of data display.
3. Includes all basic information about the data - location, collection frequency, units of measure, data quality assessment results, and supporting information in footnotes.

Data Dissemination

The true value of any scientific study can be realized only when the information is made available to the widest possible range of users. Historically, this has been limited to peer-reviewed articles in professional journals or internal publications of the sponsoring agency. At NREL, these methods of information dissemination have been joined by the recent addition of our *Renewable Resource Data Center (RReDC)* (Gardner and Rymes, 1995).

The RReDC is managed by the Resource Assessment Program at NREL under contract to the U.S. Department of Energy. This data center is accessible with a World Wide Web browser on the Internet (http://rredc.nrel.gov) and offers the following renewable energy resource information: Historical data sets, technical publications, resource distribution maps, and related technical information. User registration and feedback are also available to improve the usefulness of future RReDC developments.

Data Quality Management

To meet the needs for managing the data from various solar radiation measurement programs at NREL and to build on existing software developed for a similar purpose, NREL has recently concluded a subcontracting effort with Augustyn + Company to develop the *Data Quality Management System (DQMS).* The functional aspects of this relational data base software system are shown in Figure 4 and include the principal data manipulations: Import, quality assessment or testing, display (tables and graphs), modification (filling missing data, adjusting data for calibration drifts, etc.), reporting, and archival. The advantages of applying a relational data base management system are fully applied by the DQMS, including the organization of information about instrument calibrations, station maintenance and operation activities, and data quality. Examples of DQMS screens for establishing measurement station and record definition tables are presented in Figure 5.

References

Gardner, T.; Rymes, R. (1995). "Products Available From NREL's Renewable Resource Data Center," *Proc. of the 1995 American Solar Energy Society Annual Conference, SOLAR '95, July 15-20, 1995, Minneapolis,*. R. Campbell-Howe and B. Wilkins-Crowder (ed). pp. 210-215. Boulder, CO: American Solar Energy Society.

Maxwell, E.; Wilcox, S.; and Rymes, M. (1995). "Quality Assessment/Control of NSRDB Solar Radiation Data," Chapter 2, *National Solar Radiation Data Base (1961-1990), Final Technical Report, NSRDB-Volume 2.* Golden, CO: National Renewable Energy Laboratory. Available from the National Climatic Data Center, Asheville, NC 28801.

NREL (1988). *SERI Standard Broadband Format, A Solar and Meteorological Data Archive Format.* SERI/SP-320-3305, DE88001145. Golden, CO: National Renewable Energy Laboratory.

NREL (1993). *Users Manual for SERI QC Software, Assessing the Quality of Solar Radiation Data.* NREL/TP-463-5608, DE93018210. Golden, CO: National Renewable Energy Laboratory.

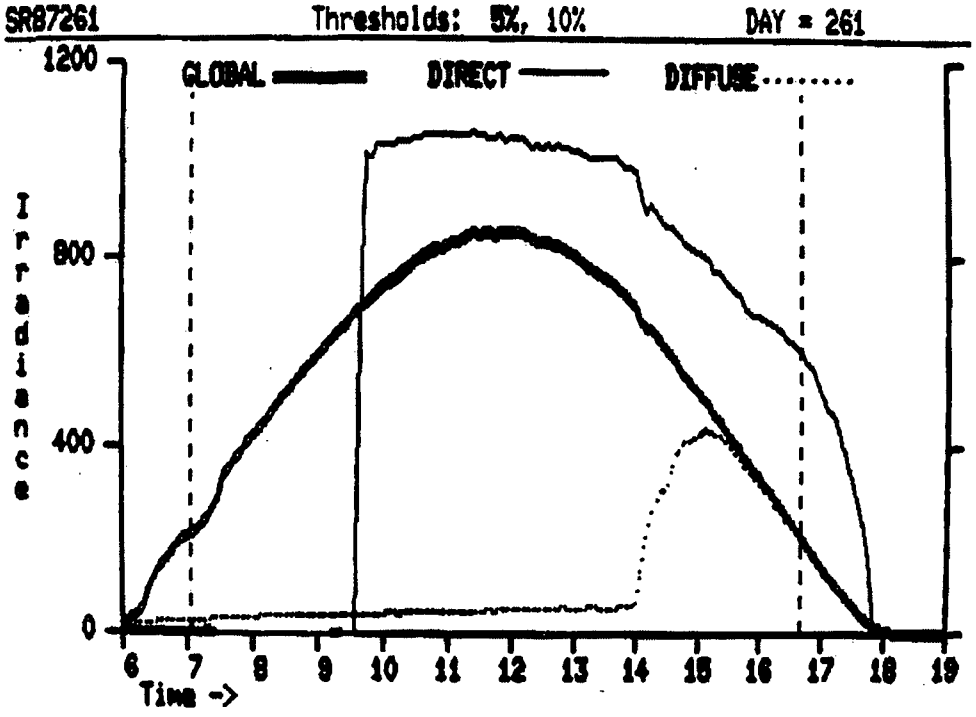

Figure 1. Time-series graph of direct normal, diffuse horizontal, and global irradiance. (Note solar tracker realigned at 09:30 and shadowband failure at 14:00)

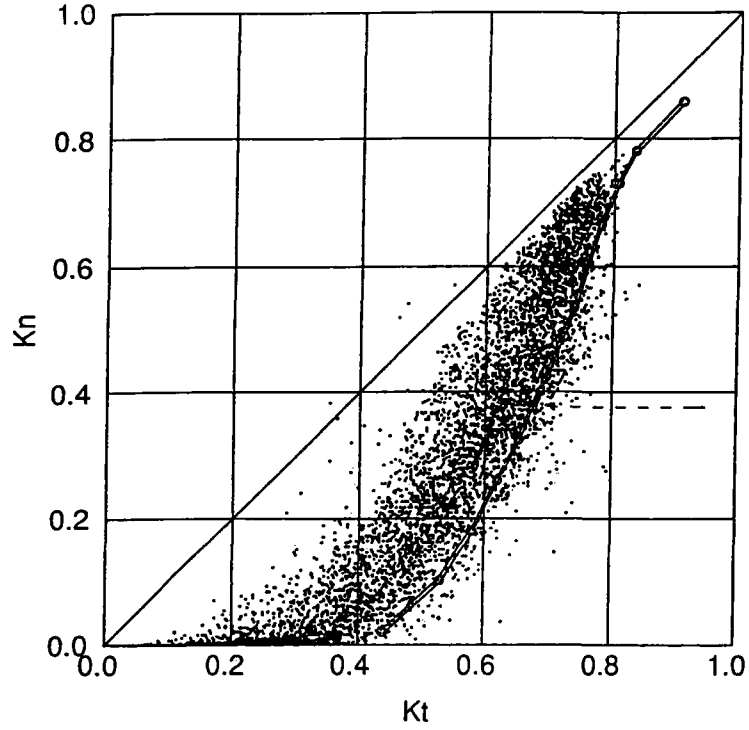

Figure 2. K-space scatter plot of hourly solar radiation data collected at Tallahassee, Florida. (1977 through 1980)

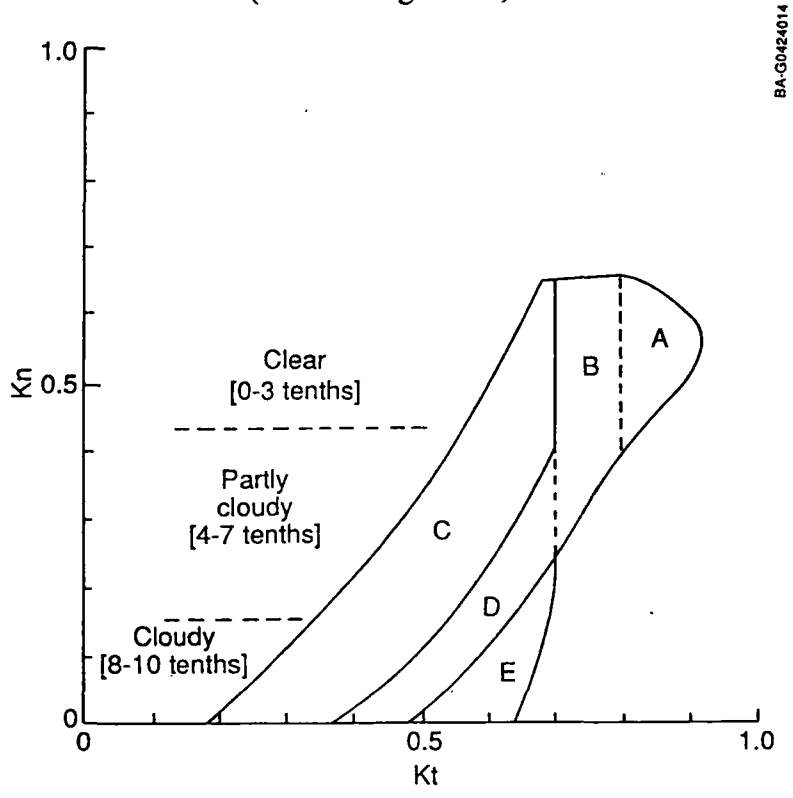

Figure 3. Regions in K-space that correspond to known atmospheric conditions.

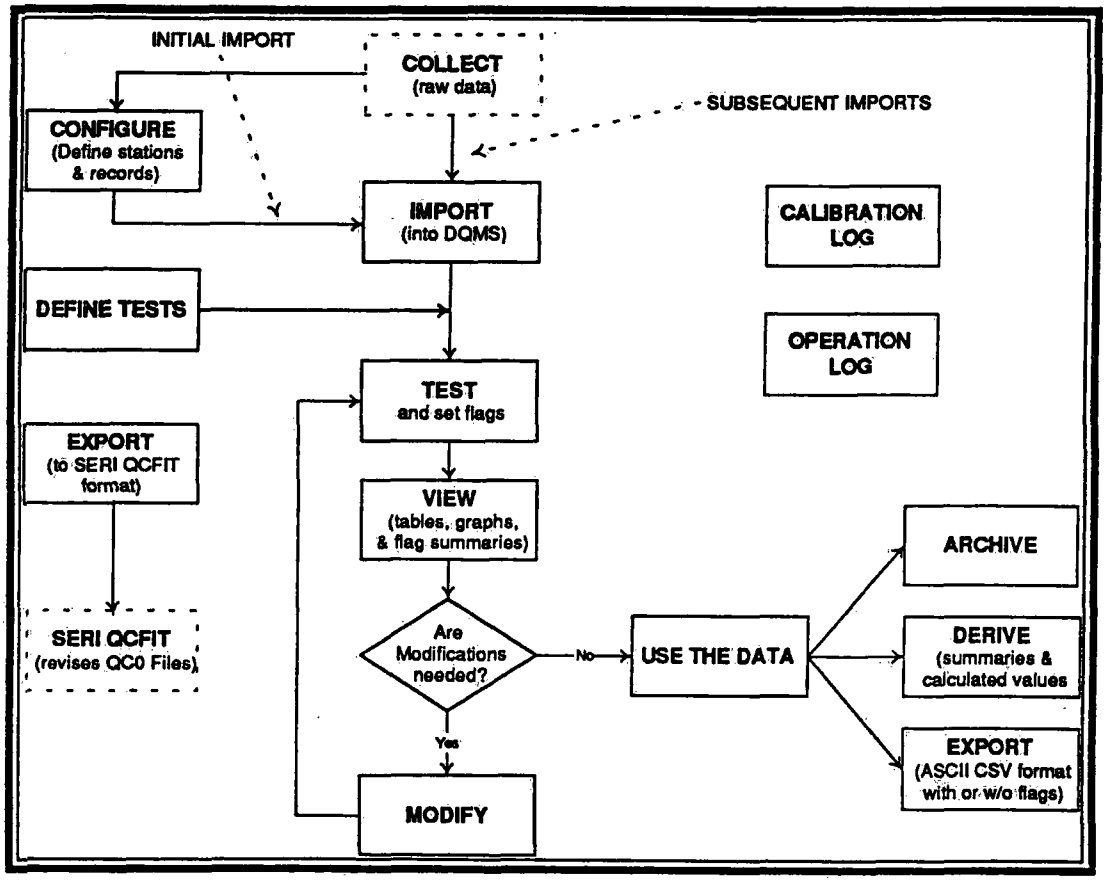

Figure 4. Main DQMS Functions--Process Flow Diagram.

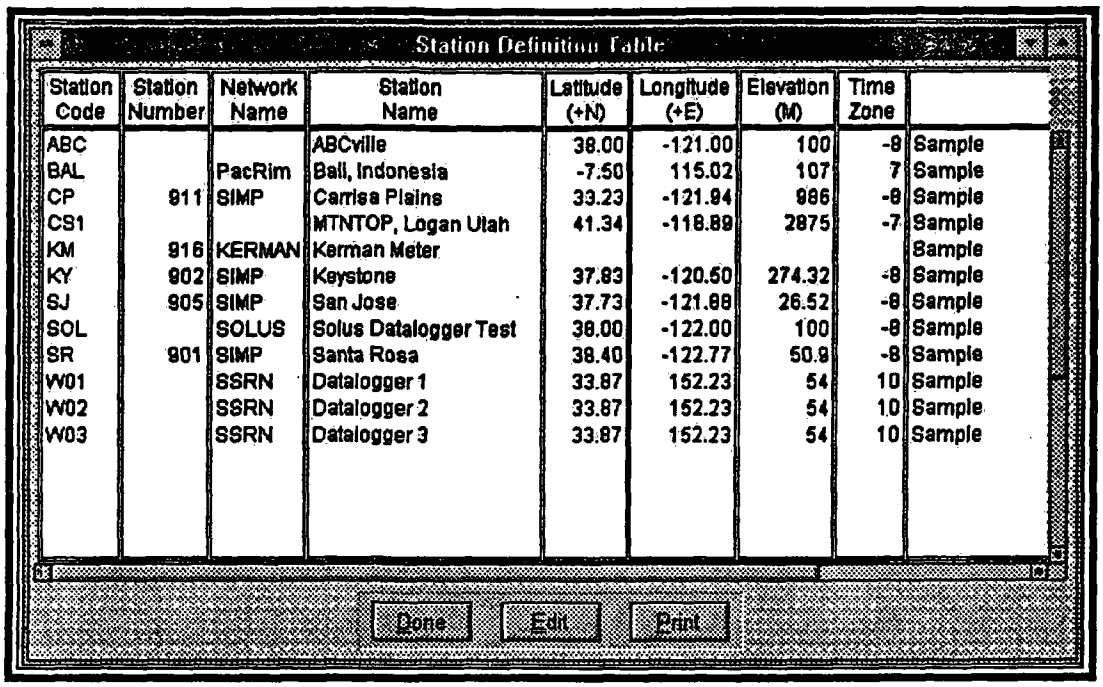

Station Definition Table

Station Code	Station Number	Network Name	Station Name	Latitude (+N)	Longitude (+E)	Elevation (M)	Time Zone	
ABC			ABCville	38.00	-121.00	100	-8	Sample
BAL		PacRim	Bali, Indonesia	-7.50	115.02	107	7	Sample
CP	911	SIMP	Carrisa Plains	33.23	-121.94	986	-8	Sample
CS1			MTNTOP, Logan Utah	41.34	-118.89	2875	-7	Sample
KM	916	KERMAN	Kerman Meter					Sample
KY	902	SIMP	Keystone	37.83	-120.50	274.32	-8	Sample
SJ	905	SIMP	San Jose	37.73	-121.88	26.52	-8	Sample
SOL		SOLUS	Solus Datalogger Test	38.00	-122.00	100	-8	Sample
SR	901	SIMP	Santa Rosa	38.40	-122.77	50.9	-8	Sample
W01		SSRN	Datalogger 1	33.87	152.23	54	10	Sample
W02		SSRN	Datalogger 2	33.87	152.23	54	10	Sample
W03		SSRN	Datalogger 3	33.87	152.23	54	10	Sample

Done Edit Print

Figure 5a. DQMS Station Definition Table.

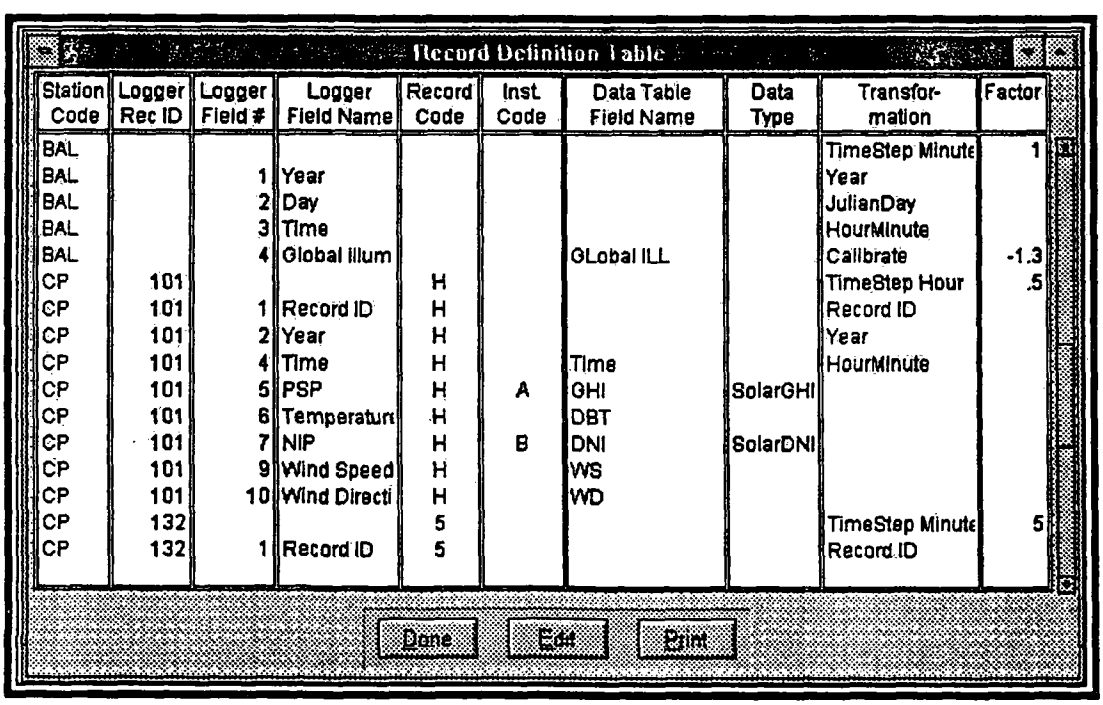

Record Definition Table

Station Code	Logger Rec ID	Logger Field #	Logger Field Name	Record Code	Inst. Code	Data Table Field Name	Data Type	Transfor-mation	Factor
BAL								TimeStep Minute	1
BAL		1	Year					Year	
BAL		2	Day					JulianDay	
BAL		3	Time					HourMinute	
BAL		4	Global illum			GLobal ILL		Calibrate	-1.3
CP	101			H				TimeStep Hour	.5
CP	101	1	Record ID	H				Record ID	
CP	101	2	Year	H				Year	
CP	101	4	Time	H		Time		HourMinute	
CP	101	5	PSP	H	A	GHI	SolarGHI		
CP	101	6	Temperatur	H		DBT			
CP	101	7	NIP	H	B	DNI	SolarDNI		
CP	101	9	Wind Speed	H		WS			
CP	101	10	Wind Directi	H		WD			
CP	132			5				TimeStep Minute	5
CP	132	1	Record ID	5				Record ID	

Done Edit Print

Figure 5b. Record Definition Table.

Absolute Cavity Radiometer Comparisons at NREL

Tom Stoffel
National Renewable Energy Laboratory
1617 Cole Boulevard
Golden, Colorado 80401-3393

Abstract

Results are summarized from comparisons of absolute cavity radiometers at NREL's Solar Radiation Research Laboratory in 1993 and 1994. The benefits of conducting such comparisons are summarized. The data collection protocol and analyses are described for the comparison of fourteen radiometers in 1993 and twenty radiometers participating in 1994.

Introduction

Fundamental to all solar radiation instrument calibrations is the need for a common reference or system of measurement. The World Radiometric Reference (WRR) was developed and is maintained by the World Radiation Center. Radiometer calibration traceability at the National Renewable Energy Laboratory (NREL) is based on direct access to the WRR through a number of absolute cavities which have participated in the regular Internation Pyrheliometer Comparisons (IPCs) at the Center. Several solar radiation measurement programs funded by the U.S. Department of Energy benefit from NREL's abilities to provide radiometer calibrations traceable to the WRR (See Figure 1). The purpose of this paper is to summarize two comparison events used to maintain this capability and transfer the calibration reference to solar measurement programs.

Benefits of Comparisons

In addition to providing radiometer calibration traceability to the WRR, there are several other reasons to regularly compare absolute cavity radiometers. A well-designed solar measurement program is typically based on the ability to calibrate field instruments using a set of reference standard radiometers. Regular comparisons of these reference instruments provides for:

- Documenation of reference instrument performance
- Development of measurement performance histories
- Continued operator training and proficiency checks
- Opportunities to conduct measurement research.

Data Collection

Comparisons of fourteen absolute cavity radiometers were completed in September/October 1993 and twenty cavities participated during the same period in 1994 at NREL's Solar Radiation Research Laboratory. Data were collected during at least three days with clear sky conditions using the following protocol:

- Equipment setup - Radiometer systems stored indoors for protection
- System warmup - Minimum of 30 minutes for thermal stabilization
- Pre-run calibration - Following electrical self-calibration procedures
- Data collection (Run) - 31 instantaneous readings at 20 second intervals (oral signal)
- Post-run calibration - Following electrical self-calibration procedures
- Repeat - For up to 15 "Runs" under cloudless sky conditions
- Equipment shutdown - Prepare system for indoor storage until next clear day.

Data collection for both of the comparisons at NREL's Solar Radiation Research Laboratory (SRRL) involved cavity systems operated manually and under computer control. The data flow summarized in Figure 2 indicates the various paths used to assemble a singe database for analysis. Data were collected by selected instruments with a protective quartz window installed at times.

Data Analysis

The basis for each comparison event is formed by computing the reference irradiance for each measurement "reading" (31 readings per "run"). The reference irradiance is computed from the weighted average of those absolute cavity radiometers having a history of participation in the IPCs and, therefore, direct calibration traceability to the WRR. Absolute cavity radiometers belonging to NREL, the National Oceanic & Atmospheric Administration, and the Eppley Laboratory, Inc. formed the reference group for both comparisons reported here. The weighting factors used to compute the reference irradiance are proportional to the estimated measurement uncertainty of the individual cavity radiometer. The uncertainty estimates are based on the random and bias errors attributed to each cavity and includes the propagation of the uncertainty associated with the individual WRR factor assigned to the instrument. The stated accuracy of the WRR (0.3%) is also part of the uncertainty estimate.

Window correction factors were also computed using data from selected cavity radiometers alternately collected with and without a protective quartz window. The windows were installed only for complete runs.

Results

Example data from Automated Hickey-Frieden absolute cavity radiometers collected during the comparisons in 1993 are presented as Figure 3. Window correction factors computed from such data were typically 1.070 ± 0.009. The data from all participating instruments, no windows installed, were generally within $\pm 0.5\%$ of the mean value for each reading and the run averages.

The results of the 1994 comparisons are presented in Table 1. Comparisons are made for selected instruments with and without protective quartz windows. For these data, the transfer of the WRR was made using the average of four cavity radiometers with direct calibration traceability to the WRR (s/n AHF-14915, TMI-67502, TMI-68018, and TMI-69036). The mean ratio of each reference cavity to the mean of the group was 0.999927 ± 0.000332[1]. Similarly, the mean ratio of the instruments under test to the reference group mean was 1.001575 ± 0.002089 (for Hickey-Frieden models) and 0.999960 ± 0.000486 (for Technical Measurements, Inc. Mark VI models). The performance of a single cavity radiometer during the 3-day comparisons is shown in Figure 4.

Acknowledgements

Graphical summary analyses of the data shown in this paper were created by Don Nelson at the National Oceanic and Atmospheric Administration's Climate Monitoring and Diagnostic Laboratory and by David Clair at the National Renewable Energy Laboratory.

[1] Range indicated by 1 x standard deviation.

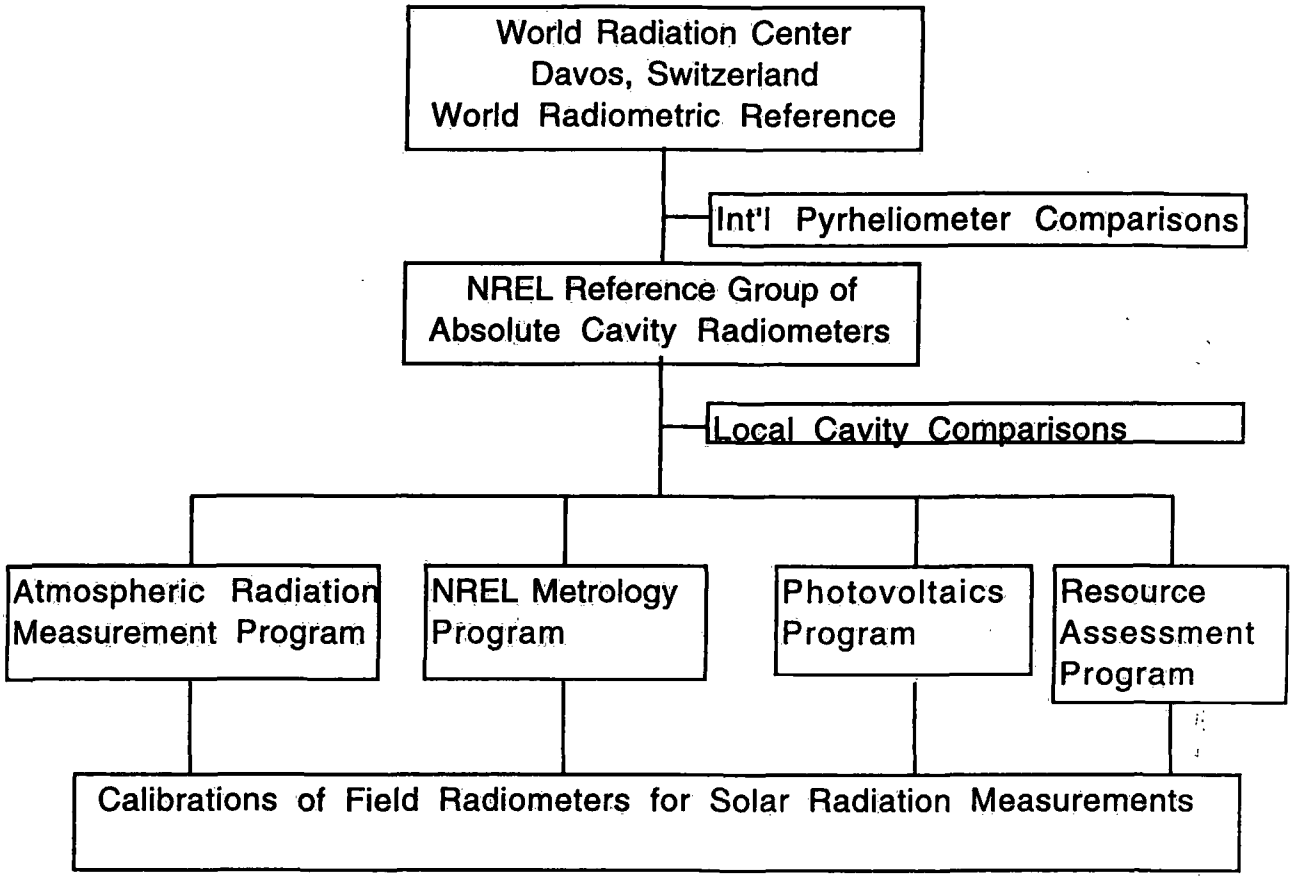

Figure 1. Solar Radiation Measurement Calibration Traceability at NREL

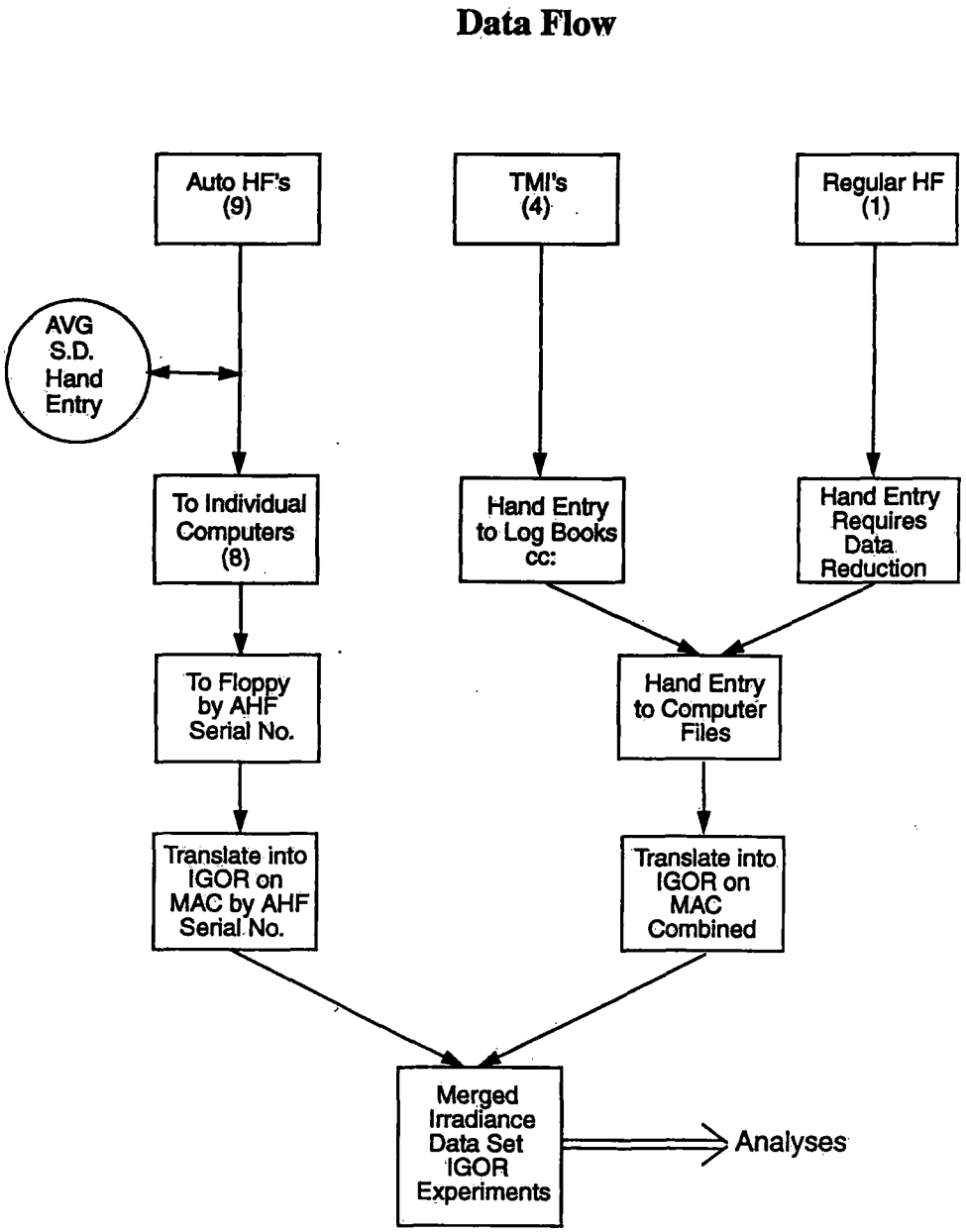

Figure 2. Data collection flow diagram for absolute cavity comparisons at SRRL

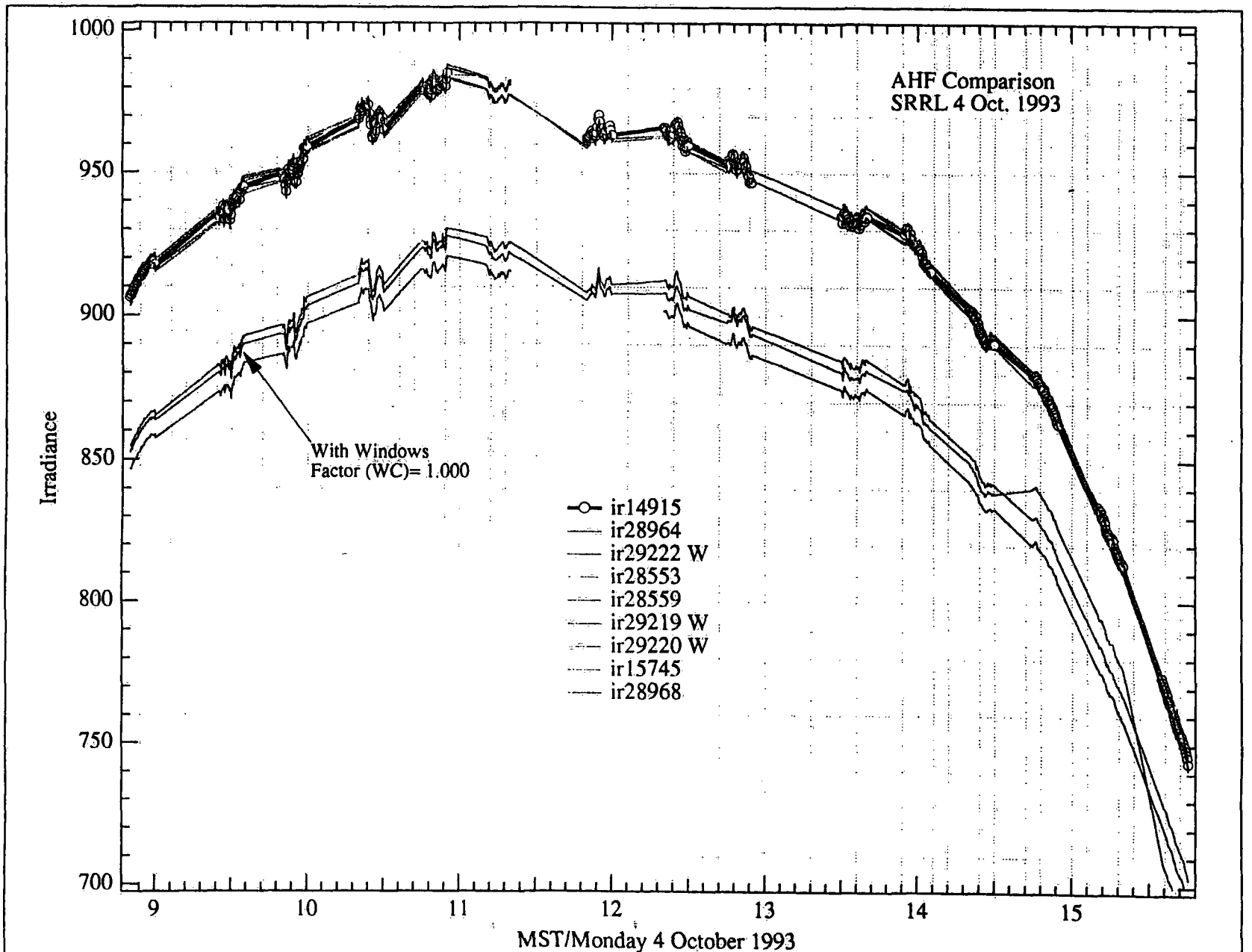

Figure 3. Example of AHF data collected on 4 October 1993 comparing instruments with and without protective windows.

Table 1. Summary Results

Results Of ARM Cavity Comparison Held October 8-10, 1994

	For Measurements Without A Window								For Measurements With A Window							
	Ratio To Reference Irradiance			New WRR Factor					Ratio To Reference Irradiance			New WRR Factor				
	Average	Uncertainty		Average	Uncertainty With Respect To WRR				Average	Uncertainty		Average	Uncertainty With Respect To WRR			
	Ratio	Std. Dev.	d. f.	Factor	Bias	Random	U99	U99 With Respect To SI Units	Ratio	Std. Dev.	d. f.	Factor	Bias	Random	U99	U99 With Respect To SI Units
Cavities In Reference Group																
AHF 14915	0.999522	0.000387	1226	---	---	---	---	---	---	---	---	---	---	---	---	---
TMI 67502	0.999793	0.001067	389	---	---	---	---	---	---	---	---	---	---	---	---	---
TMI 68018	1.000144	0.000273	1226	---	---	---	---	---	---	---	---	---	---	---	---	---
TMI 69036	1.000247	0.000292	1226	---	---	---	---	---	---	---	---	---	---	---	---	---
Other Cavities																
AHF 15745	0.997720	0.000495	389	1.002286	0.000241	0.000497	0.001236	0.004004	---	---	---	---	---	---	---	---
HF 28552	1.002257	0.000742	464	0.997753	0.000207	0.000753	0.001712	0.004512	---	---	---	---	---	---	---	---
AHF 28553	1.003156	0.000422	712	0.996854	0.000207	0.000420	0.001047	0.003847	---	---	---	---	---	---	---	---
AHF 28964	1.002174	0.000389	141	0.997831	0.000209	0.000387	0.000984	0.003782	---	---	---	---	---	---	---	---
AHF 28968	0.999291	0.000540	1226	1.000709	0.000197	0.000541	0.001280	0.004089	---	---	---	---	---	---	---	---
AHF 29220	1.001618	0.000635	924	0.998385	0.000198	0.000633	0.001463	0.004272	0.945814	0.000483	265	1.057290	0.000198	0.000540	0.001278	0.004087
AHF 29222	1.000343	0.000653	650	0.999658	0.000182	0.000652	0.001486	0.004310	0.933076	0.002144	278	1.071730	0.000182	0.002462	0.005106	0.007929
AHF 29226	1.003891	0.000504	1193	0.996124	0.000159	0.000500	0.001159	0.004004	---	---	---	---	---	---	---	---
AHF 29227	1.003725	0.000411	1157	0.996289	0.000169	0.000408	0.000985	0.003821	---	---	---	---	---	---	---	---
TMI 67603	1.000104	0.000489	836	0.999896	0.000163	0.000489	0.001140	0.003982	---	---	---	---	---	---	---	---
TMI 67811	0.999761	0.000463	743	1.000239	0.000163	0.000463	0.001088	0.003930	---	---	---	---	---	---	---	---
TMI 68017	0.999921	0.000393	1195	1.000079	0.000169	0.000393	0.000955	0.003791	---	---	---	---	---	---	---	---
TMI 68020	1.000670	0.000328	327	0.999330	0.000183	0.000327	0.000838	0.003660	---	---	---	---	---	---	---	---
TMI 68022	0.999344	0.000917	836	1.000657	0.000163	0.000918	0.001999	0.004841	---	---	---	---	---	---	---	---

Analysis Of Ratios For Cavities In Ref. Group	
Mean	0.999927
Std. Dev.	0.000332

Analysis Of Ratios For Cavities Without Windows & Not In Ref. Group		
	HF/AHF	TMI
Mean	1.001575	0.999960
Std. Dev.	0.002089	0.000486

Analysis Of Ratios For Cavities With Windows & Not In Ref. Group		
	HF/AHF	TMI
Mean	0.939445	---
Std. Dev.	0.009008	---

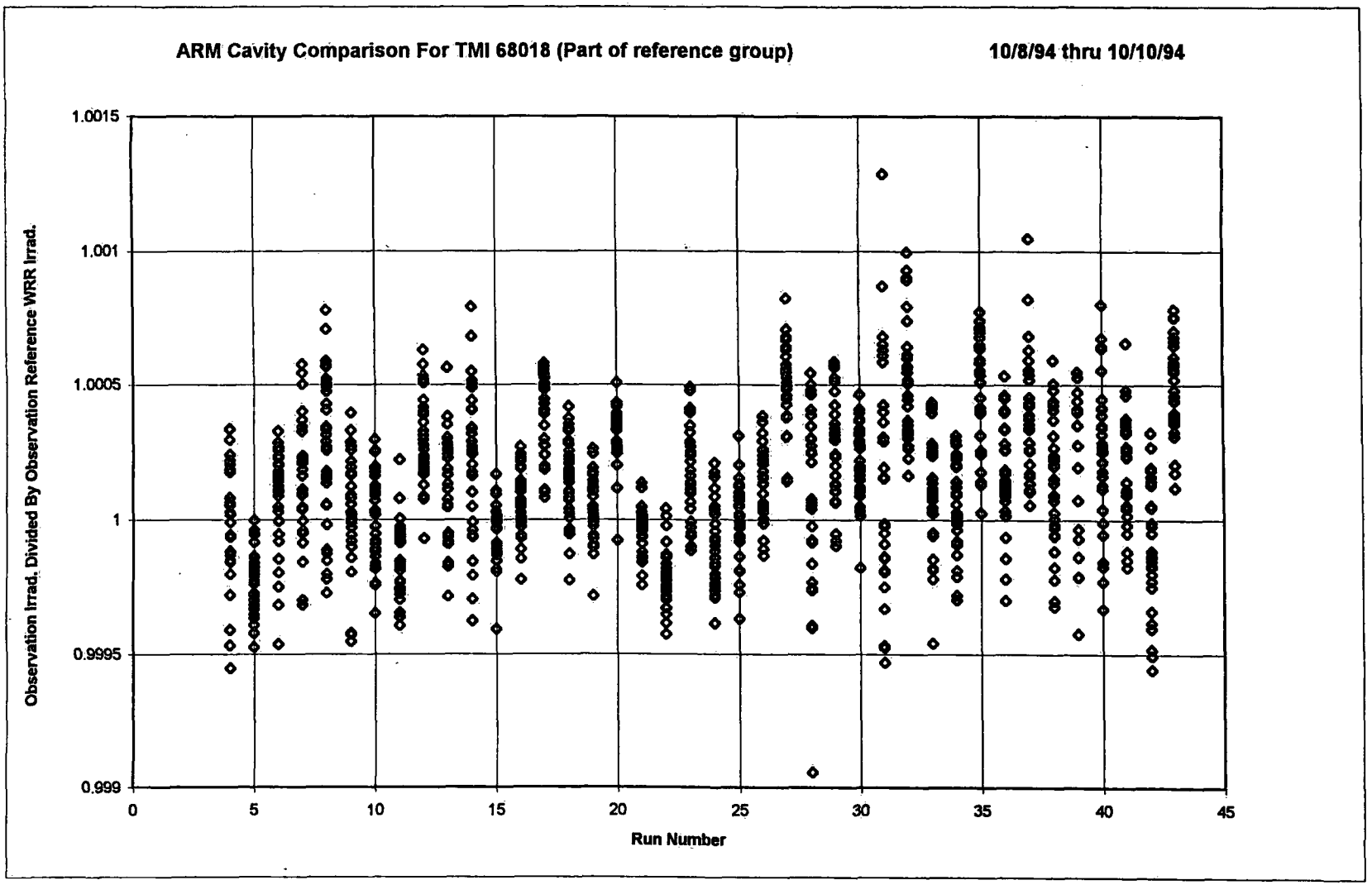

Figure 4. Measurement performance of Technical Measurements, Inc. Model MK VI cavity radiometer serial number 68018 for all data collected during 1994 comparisons based on the average irradiance computed from the reference group.

Characterization of Pyranometer in JMA

HIROSE Yasuo
Observations Division, Observations Department
Japan Meteorological Agency, Tokyo

Introduction

Pyranometer calibration in the Japan Meteorological Agency(JMA) has been carried out by outdoor comparison with reference pyranometer under global solar radiation. The main purpose of pyranometer characterization in JMA is to make accurate measurement of global solar irradiance as the calibration reference by applying characteristics correction to the reference pyranometer. Systematic procedures and the apparatuses used for the characterization are detailed in [1].

In this paper a complement to [1], some results of long-term comparison showing how the characteristics correction works, and an unresolved problem are presented.

Instrument Equations

The instrument equations employed for the characterization and the characteristics correction of pyranometer are as follows:

pyranometer

$$V = k0 \cdot h(t,a) \cdot a \qquad (1)$$

$$a = g(z, \phi) \cdot S \cdot \cos z + U \cdot Ed \qquad (2)$$

$$Eg = S \cdot \cos z + Ed \qquad (3)$$

where

V: output of instrument, **t**: body temperature of instrument,
S: direct solar irradiance, **Ed**: diffuse solar irradiance,
Eg: global solar irradiance,
(z, ϕ): direction of direct solar radiation,
(z', ϕ'): direction of diffuse solar radiation,
$h(t,a)$: thermal response of instrument; $h(t0,a0) \equiv 1$,
k0: responsivity of instrument at $t=t0$, $a=a0$,
$g(z, \phi)$: directional response of instrument; $g(0, *) \equiv 1$,
U: mean directional response for diffuse solar radiation; defined as follows, assuming uniform radiance through hemisphere:

$$U = \int \Omega \, g(z', \phi') \cdot \cos z' \cdot d\Omega \; / \; \pi \qquad (4)$$

As the ratio of diffuse irradiance to global irradiance varies depending on the sky conditions, the directional response of pyranometer can not be corrected using single instrument of pyranometer even if the characterization of pyranometer has completed. For the correction of directional response of pyranometer, diffuse or direct component must be separated from global radiation by using the combination of, for example, a pyranometer and a pyrheliometer, or a pyranometer and a diffusometer, etc. The instrument equations of those are as follows:

pyrheliometer

$$V = k0 \cdot h(t,S) \cdot S \qquad (5)$$

diffusometer

$$V = k0 \cdot h(t,a) \cdot a \qquad (6)$$

$$a = U \cdot Ed \qquad (7)$$

Though the parameter **U** is a compromised quantity, it is useful in correcting the directional response, especially in case of pyranometer having a large directional response, as shown in [2].

Comparisons

Some results of long-term comparisons between characterized pyranometers are shown in **Fig.1**. The instruments **PSP25918F3(EPPLEY)** and **F83006(EKO)** were continuously calibrated against the calibration reference pyranometer **F85035(EKO)** in **1993-1994**. In the figure dotted marks represent actual calibration factors obtained at each calibration series. The continuous curves are calculated responsivities for various sky conditions of **F (=Ed/Eg)**, assuming the normal irradiance and air temperature at the calibration site Tsukuba. The responsivity of the calibration reference was the mean value of **F=0.3,0.5**, and **0.7**, and changed every day along its calculated responsivity curves through seasons. As seen in the figure actual values agree very well with calculated values, which suggests a good consistency of the characterization in these cases.

Problem unresolved

There are another results of comparisons exampled in **Fig.2**. In this case the calculated responsivities seem to be about 0.6 % higher than actual calibration factors at each calibration series. The discrepancy might originate from the uncertainty in the responsivity **k0**, as shown in **Fig.3**, which is determined by comparison with windowless absolute pyrheliometer using collimation tube. The effect of the fluctuation of the IR part of direct solar radiation at collimation tube comparison should be examined as one of the possibilities[3].

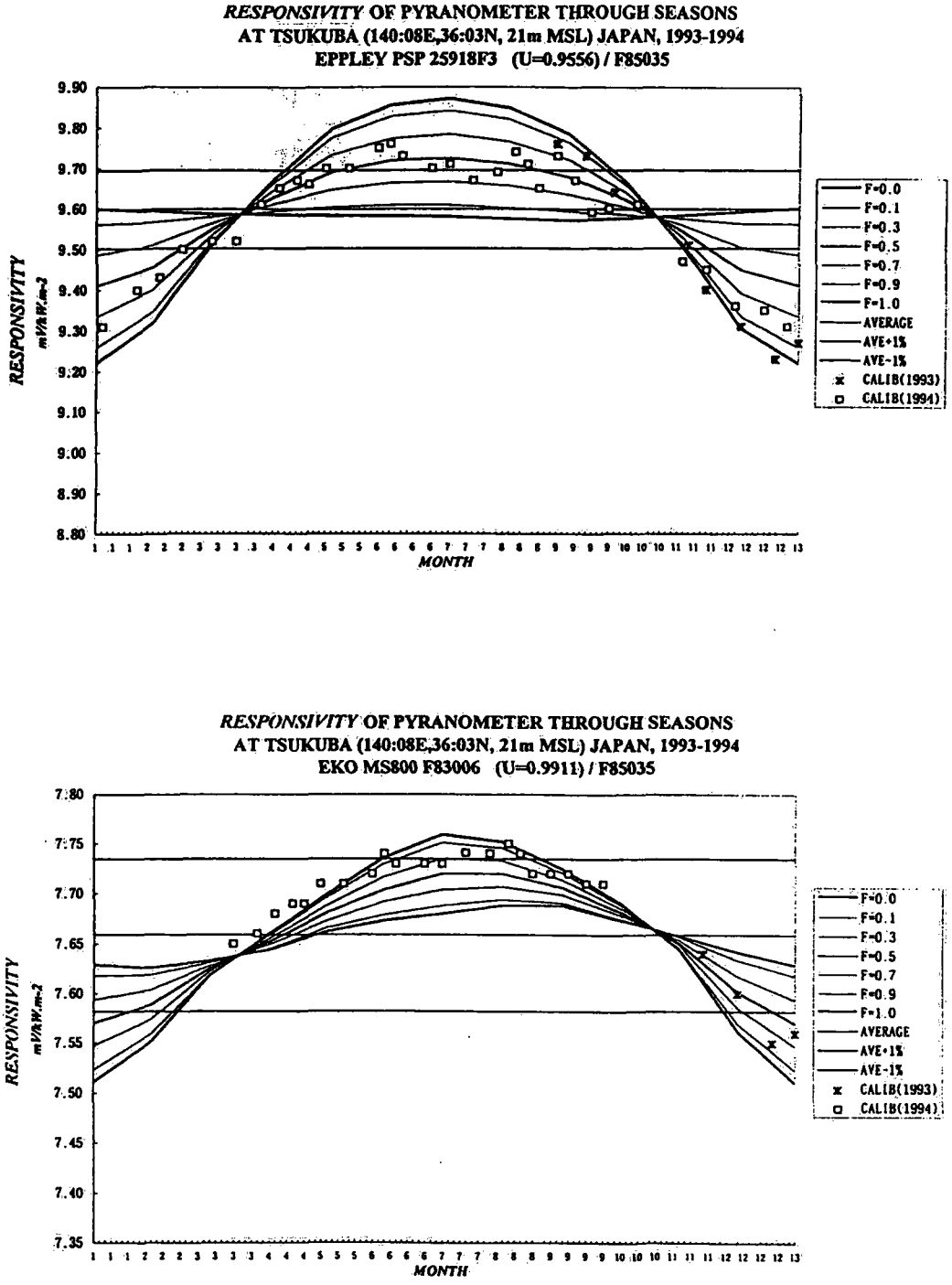

Fig.1 Examples of long-term comparisons between characterized pyranometers. In case of PSP25918F3 calibration factors seem to be corresponding to clear winter(November-February) and cloudy summer(June-August).

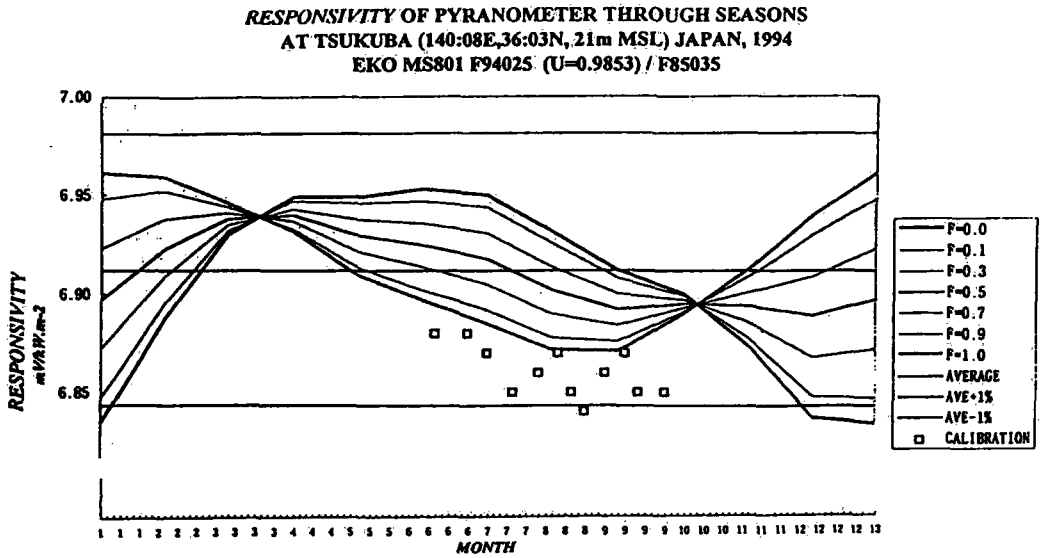

Fig.2 Example of long-term comparisons showing a discrepancy between calculated values and actual calibration factors.

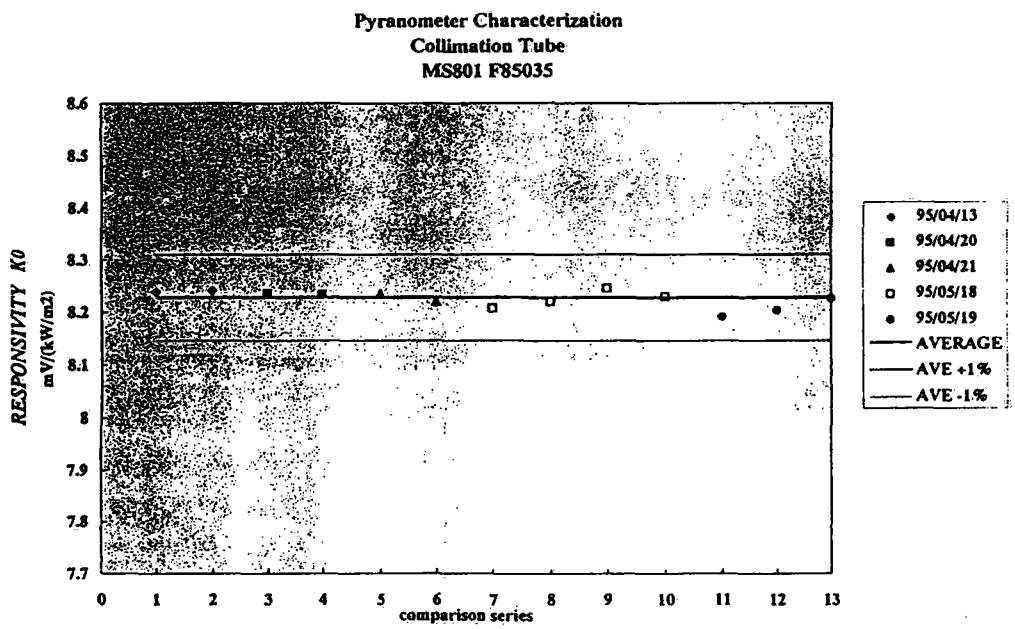

Fig.3 Uncertainty of collimation tube comparison. The fluctuation of **k0** amounts up to about 0.7 % of the mean value.

References

[1] HIROSE,Y(1994);Determination of Genuine Directional Characteristics of Pyranometer, Instruments and Observing Methods Report No. 57(TECO-94), WMO/TD-No.588.

[2] HIROSE,Y(1986);On the Trial of Calculating Global Solar Irradiance in Consideration of the Characteristic Functions of Pyranometer, Japan J.Met.Res.,vol.38,No.3.

[3] Fröhlich,C(1995);Meteorological Radiation Quantities and History of Radiation Measurements, IPC VIII Davos 1995.

NOAA CLIMATE MONITORING & DIAGNOSTICS LABORATORY (CMDL) SURFACE RADIATION MONITORING SITES

OCTOBER 1995

Currently, the CMDL operates seven solar & thermal radiation monitoring sites. The seven sites are listed below.

- Barrow Alaska (BRW)
- Mauna Loa Observatory, Hawaii (MLO)
- Cape Matatula, American Samoa (SMO)
- South Pole, Antarctica (SPO)
- Kwajalein Atoll (KWJ)
- Bermuda (BER)
- Boulder Atmospheric Observatory (BAO, 300m tower)

Four of the seven sites represent the original NOAA GMCC baseline observatory network which date from the early 1970's. These sites are Barrow Alaska, Mauna Loa Hawaii, Tutuila Island American Samoa, and the Clean Air Facility at South Pole Station Antarctica. The United States National Science Foundation established and maintains the South Pole Station and the CMDL presence is one of many scientific programs which operate there with NSF permission and support. Three other monitoring sites have been added during the past decade: the BAO, Kwajalein and Bermuda. Data from all sites are acquired on a daily basis and processed in Boulder.

CMDL BASELINE SITE SURFACE BROADBAND INSTRUMENTATION

- Pyranometers
- Pyrheliometers
- Pyrgeometers (BRW, MLO, SPO, KWJ, BER, BAO)
- Filters (695nm: BRW, MLO, SMO, SPO, BAO)
- Diffuse (tracking disk at BAO, BRW, SPO, MLO, SMO)
- Cavity AHF #30499 (MLO)
- Net SW/LW (BRW,SPO,BAO)

Five the the seven CMDL monitoring locations are also designated BSRN, and the data from these sites are processed for submission to the BSRN archive. The five BSRN sites are Barrow, Kwajalein, Bermuda, BAO, and South Pole.

CMDL BSRN SITE BROADBAND INSTRUMENTATION

- Pyranometers
- Pyrheliometers
- Pyrgeometers (BRW, SPO, KWJ, BER, BAO)
- Filters (695nm: BRW, SPO, BAO)
- Diffuse (tracking disk at BAO, BRW, SPO)
- Net SW/LW (BRW,SPO,BAO)

SOLAR RADIATION CALIBRATION FACILITY(SRCF)

Operational support, sensors, and sensor calibration for the CMDL surface radiation monitoring sites is provided by the CMDL Solar Radiation Calibration Facility. The NOAA Solar Radiation Calibration Facility (SRCF) in Boulder Colorado dates from 1975, when its functions were transferred fron NOAA National Weather Service in Silver Spring Maryland to Boulder. Since 1990, when the NOAA Climate Monitoring and Diagnostics Laboratory (CMDL) was created, the Solar Radiation Facility has resided within the CMDL organization as part of the Solar & Thermal Atmospheric Radiation (STAR) group. Dr. Ellsworth Dutton is the group chief. The functions of the SRCF

- Calibrations/Characterizations of CMDL sensors
- Calibration/Characterization for other labs/research groups
- Calibration/Characterization Development
- Development of operational solar radiation monitoring products

GEF/GAW BASELINE STATIONS

In addition to the suppport for the complement of monitoring sites described above, the CMDL SRCF in collaboration with the WMO has assisted in the establishment of solar radiation monitoring capability at four baseline sites which are part of the Global Atmosphere Watch. The CMDL purchased instrumentation, constructed data acquisition and data archiving hardware and software, trained personnel and assisted in installation at four sites listed below:

- Algeria (Tamanrasset)
- China (Waliguan)
- Argentina (Tierra del Fuego)
- Indonesia (Sumatra)

During 1994, personnel from each of the four countries, Algeria, China, Argentina and Indonesia spent four weeks each in Boulder learning how to install, operate and calibrate the solar sensors purchased for each site as well as data examination and archival. All equipment for each site was assembled, tested, calibrated and installed in a test configuration and operated in a manner consistent with planned site installations. This experience enabled each participant to successfully return home and install the system at their site and begin monitoring operations. A feature of these Baseline GAW solar monitoring sites is that each site was equipped with an automated cavity system and the personnel were trained to use the cavity as a tool to maintain their own instrment calibrations. As solar radiation twinning partner to the GEF/GAW baseline sites, CMDL will continue collaboration with these GAW baseline sites with the hope that these sites will become contributors to the current worlwide network of high quality surface radiation monitoring sites.

GEF/GAW BASELINE SITE SURFACE BROADBAND INSTRUMENTATION

- Pyranometers
- Pyrheliometers
- Filters (695nm)
- Diffuse (shadowband)
- Cavity Radiometer

Figure 1 illustrates the current locations of the CMDL solar radiation monitoring sites as well as the GEF/GAW baseline sites.

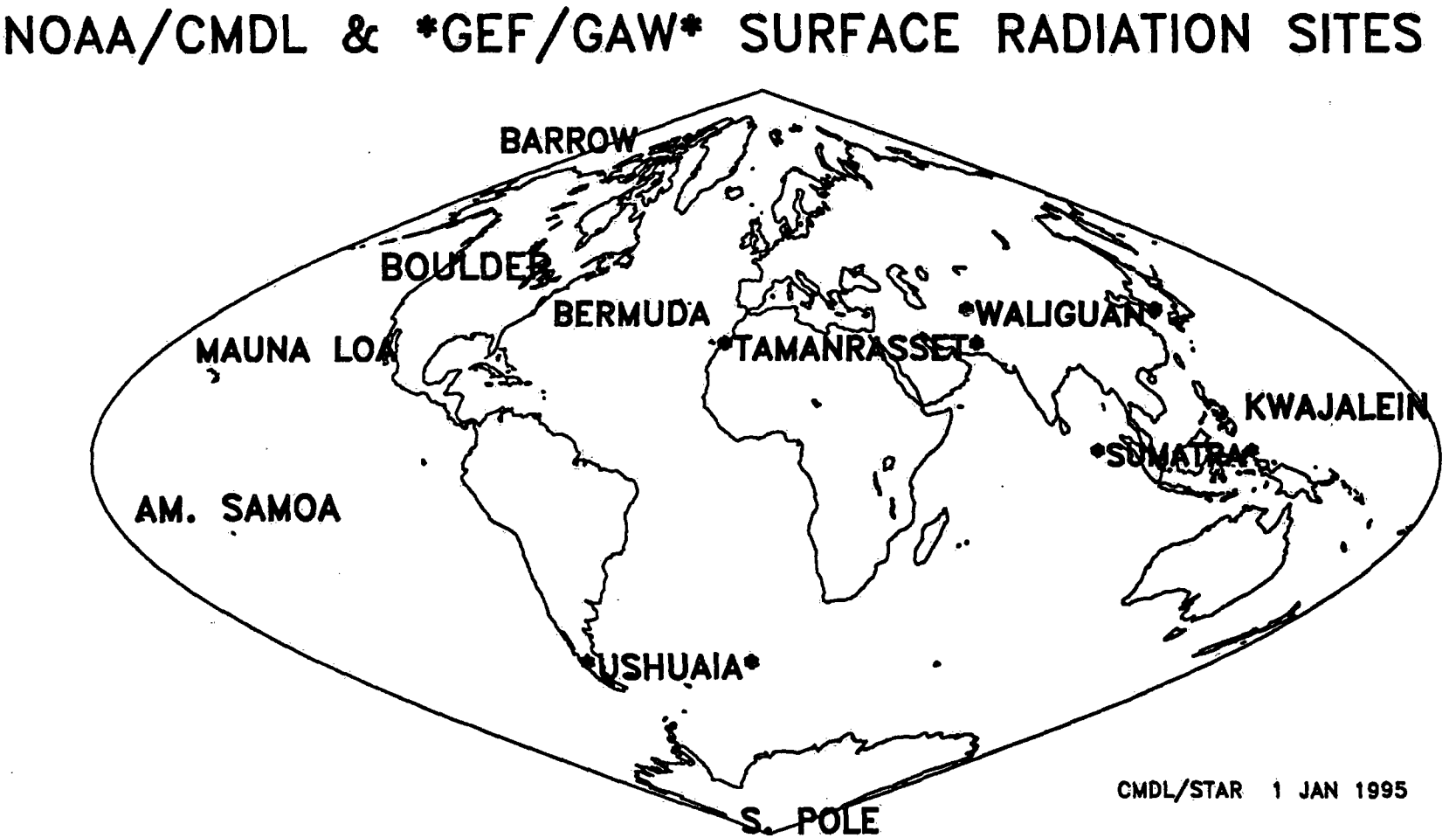

Figure 1: CMDL and GEF/GAW surface radiation monitoring sites, October 1995

ATMOSPHERIC TURBIDITY AND VOLCANIC ACTIVITY

Alexandre Joukoff and Jean Tempels
Institut Royal Météorologique de Belgique
Avenue Circulaire, 3
B - 1180 Bruxelles

1 Introduction

Atmospheric turbidity Linke factor constitutes an indicator of the general state of the atmosphere, it represents the ratio between the attenuation of the direct beam solar radiation through the actual atmosphere and the attenuation through an ideal dry and clean atmosphere. It depends upon the water vapour content of the atmosphere and upon the total load of the air pollution as well of anthropogenic origin (industrial activity, domestic heating, terrestrial and aerial traffic) as from natural sources (volcanic eruptions, sand storms, ocean spray)..

A trend or a change of the mean value in the series of turbidity values are generated by a significant modification of the atmospheric constituents. The method developed by Vannitsem et Demarée [1] for the study of Sahelian droughts has been applied to the long time series of the direct beam solar radiation observed in Uccle (Belgium).

A first study of the stability of the atmospheric turbidity in Uccle by Dogniaux et Sneyers [2] for the period 1951-1970, has shown an increase of the turbidity at an annual mean rate of 0.013 for these twenty years. Such an increase has been interpreted as a consequence of the air pollution level as resulting from human activities. This trend disappears when one considers the series extended to 1993.

2 Atmospheric turbidity

The fundamental relation describing the attenuation of the direct beam solar radiation by the atmosphere is given by:

$$I = \frac{1}{S} I_0 e^{-K_R m T_L}$$

where I, I_0 are the solar direct beam radiation respectively at the ground level and outside the atmosphere, the adopted value for the solar constant is 1367 W/m²,

S is the reduction factor to the mean Sun-Earth distance,

K_R is the extinction factor of clean and dry air per unit air mass (Rayleigh diffusion),

m is the relative air mass,

T_L is the Linke turbidity factor.

The Linke factor includes all the diffusion and absorption effects (excluding the Rayleigh diffusion), integrated over the whole spectrum, such as those of water vapour, absorbing gases, aerosols and all kinds of air pollution; it indicates the number of clear and dry

atmospheres required for reducing the solar extraterrestrial radiation in the same proportion than the actual atmosphere.

3 Data acquisition and processing

The Uccle solar direct beam measurements during 1951-1993 have been processed to derive the Linke turbidity factor for clear sky half hours (our integration standard): 30 minutes of sunshine are required from both the Campbell-Stokes heliograph and the pyrheliometric measurements to define a clear sky half hour. Values of Linke factor exceeding 7 are not considered as clear sky (presence of haze or light clouds).

4 Variation of the atmospheric turbidity

Annual means of the Linke turbidity factor are presented on *figure 1*. AM values are usually lower than PM values, due to the daily cycle of evaporation giving higher amounts of water vapour in the afternoon.

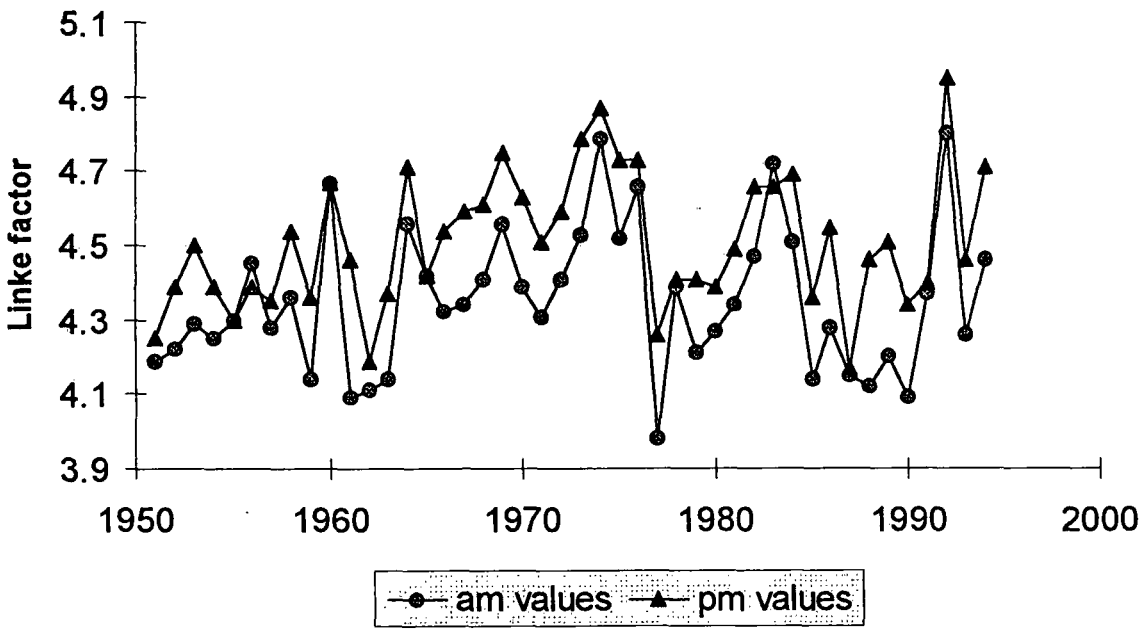

Figure 1. Annual means of the Linke turbidity factor

The annual cycle of the Linke factor in Uccle is shown on *figure 2*, with a maximum during the summer and a minimum in the winter.

Such a cycle corresponds to the evolution of the air masses reaching Belgium: during the winter, clear skies are mainly observed during cold and dry periods, while during the summer time, humid subtropical or maritime air masses dominate.

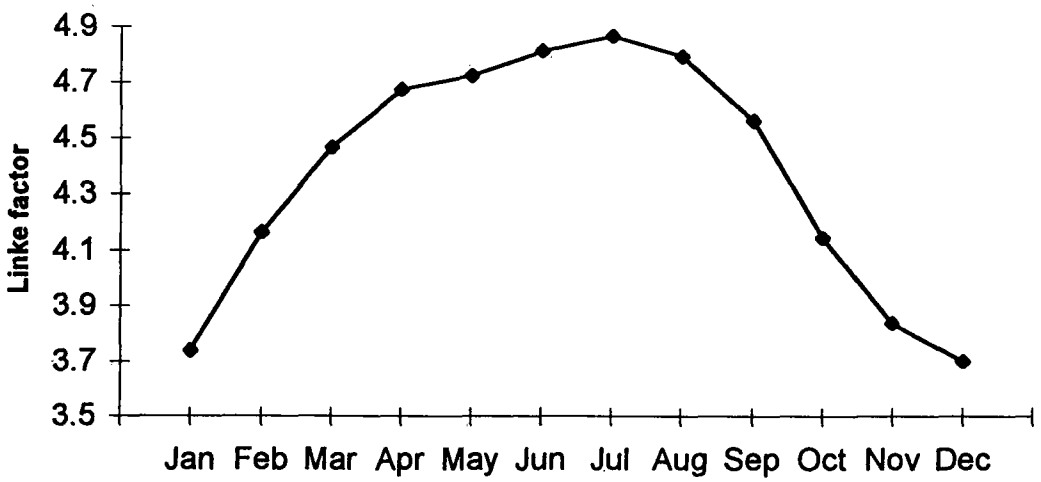

Figure 2. Monthly means of the Linke turbidity factor (1951-1993)

5 Statistics

The method used to show trends in the mean turbidity factors time series has been proposed by Vannitsem et Demarée [1], it is essentially based on three tests:

- Mann-Kendall test, allowing for the detection of a unique trend within the series,
- Lombard test, allowing to evaluate the number of significant changes in the mean,
- Pettitt test, allowing to estimate the position of a change in the mean, but only one.

All three tests are non-parametric: no hypothesis is done on the form of the distribution function of the series. Applying the tests on the whole series from 1951 to 1993, one can not find a significant trend (test de Mann-Kendall), but a change is revealed in the early sixties, however not significant for the Pettitt test. If one limits the series to 1975, a trend (increase) appears clearly starting in the begin of the sixties, the Pettitt test gives a change around 1963, confirming the results of Dogniaux and Sneyers for this period.

6 Relation between the turbidity and the volcanic eruptions

Atmospheric turbidity depends upon the global condition of the atmosphere and varies as function of the aerosol and dust contents. Explosive volcanic eruptions, such as this of Mount Pinatubo in 1991, increase the aerosol load in the stratosphere. The evolution of the atmospheric turbidity has been related to explosive volcanic eruptions. *Figure 3* shows the cumulated sums of the deviations of the monthly means of the atmospheric turbidity from the monthly means for the reference period 1951-1960, some volcanic eruptions known to have produced sufficient quantities of materials injected into the stratosphere to influence the solar radiation are indicated on the curve [4].

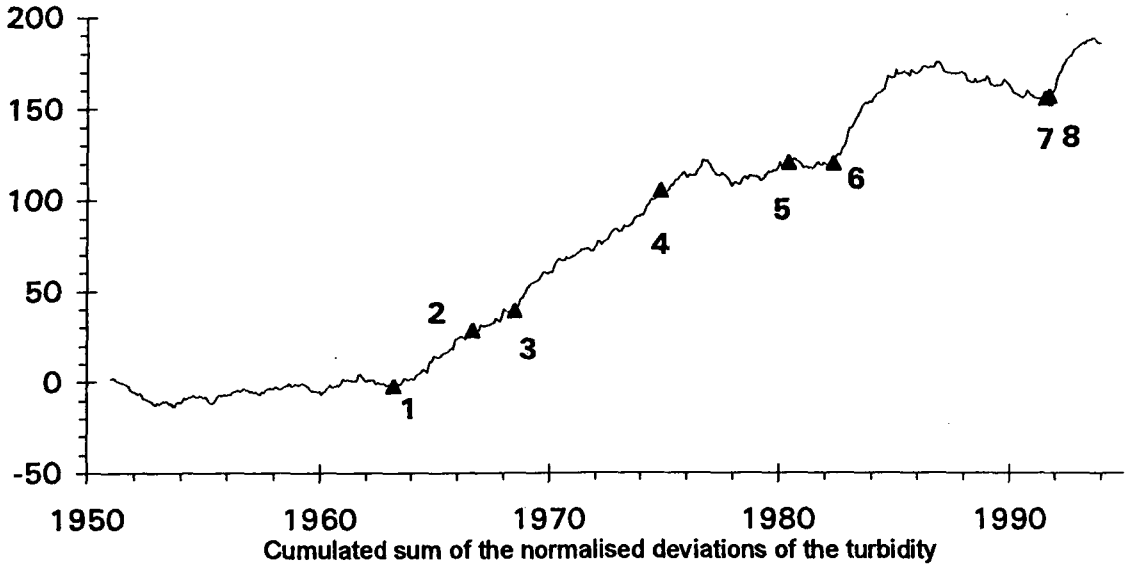

Cumulated sum of the normalised deviations of the turbidity monthly means from the 1951-1960 means.

*	Eruption date	Volcano	VEI	DVI
1	03/1963	Agung, Bali, 8°S - 116°E	4	800
2	08/1966	Awu, Celebes, 4°N - 125°E	4	200
3	06/1968	Fernandina, Galapagos, 0°S - 92°W	4	50-100
4	10/1974	Fuego, Guatemala, 14°N - 91°W	4	250
5	05/1980	St. Helens, USA, 46°N - 122°W	5	500
6	04/1982	El Chichon, Mexico, 17°N - 93°W	4	800
7	06/1991	Pinatubo, Philippines, 15°N - 120°E	5	1000
8	08/1991	Hudson, Chile, 46°S - 73°W	5	----

VEI = Volcanic Explosivity Index ; **DVI** = Dust Veil Index

Figure 3. Atmospheric turbidity and volcanic eruptions

Finally, using data furnished by M. Sato [3], it has been possible to connect the atmospheric turbidity to the stratospheric optical depth for the 0.55 μm wavelength. This is shown on *figure 4*. A clear correlation appears between main volcanic events an the rise of the turbidity following the Mount Agung eruption in 1963 and that of El Chichon.

The effects of the aerosols and dust injected during a volcanic eruption decrease slowly, and after about two years, the turbidity recovers its pre-eruption value, if no other eruption occurs.

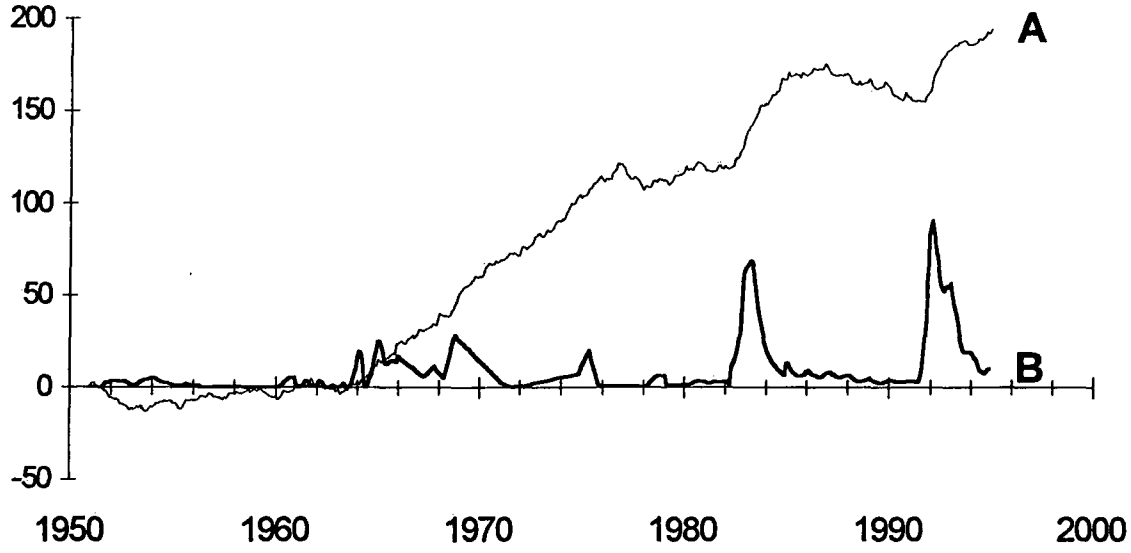

Figure 4. Atmospheric turbidity and stratospheric optical depth:
A: cumulated sum of the deviations of the turbidity monthly means from the values for the period 1951-1960;
B: stratospheric optical depth (values*500).

7 Conclusion

It clearly appears that the changes in the atmospheric turbidity are related to volcanic eruptions. The observed trend or change in the mean value which are found in the turbidity around 1963/1964 by the statistical study corresponds to the start of volcanic activity at this time; the first half of our century is considered as relatively quiet as far as the explosive volcanic activity is concerned.

8 Acknowledgements

The authors are grateful to. S. Vannitsem et G. Demarée for the statistical approach they have developed and for the statistical tests techniques, to C. Tricot et M. Sato for giving access to the stratospheric optical depth data.

9 References

[1] Vannitsem S. et Demarée G., 1991. Détection et modélisation des sécheresses au Sahel. Hydrol. continent., vol. 6, n°2 : 155-171

[2] Dogniaux R. et Sneyers R., 1972. Sur la stabilité du trouble atmosphérique à Uccle au cours de la période 1951-1970. I.R.M. Publications, Série A, n° 75

[3] Sato M., Hansen J.E., Mc Cormick P. and Pollack J. B., 1993. Stratospherical aerosol estimated optical depths, 1850-1990. N.A.S.A. preprint

[4] Lamb H. H., 1970. Volcanic dust in the atmosphere ; with a chronology and assessment of its meteorological significance. Phil. Trans. Roy. Soc. London 266A : 425-533

RELATED BSRN ACTIVITIES IN COLIMA, MEXICO

IGNACIO GALINDO
Centro Universitario de Investigaciones
en Ciencias del Ambiente (CUICA), Universidad de Colima,
P.O. BOX 380, 28000 Colima, Colima, México.
Tel. 52 (331) 3 11 65, Fax: 52 (331) 3 07 09
Internet galindo@volcan.ucol.mx

SUMMARY

The University of Colima has a research project on solar radiation studies which entails radiometer calibrations and comparisons, a measurement program of solar irradiance fluxes, and a program of measurements of atmospheric particles (aerosol) and gases together with meteorological observations. There is also a satellite receiving ground station for AVHRR satellite imagery. The aim of the project is the physical and chemical characterization of the atmospheric regional environment. High quality measurements performed at different heights on the Volcán de Fuego de Colima provide data for validating satellite-based determinations of the surface radiation budget. The project is also designed to monitor long-term trends in surface radiation fluxes. Since the goals of the project are similar to those of BSRN, the question arises if the Colima network should be part of that program.

1. INTRODUCTION

The research project of the Centro de Investigación en Ciencias del Ambiente from the University of Colima has within its lines of work measurement programs of surface solar irradiance fluxes together with meteorological parameters at sites under different environmental conditions (height, topography, vegetation etc.), particles (aerosol) and atmospheric gases are also determined. There is also a satellite receiving ground station for AVHRR satellite imagery. Preliminary results indicate that there are two main pollution sources in the area, a natural source, namely The Volcán de Fuego de Colima (3,850 m., a.s.l.) and a sugar mill which lies 5 km from the city of Colima.The Volcán del Fuego de Colima (3,850 m., a.s.l.) is an active volcano considered the most dangerous volcano in Mexico by several authors. It lies only 30 km north from the city of Colima. Airborne measurements of sulfur dioxide emission rates in the gas plume from the volcano are monthly made using a UV Correlation Spectrometer (COSPEC). The main research objective of this Center is the physical and chemical characterization of the regional environment which implies the study of the interaction between two very complex physical systems like an active volcano and its surrounding atmosphere. This research entails both theoretical and observational approaches, the link between them lies in the measurement programs. Since part of our activities are basically related with the measurement program of the Basic Solar Radiation Network (BSRN) project, in what follows I shall concentrate on the measurements program.

2. MEASUREMENT PROGRAM

The basic measurements include volcanic gases and particles (aerosols) from the fumarole, short-wave total and spectral fluxes, and meteorological parameters. At present there are four stations operating: CUICA (19.2oN, 103.7oW, 577 m.,a.s.l.), Rancho Buenos Aires (19.3oN, 103.7oW, 465 m.,a.s.l.), Rancho El Refugio (19.4oN, 103.7oW, 1,390 m.a.s.l.) and Volcancito (19.5oN, 103.6oW, 3500 m.,a.s.l.). Fumarolic sulfur dioxide is monthly measured by means of a UV-Correlation Spectrometer (COSPEC) which is mounted in an aircraft. Perpendicular traverses below the plume are made. SO_2 concentrations are determined. Particles (aerosols) are determined with a cascade impactor, filters and photovoltaic counter of particles. Chemical analysis of aerosol samples is made at the Facultad de Ciencias Químicas of the same University and X-ray fluorescence at the University of Guadalajara, Mexico.

Solar Irradiance Measurements

Short-wave total and spectral fluxes:
-global short-wave downward irradiance,
-diffuse short-wave downward irradiance,
-UV-global (290-385 nm) downward irradiance,
-UV-diffuse (290-385 nm) downward irradiance.
-UVB-global (250-320 nm) downward irradiance.

To be implemented, starting February 1996
-long-wave downward irradiance,
-reflected short-wave irradiance,
-direct broad irradiance with automatic driven sun-tracker,
-global short-wave spectral (380-950 nm) measurements.

Quality control of the irradiance measurements is obtained through a radiometer calibration and comparison program by means of the cavity radiometer HF-28765. automatic solar tracker and data acquisition system.

Meteorological measurements

-air temperature, dew-point temperature, humidity, atmospheric pressure, wind speed and direction.
-radiosonde observations (11 and 23 GMT) from the Meteorological Observatory from Manzanillo, Colima, 100 km southwest from Colima city.

2.1 INSTRUMENTS

Most of the radiometers used are from Eppley Laboratory, Inc. including the H-F absolute radiometer. UVB radiometers arethose designed by Berger and Robinson. Shading devices are those provided from Eppley. No attempt has been made to ventilate these instruments, however

a comparison under real conditions ventilated/non ventilated will be made soon. Meteorological instruments are those provided by Campbell Instruments from several manufacturers.

2.2 DATA ACQUISITION SYSTEMS

Electronic card devices are incorporated into a 286 ATX computer to run with a one minute cycle time, data are storage in the PC memory for each measured parameter. Data downloading on the network of the PC is started automatically every 20 minutes into a high-density diskette. Every four days diskettes are changed. Statistical processing of the information is performed at CUICA. We are also using Campbell Scientific CR10 and 21X data loggers. The data loggers are running with a five minutes cycle time for meteorological parameters and one minute sampling time for irradiance fluxes. Data are stored at the output part of the logger memory.The information is radiotransmitted to the Campus where downloading is started automatically every 20 minutes. Transfer and archiving of the data is performed once a day at midnight and renamed according to the present day so that full-day files are available for evaluation on the next morning.

2.3 THE SITES

The economy of the state of Colima is mainly based on agriculture, breeding cattle, and fisheries. With the exception of the Manzanillo's seaport there is almost no industrial development. The main pollution sources for the city of Colima are one sugar mill and volcanic dust. Therefore atmospheric transparency is quite good. It is only during January and February that there is soot and some smoke in the atmosphere due to burning of crop remnants in preparation for the next agricultural cycle. The vicinity of the volcano to the city permits the emplacement of observations sites at different heights under a exceptionally clear atmosphere. At present time we have four stations located at 465, 577, 1,390 and 3,500 m. a.s.l., respectively. Radio telemetry is used for communication with the stations and data downloading.

3. REMOTE SENSING OBSERVATIONS

Satellite Receiving Workstation .- This is an S-band station that receives HRPT data directly from the TIROS polar orbiting satellites. The system has an integrated software such that when images confirm the first releases of volcanic ash plumes, the trajectory of the plume can be followed. Warning reports will be delivered to Civil Aviation Authorities.

4. FURTHER DEVELOPMENTS

Located in the Coquimatlán campus (10 km from Colima city), there is a wind mill tower 90 m. height which is not in use anymore. There exist a project to use this facility for a type BSRN station which main objective would be validation of satellite derived surface irradiance. The site meets the specific requirements since the area is quite flat and homogeneous mainly devoted for

agriculture and cattle breeding. It is expected to have in operation this station during 1996. The objective of the station is to provide the highest possible quality, high sampling rate observations of the short and longwave fluxes together with surface and upper-air observations and other supporting observations. The quality standards will be those required for the BSRN stations.

Other site that we have chosen for next future observational developments is Isla Socorro, site of the Everman volcano. The island is located in Revillagigedo's Archipelago in the middle of the Pacific Ocean, 800 km west from Manzanillo, Colima. The island has been declared a forest reserve where no constructions are allowed. The only inhabitants there is a 60 men Mexican Navy post. Actually there is a meteorological observatory with regular radiosonde observations.

5. CONCLUDING REMARKS

The University of Colima has dedicated great efforts to build up a modern environmental research center which aim is the study of the regional atmospheric environment. The measurements program objective is to provide the highest possible quality, high sampling rate observations of the short and longwave surface radiation fluxes at a reference station located in a 90-m high tower together with surface and upper-air meteorological data and other supporting observations such as particles (aerosol) and gases (SO_2, NOx and O_3). The consistent set of measurements will provide data for the calibration of satellite derived estimates of surface radiative fluxes. The satellite data set from the AVHRR digital imagery will integrate, together with the surface data, a unique data set for theoretical computations of radiative fluxes This research center is willing to receive visiting scientists from abroad that could developed their research projects using our facilities.

Sunshine Duration Measurement using a Pyranometer

J. Oliviéri
Météo-France

1. Introduction.

It is well known that sunshine duration and Global exposure are strongly correlated. A Angström then J. A. Prescott and others proposed very simple formulae to estimate Global exposure from the number of bright sunshine hours and vice versa. Nevertheless such formulae are valid only if we consider sunshine hours totaled during one month or at least 10 days. Our intention is different. We think that it is possible to use the Pyranometer as a sunshine recorder. This presents a double advantage : sunshine duration ***and*** Global Irradiance (which is a more interesting datum) are measured at the same time for a very reasonable price.

2. The Method.

The measured Global Irradiance is compared every one minute (for example) to the value of the product Fc*Mod,

- Mod represents the Global Irradiance obtained from a cloudless day model,
- Fc represents a coefficient the empirical value of which is close to 0.7. Its real value depends on the period of the year, and probably on the site location.

We consider that if the measured Global Irradiance is superior to the product above mentioned, the Direct Irradiance of the Sun is superior to 120 W/m². If the Direct Irradiance reaches or exceeds this threshold level the number of minutes of bright sunshine is increased of one unit.

The models that were presently tested are:

- ***Model 1:*** $G = 1030 (\sin h)^{1.22}$
  where h represents the elevation of the Sun.
- ***Model 2:*** The ASHRAE Algorithm improved by M. Iqbal [See An Introduction to Solar Radiation - Academic Press].

The results obtained for the moment are correct. For twelve months running - July 1994 to June 1995 - hours of sunshine are within 1% of the Pyrheliometric Reference. For each month during this period, the errors are within ± 0% to ± 3.5% of the Reference. Of course daily and hourly errors may be larger. But usually the sunshine profile of the day is acceptable.

Figure 1 that follows, represents the Global, Direct Irradiances, and the products Fc*Mod versus Time. The functions *product* are noted F1 and F2, the factor Fc is equal to 0.65 in the two cases. ***Table 1*** represents the results of the sunshine duration obtained using the two models for the same day : June 1, 1995.

Remark: We are testing an other model that seems more interesting especially on the tails of the day.

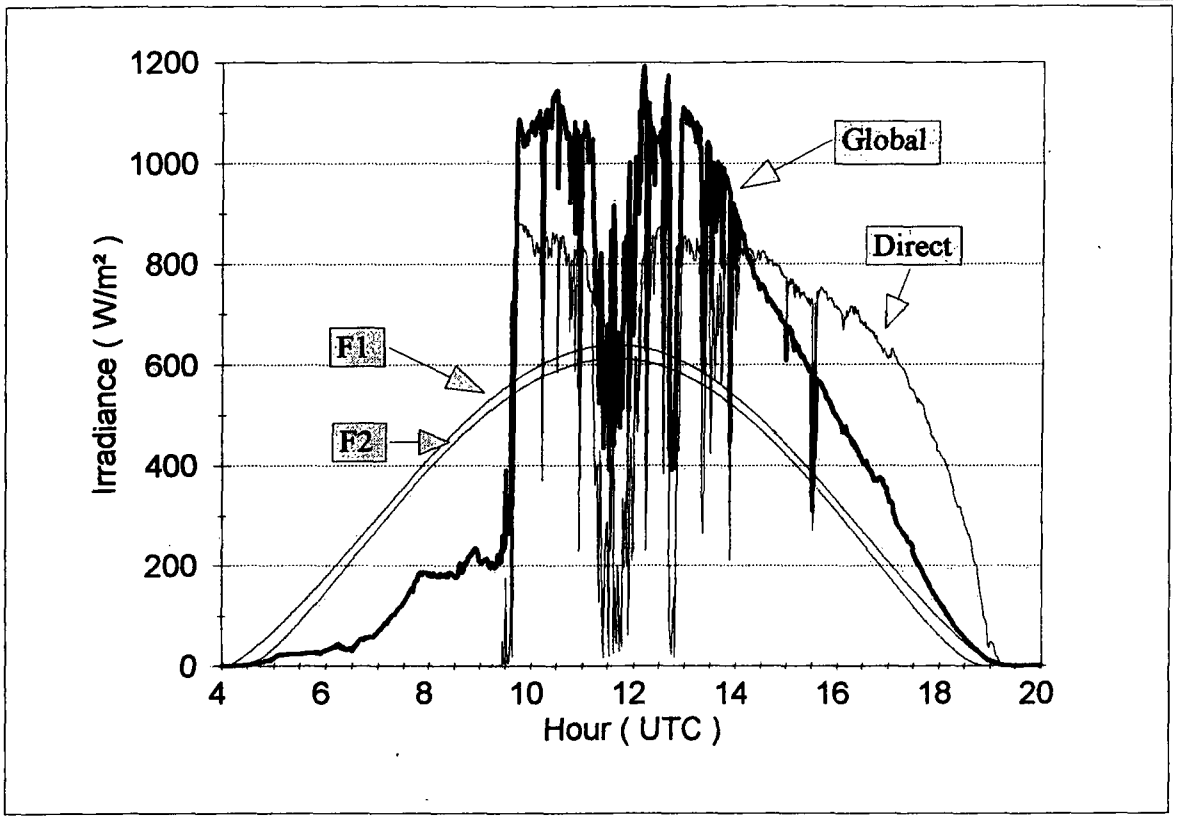

Figure 1 : Measured Global and Direct Irradiances on June 1, 1995 at Carpentras.
F1 and F2 : Products of Models 1 & 2 and Factors Fc.

UTC	SS(NIP)	SS(Mod1)	SS(Mod2)
5	0	0	2
6	0	0	0
7	0	0	0
8	0	0	0
9	0	0	0
10	23	21	21
11	60	59	59
12	50	42	44
13	53	51	52
14	60	59	59
15	60	60	60
16	60	58	59
17	60	60	60
18	60	60	60
19	51	60	60
SS Day:	**537**	**530**	**536**
ERR %	**0**	**-1.3**	**-0.2**

Table 1 : Hourly and Daily SunShine durations
(in minute) using two Models.

EPPLEY PYRGEOMETER EXPOSURE COMPARISON EXPERIMENT

R.P. Cechet[1], P.M. Novotny[2] & A.J. Prata[1]

1. CSIRO Division of Atmospheric Research, P.M.B. No. 1, Aspendale (VIC) AUSTRALIA 3195
2. Australian Bureau of Meteorology, G.P.O. Box 1289K Melbourne (VIC) AUSTRALIA 3001

1. INTRODUCTION

The Eppley infrared radiometer (pyrgeometer) manufactured by The Eppley Laboratory Inc., was designed to directly measure thermal atmospheric irradiance. At its release onto the international market in 1970, it was considered an accurate instrument with high sensitivity and a rapid response time (Drummond et. al., 1970). The Eppley Laboratory pyrgeometer remains the only instrument of its type that is commercial and well known in the international scientific community. It is generally considered as the standard monitoring instrument for surface downwelling thermal radiation, and it is being used by the World Climate Research Programme (WCRP) Baseline Surface Radiation Network (BSRN) to monitor long-term trends in radiation fluxes and to obtain high quality data for comparison with general circulation (global climate) models (GCM's) and for validating remotely sensed methods of determining components of the surface radiation budget.

The BSRN accuracy requirement for global solar irradiance is 2% (considered realistic), whereas the targeted uncertainty for the downwelling thermal radiation is presently 5%; ($\pm$20Wm^{-2} for a moist tropical environment and $\pm$15Wm^{-2} for a sub-tropical maritime environment). The lack of a widely available absolute standard longwave radiometer as well as a standardised calibration procedure for longwave instruments has caused this reduced accuracy requirement for the downwelling thermal radiation flux. In addition, questions have been raised as to whether the present instruments designed to measure thermal atmospheric irradiance are adequate to meet BSRN objectives as the range of absolute measurement errors may exceed 15% (WCRP-64, 1991).

During the FIRE II field experiment at Coffeyville, Kansas, November-December 1991, an intercomparison of 17 broadband radiometers (14 pyrgeometers and 3 pyrradiometers) measuring downwelling thermal radiation was conducted (DeLuisi et al., 1992). To study differences in performance, some pyrgeometer domes were ventilated and shaded as recommended by the BSRN (after Ohmura and Schroff, 1983) while other domes were exposed to solar radiation and natural ventilation. A variety of instruments (chiefly Eppley pyrgeometers ranging in age from new to 20 years old) were obtained from 14 different owners. Calibrations were supplied by the owners (generally manufacturer's calibration), however due to the non-availability of an operational absolute radiometer for comparison, the simple melting ice dome calibration procedure was used to compare all the instruments. The calibration factors resulting from these ice cavity calibrations were in the mean 4.7% higher (range: +1.6 to +9%) than the values provided by the owners. Under operational conditions during FIRE II, the 8 shaded and ventilated Eppley pyrgeometers displayed a spread of 10 to 20 Wm^{-2} during both daytime and nighttime operation, even after the instruments had been calibrated on-site by the same method.

There is a scarcity of long-term measurements of the downwelling longwave flux from continental stations. A number of continental sites are available as monthly means in the Global Energy Balance Archive (GEBA) (Ohmura and Gilgen, 1991). Of note are observations at Hamburg, Germany which commenced in 1954 and also Bergen, Norway where observations commenced in 1965. A number of research organisations and government agencies worldwide have commenced regular monitoring of the downwelling longwave flux since the mid 1980's. Many of these organisations and research bodies are associated with the BSRN, as BSRN stations are nationally operated, with guidelines for site selection, measurement uncertainty requirements, acceptable instrumentation, and data acquisition and management established by a BSRN expert working group (WCRP-54, 1990: WCRP-64, 1991). The BSRN recommendation that pyrgeometer domes be ventilated and shaded is not expected to be uniformly adopted by all national agencies due to the cost of setting up the installation. It is expected that a number of other useful datasets outside the BSRN framework will also become available over the next few years where different pyrgeometer exposures are adopted.

We considered that it is important that an evaluation of the significance of the various pyrgeometer exposures be undertaken to indicate the likely uncertainties in the observed mean daily, monthly and annual downwelling longwave fluxes for each exposure. In our study, we consider that the accurate reference measurement of downwelling longwave flux is obtained from an instrument exposure where the dome is properly ventilated and sun shaded following the recommendations of a recent report into state-of-the-art broadband infrared radiometry (IEA, 1993). Correction algorithms based on meteorological parameters and the downwelling shortwave flux are required so that in future when using data obtained from a number of sources with different exposures, one can minimise the uncertainty in the observed fluxes when comparing with satellite measurements or model output.

We have assembled a near identical set of eight Eppley pyrgeometers manufactured in the same batch. Following laboratory calibration against the Australian longwave standard, all instruments were setup under normal exposure to downwelling thermal radiation in a hot and dry boundary layer environment to determine long-term biases. The instruments were then arranged in 4 different exposures; normal, ventilated, shaded, and shaded and ventilated to investigate the magnitudes of differences in output. This paper describes the aim, methodology and the focus of our initial efforts in evaluating the differences between the exposure of operational systems (Eppley PIR instruments) for measuring downwelling thermal radiation. Initial efforts concentrate on comparison of the instruments under similar exposure in situations where large measurement errors due to direct solar heating are experienced. Some preliminary results of the 4 different exposures obtained from a test site in central Australia are shown.

2. THE EPPLEY PYRGEOMETER

The Eppley pyrgeometers used in this study incorporate a silicon dome with an interference filter that isolates the infrared (4 - 50 μm) part of the spectrum. These instruments are a modified version of the former Eppley pyrgeometers that included a KRS-5 (binary thallium iodide-thallium bromide) dome. The eight Eppley pyrgeometers acquired for this experiment were assembled in the same batch. The strategy in assembling this set of instruments was to minimise differences in dome transmittance, thermistor characteristics, dome coupling to instrument body and general instrument manufacture and also to eliminate effects due to instrument degradation. We speculate that these differences were in part responsible for the large biases displayed in the Coffeyville data (DeLuisi et al., 1992) and that bias errors due to inherent instrument (random) errors are in fact much lower than the reported bias values (see Section 3: Calibration and instrument comparison).

The diurnal variation of the Eppley pyrgeometer performance was questioned from the first days of its experimental use. Albrecht et al. (1974) in pyrgeometer aircraft measurements noticed that the cooling of the dome relative to the body of the radiometer reduced the output from the instrument. They proposed that the dome be monitored with a thermistor and the longwave radiation be calculated on the basis of energy balance considerations as detailed below (Albrecht and Cox, 1977):

$$L = EC + \varepsilon_o \sigma T_s^4 - K\sigma (T_d^4 - T_s^4) \quad (1)$$

Term (a) (b) (c)

where L is the incident irradiance, E the voltage output from the pyrgeometer thermopile, C the calibration constant of the thermopile, ε_o the emissivity of the thermopile surface, σ the Stefan-Boltzmann constant, T_s the temperature of the thermopile cold junction, T_d the temperature of the dome and K is a calibration constant (here refered to as the "dome minus sink" flux calibration constant) which relates the difference in the dome and thermopile cold junction (sink) longwave fluxes.

Enz et al. (1975) noted that an additional source of longwave radiation developed as the dome was heated by the sun. They vented air onto the dome in order to minimise heating and achieved an improvement of 50-65% based on values from shading tests obtained prior to ventilation. Shading tests showed that biases were a predictable function of incident solar radiation intensity, however the application of this simple empirical relationship was only practical on clear days. Another early effort to investigate this problem was by Campbell et al. (1978) where they redesigned the aluminium housing to act as a heat sink for the dome and also used a different type of thermopile.

In order to eliminate the diurnal response problems described above, in 1976 Eppley Laboratory Inc. introduced a pyrgeometer with a silicon dome. The silicon dome exhibits a transmissivity of about 0.5 for the wavelength interval 4-50μm and is opaque for wavelengths less than 3μm (Eppley 1976). Although the silicon dome pyrgeometer does represent an improvement on the KRS-5 model, limitations are still experienced with regard to dome heating (Weiss, 1981), however their magnitude has been decreased by more than 50% (Alados-Arboledas et al., 1988).

3. CALIBRATION AND INSTRUMENT COMPARISON

The aim of this study is to evaluate the differences between the exposure of operational systems (Eppley PIR instruments) for measuring downwelling thermal radiation. Firstly the thermopile calibration constant and the dome-sink flux calibration constant was determined in laboratory calibrations. Then prior to the instruments being setup with different exposures, they were first deployed at our calibration site in Melbourne, Australia with similar exposure (in our case we used the normal exposure; no shading or ventilation) to determine whether any bias errors exist between the instruments.

Laboratory calibrations were repeatedly carried out against the Australian longwave standard in an effort to determine the calibration error, and also to determine if there existed a difference between the manufacturer's calibration and the calibration using the Australian standard. The Australian longwave standard is detailed in Collins (1968). It was noted earlier that for the Coffeyville experiment a difference of 4.7% was found between the owners calibration (chiefly manufacturer's calibration) and the ice cavity calibration. Both Eppley and ice cavity calibrations use a cold downward

facing cavity whereas the Australian standard uses a hot (393K) downward facing cavity. There was the possibility that the inside cone skin temperature was not in agreement with the cone temperature transducers and we were interested to see whether there was a significant difference between the calibrations against the Australian standard and the manufacturer's (Eppley) calibrations.

Eppley Instr. Number	Eppley Calib. ❶	Aust. Calib. Nov.94 ❷	❷-❶	Aust. Calib. Nov.95 ❸	❷-❸
29069	3.89	4.20	0.31	4.14	0.06
29070	4.17	4.44	0.27	4.36	0.08
29071	4.28	4.47	0.19	4.42	0.05
29072	3.92	4.16	0.24	4.11	0.05
29073	4.38	4.48	0.10	4.43	0.05
29074	4.08	4.35	0.27	4.33	0.02
29075	4.25	4.46	0.21	4.40	0.06
29076	4.27	4.53	0.26	4.48	0.05
Average			0.23		0.05

TABLE 1. Eppley pyrgeometer thermopile calibration constant for the eight instruments used in the exposure comparison experiment. All units are $\mu V/(Wm^{-2})$.

The results which are shown in Table 1 indicate that the Australian calibration of the thermopile constant is not within 5% of the manufacturers (Eppley) calibration. There exists an average positive bias of 0.23 $\mu V/(Wm^{-2})$ (5.6%), which is similar to the positive bias of 4.7% determined at Coffeyville (DeLuisi et al., 1992) from comparison of ice cavity calibrations with calibrations provided by the owners (chiefly Eppley calibrations). Our results are based on the Australian National Standard Calibration Facility which has a 95% confidence level uncertainty of 2.5% (as endorsed by the National Association of Testing Authorities; NATA). The repeatability of the thermopile constant determination was ±1%. Differences in the magnitude of the downwelling thermal flux, using the Eppley calibration instead of the Australian calibration and employing equation (1) for the calculations, are shown in Table 2. The magnitude of the differences increases with increase in the temperature difference between the thermopile (sink) and that of the environment being viewed. It should be noted that we have assumed a value of 4.0 for the dome-sink flux calibration constant, K. At this stage we have not assembled apparatus to accurately measure this constant and have accepted advice from the Eppley Laboratory Inc. to set the constant to a typical value of 4.0 (possible range 3.6 to 4.4) for all instruments as they are from the same batch. This is likely to cause little error in comparing exposures.

Following laboratory calibration against the Australian longwave standard, all instruments were setup under normal exposure to downwelling thermal radiation in a hot and dry boundary layer environment to determine long-term biases. Firstly, long-term bias (baseline bias) was determined from measurements made early in the morning prior to sunrise (2am to 6am) under clear sky conditions (no dew formation) and when the atmosphere exhibits greatest stability. Data displayed in Table 3 show that these biases are consistent from night to night.

sink radiative flux (Wm^{-2})	350	400	450	500	550
sink tmperature (deg. Celcius)	7.1	16.7	5.3	33.3	40.7
t'pile radiative flux(Wm^{-2})	0	-50	-100	-150	-200
Difference; total flux (Wm^{-2})	0	-2.9	-5.8	-8.6	-11.5

TABLE 2. Differences in total downwelling thermal flux for Eppley minus Australian calibration where the downwelling IR is held constant at 350 Wm^{-2}.

Secondly, biases due to the diurnal heating cycle (diurnal bias) were determined from measurements made near local noon (11am to 2pm). The days considered experienced clear sky conditions. However, windspeeds were generally between 10 and 15m/s which limited the effect of dome heating. Values of the "dome-sink flux" (equation 1, term c) were between 20 to 40 Wm^{-2} around the time of local noon. This magnitude compares well with the results of Culf and Gash (1993) (2.7% of the total solar radiation). The weather conditions and calculated biases are displayed in Table 4. Baseline biases shown in Table 3 have been removed from the data. Once again, as was shown for the baseline biases, the biases determined near local noon (diurnal bias) appear consistent from day to day.

Instrument: Date	05/12/94	06/12/94	10/12/94	11/12/94	12/12/94	Average
29075(average)	341.9	350.2	292.1	319.0	345.6	
29075-29069	-6.7	-7.0	-6.8	-6.8	-6.9	-6.8
29075-29070	1.3	1.2	0.2	-0.8	1.1	0.6
29075-29071	-2.8	-3.1	-2.7	-2.9	-2.8	-2.9
29075-29072	1.8	1.8	1.6	1.5	1.8	1.7
29075-29073	1.8	1.1	1.8	1.3	1.3	1.4
29075-29074	-2.1	-2.5	-1.5	-1.4	-2.3	-2.0
29075-29076	0.2	-0.3	1.0	1.1	0.0	0.4

TABLE 3. Differences in downwelling thermal radiation for each Eppley pyrgeometer relative to instrument 29075 (clear sky nighttime measurements during stable boundary layer conditions). Note: All data are in units of Wm^{-2}. and the Albrecht and Cox formulation (equation 1) was used for the calculations.

Date	05/12/94	06/12/94	10/12/94	11/12/94	12/12/94	Average
Weather: Temp (°C)	clear high 30s	clear high 30's	light winds mid 20's	clear mid 30's	windy high 30's	.
29075(av'ge)	382.3	386.4	326.5	361.2	382.8	
29075-29069	0.3	0.9	-0.4	-1.2	0.9	0.1
29075-29070	1.0	1.6	1.7	0.5	0.9	1.1
29075-29071	2.3	2.1	1.4	2.0	1.8	1.9
29075-29072	5.2	5.1	4.3	4.8	4.9	4.9
29075-29073	2.5	2.5	3.7	3.0	2.1	2.8
29075-29074	-2.9	-2.5	-1.8	-2.9	-2.3	-2.5
29075-29076	-5.5	-5.0	-4.7	-5.5	-4.0	-4.9

TABLE 4. Differences in downwelling thermal radiation for each Eppley pyrgeometer relative to instrument 29075 (clear sky daytime measurements [11am to 2pm]). Baseline (steady-state) biases shown in Table 3 have been removed from this data. Note: All data are in units of Wm^{-2}.

The above dataset of 5 clear and hot days was initially only meant to give us an indication of the size of the relative biases compared to the total downwelling flux measurement. The magnitude of baseline steady-state biases are likely to vary with temperature whilst diurnal biases are likely to vary with temperature and more strongly with windspeed. We have adopted the values of the baseline biases for the work detailed below in light of their remarkable consistency over the temperature range from which measurements were carried out and also due to the fact that we will be working in a similar thermal environment. Further work is planned regarding the magnitude of the baseline bias and its variation with temperature and also the relationship between diurnal bias and windspeed at our experimental installation once we have accurately determined the dome-sink flux constant K in the laboratory.

4. EXPERIMENTAL INSTALLATION AND SOME PRELIMINARY RESULTS

Our experimental installation is located at Alice Springs (Central Australia), immediately adjacent to the only Australian BSRN site. It was hoped that any valuable results to come out of this work could be directly applied to BSRN data. Alice Springs is located on an elevated plateau (600 metres above sea level) and is characterised by a hot arid environment with generally light to moderate winds during the summer months. Summer [December to February] average daily maximum temperatures and sunshine duration (deg. C, hours) are 35.3, 10.2; 36.1, 10.2; 34.9, 9.8; for each month respectively. Hot days, where low windspeed conditions occur, are common and dome heating effects would be most prevalent on these days. The installation is at latitude 23° and therefore the solar zenith angle at local noon is near zero (overhead).

The pyrgeometers were exposed in 4 different arrangements; normal, ventilated, shaded and shaded and ventilated to investigate the magnitude of differences in output. The first installation occurred in March 1995, unfortunately missing the best season for measurements due to delays with equipment construction. Further equipment problems were encountered after installation with the result being that the equipment ran intermittently for 2 months. Some preliminary data from this period is shown below. The equipment was re-installed in January 1996 and is expected to run for 12 months.

Figure 1 relates to data acquired at Alice Springs on March 6th 1995. Conditions were initially cloudy with a thick middle-level cloudbank over the area until about 4am local time. The western (trailing) boundary of the cloudbank was very distinct, and following its passage conditions remained clear, relatively dry with light to moderate winds (steady at around 10 m/s) for the remainder of the day. The screen maximum temperature was 33°C and the land surface temperature was 55°C. Four pyrgeometers are under consideration here and their exposures were as follows; 29075 (shaded & ventilated), 29070 (normal), 29073 (ventilated) and 29074 (shaded). Data are minute averages of readings acquired every second.

The top panel of Figure 1 relates to the total downwelling flux for the shaded and ventilated pyrgeometer (29075). Panels 2, 3 & 4 relate to terms (a) (b) & (c) in the Albrecht and Cox formulation (equation 1); the thermopile, sink and "dome minus sink" (d-s) flux components, which when added together make up the result shown in panel 1. The jump in the thermopile and (d-s) fluxes is due to the sun-tracker being disabled at solar noon and then being reinstated just before 3pm local time (ventilation maintained thoughout). The effect is that the pyrgeometer dome heats and radiates at a higher temperature than that of the thermopile cold junction (sink) and this extra flux reduces the magnitude of the thermopile flux as the incoming flux increases and approaches the magnitude of the sink flux. Removing the shade gradually increases the sink temperature by approximately 1°C while the dome temperature rapidly increases by approximately 2°C. Panel 1 indicates that the Albrecht and Cox formulation, which although only a simple approximation to the radiation exchange occurring in the instrument, performs very well under these transient conditions of operation with only a slight deviation evident on the total flux plot.

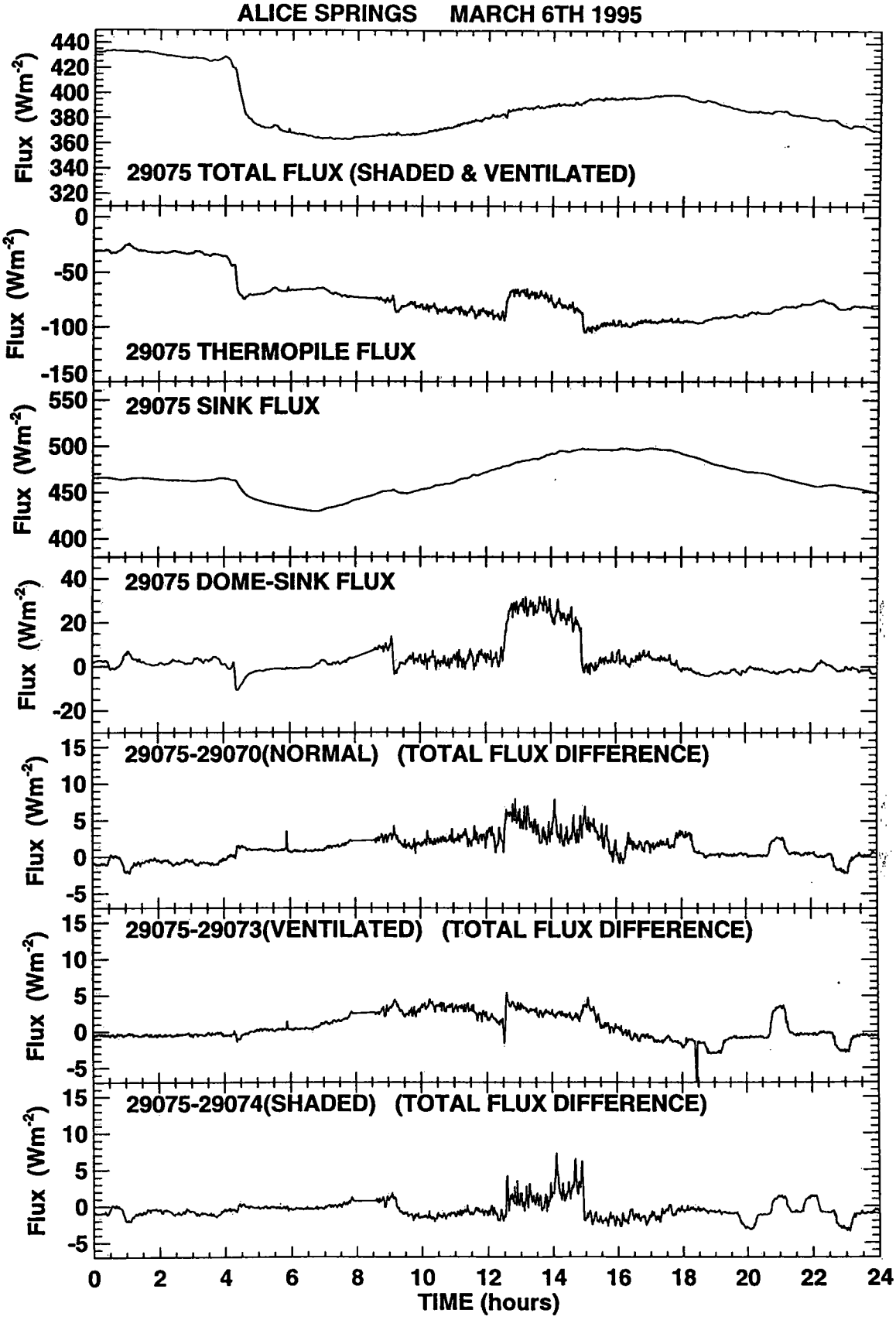

Figure 1. Pyrgeometer data at Alice Springs 6/3/1995

Figure 1 panels 5, 6 & 7, show the difference between the shaded and ventilated pyrgeometer (29075) and instruments exposed in the other 3 arrangements. The shaded and ventilated pyrgeometer (29075) and the shaded pyrgeometer (29074) use the same sun-tracker, therefore when shading was suspended we are comparing a ventilated exposure (29075) with a normal exposure (29074). Differences are very small under the chiefly moderate windspeeds experienced on this day; less than ±2 $W.m^{-2}$ averaged over the complete day. Of note is the slight parabolic shape of the differences shown in panel 5 & 6 (29075-29070, 29075-29073) compared to the flat difference response shown in panel 7 (29075-29074). The parabolic shape, which occurs during the diurnal warming cycle, is due to the assumption that the (d-s) flux constant K is the same for all instruments where in fact there appears to be some small difference for some instruments.

5. CONCLUSIONS & FUTURE WORK

As the early results of this study are only in a preliminary form, it is very difficult to make any assessment of the bias errors between different exposures even on a daily averaged basis. The early results do not contain data from the warmest months (December to February), and we have few days with temperatures above 30°C with light winds. Analysis of the 1996 data is expected to provide daily and monthly averaged biases for the different exposures.

The data displayed in Figure 1 gives the indication that these biases will in fact be quite small (of the order of a few Wm^{-2}) under most conditions. Under light wind or calm conditions with hot and dry days, biases are likely to be higher which will have a significant effect on the daily average. However, indications from meteorological records are that these days occur on less than 25% of cases and therefore mean monthly averages will not change to the same extent.

The Albrecht and Cox formulation appears to work remarkably well in handling the heating of the dome of the pyrgeometer relative to the body of the instrument. We are also interested in data obtained under normal exposure at many locations around the globe. It is reassuring that the performance of the Albrecht and Cox formulation under transient conditions (clouds) based on experience not included in the paper, has also been impressive.

We are concerned that the calibration of the thermopile constant of our 8 pyrgeometers showed on average a positive bias of 5.6% relative to the manufacturer's (Eppley) calibration values. This is similar to the positive bias of 4.7% determined at the FIRE II field experiment at Coffeyville (DeLuisi et al., 1992). The Coffeyville experiment highlighted the calibration biases between different laboratory standards and also between instruments after on-site calibrations. Our preliminary data shows that exposure biases are likely to be smaller than calibration biases between laboratories. There is an urgent need for an absolute standard longwave radiometer as well as a standardised calibration procedure for longwave instrumentation. The lack of a suitable standard has reduced the accuracy requirements for BSRN, and also has raised questions as to whether the present instruments designed to measure thermal atmospheric irradiance are adequate to meet BSRN objectivies. We strongly believe that it is the calibration standard and procedure, not the instrument design, that requires serious review.

ACKNOWLEDGMENTS

The enthusiastic assistance provided by the technicians stationed at the Bureau of Meteorology Alice Springs airport field site was greatly appreciated. Regular cleaning and checking of the instruments and data output provided by the observing staff at the Alice Springs airport field site was also much appreciated. A note of gratitude to G. Rutter for his technical assistance in the design of the data management software and setting up the field equipment.

REFERENCES

Alados-Arboledas, L., J. Vida and J.I. Limenez, 1988: Effects of solar radiation on the performance of pyrgeometers with silicon domes. J. Atmos. Oceanic Technol., 5, 666-670

Albrecht, B., M. Poellot and S.K. Cox, 1974: Pyrgeometer measurements from aircraft. Rev. Sci. Instrum., 45, 33-38

Albrecht, B. and S.K. Cox, 1977: Procedures for improving pyrgeometer performance. J. Appl. Meteor., 16, 188-197

Campbell, G.S., J.N. Mugaas and J.R. Kink, 1978: Measurement of long-wave radiant flux in organismal energy budgets: A comparison of three methods. Ecology, 59, 1277-1281

Collins, B.G., 1968: A long wave radiation source for net pyrradiometer calibration. J. Sci. Inst.. Ser 2, 1, 62-64

Culf, A.D. and J.H.C. Gash, 1993: Longwave radiation from clear skies in Niger: A comparison of observations with simple formulas. J. Appl. Meteor., 32, 539-547

DeLuisi, J., K. Dehne, R. Vogt, T. Konzelmann, and A. Ohmura, 1992: First results of the baseline surface radiation network (BSRN) broadband infrared radiometer intercomparison at FIRE II. IRS '92: Current problems in atmospheric radiation, 559-564

Drummond, A.J., W. J. Scholes and J. H. Brown, 1970: A new approach to the measurement of terrestrial long-wave radiation. WMO Tech. Note No. 104, 383-387

Eppley, 1976: Instrumentation for the measurements of components of solar and terrestrial radiation. Unpublished document by Eppley Laboratory Inc., Newport, 12pp

IEA, 1993: IEA (SCHP) Comparison of longwave radiometers in Hamburg 1989/90 (Report of Task 9)

Ohmura, A. and K. Schroff, 1983: Physical characteristics of the Davos-type pyrradiometer for short-wave and long-wave radiation. Arch. Met. Geophys. Biol., Ser. B, (33), 57-76

Ohmura, A. and H. Gilgen, 1991: Global Energy Balance Archive GEBA. Rep.2: The geba database: Interactive applications, retrieving data (Heft 44). Geographisches Institut, ETH Zurich. 66pp

WRCP-54, 1990: Radiation and climate (Workshop on implementation of the Baseline Surface Radiation Network. Washington D.C. U.S.A., 3-5 Dec.), WMO / TD No. 406

WRCP-64, 1991: Radiation and climate (Second workshop on implementation of the Baseline Surface Radiation Network. Davos Switzerland, 6-9 Aug.), WMO / TD No. 453

The Global Radiation in the Past 100 Years in Potsdam

Klaus Behrens
Meteorological Observatory Potsdam
German Weather Service

1 Introduction

Since the 1st of January 1893 regularly meteorological observations have been made at the Meteorological Observatory in Potsdam, Germany. Traditionally, the measurements of radiation components play an important role in the scientific work at the Observatory (Spänkuch 1993, Körber 1993). The duration of sunshine is one of these elements. Global radiation has been recorded since the beginning of 1937.

Global radiation is one of the most important meteorological elements in climatology, because it characterizes the potential, from the Sun irradiated energy at the surface. Global radiation integrates the influences of the solar radiation at the way through the atmosphere. The exact knowledge of the temporal and spatial distribution of radiation components is necessary for solving basic problems in meteorology (Raschke 1989). Therefore the course of annual and selected monthly totals of the global radiation at Potsdam in the past 100 years are discussed in connection with other meteorological elements.

2 Data Base

2.1 Direct Measurements

Hourly values of global radiation have been recorded since the 1st of January 1937 with thermoelectrical pyranometers with the exception of only a few short periods during World War II and in 1946/47 when it was necessary to use a ROBITZSCH-Pyranograph (Robitzsch 1932). The registration was lack only in some few cases in the first decade. Unfortunately, as a result of the war, the radiation data are missed completely for the years 1944 and 1945.

From 1937 up to 1967 the MOLL-GORCZYNSKI-Pyranometer (Gorczynski 1926, e. g. Bener 1950, Hinzpeter 1952), the so-called Solarimeter, were used. In 1968 these instruments were replaced by SONNTAG-Pyranometers (Sonntag 1963, 1975).

From the beginning up to the end of 1968 the voltages of the pyranometers were recorded by a strip recorder. The recording strips had to be manually planimetered and then the hourly totals had to be calculated. Later on the data were recorded by different types of electronic equipment.

Calibrations of the instruments were done by the shadow-method at suitable weather conditions preferably at least once a month. As in wintertime often monthly calibrations are not possible, the instruments have been compared since the midseventies with the Observatorie's standard pyranometer.
The calibrations, using the shadow-method, were at first done by the MICHELSON-MARTEN-Actinometer No. 515 and has been done since 1946 by the LINKE-FEUSSNER-Actinometer No. 27. These instruments were regularly compared with the Silverdisc-Pyrheliometer No. 12 and the ANGSTRÖM-Pyrheliometer No. 140 and later on, since 1983, by an Absolute Radiometer PMO 6. These standard instruments were at every time close connected to the different pyrheliometric scales by many international comparisons.

As a result of the installation of the WRR in 1981 a general data homogeneization and rehabilitation was undertaken and missing data were supplemented. All hourly values were checked and converted into this reference scale, the WRR, and in SI-Units (J/cm²). This step was necessary, because formerly the data were registered in Smithsonian Scale rev. 1913 and later in International Pyrheliometric Scale 1956 (IPS 1956) as well as in calories.
Table 1 summerizes the radiation scales and the correction factors needed to bring the Potsdam radiation data to WRR (Schöne 1973, Fröhlich 1975).
Getting a complete series of global radiation, single missing daily totals were substituted using the relation between duration of sunshine and global radiation.

As since the beginning in 1937 the radiation components global radiation, direct radiation at normal incidence and sky radiation have been measured independently from each other, a permanent check of the hourly sums using the equation

$$I \sin h + D - G = \delta$$

was possible, assuming $\delta = 0$, with I direct radiation at normal incidence, D sky radiation, G global radiation and sinh the sinus of the sun height.
Taking into account all measures of quality protection as well as of the estimated errors for the instruments used (Bener 1950, Schieldrup Paulsen 1968, Sonntag 1975) we may assess the uncertainty of the global radiation within ±3 %, measured by thermoelectrical pyranometers. A similar estimate was given by Stanhill and Moreshet (1992).

Table 1
Radiation scales used at Potsdam

Period	Standard instrument	Scale	Correction factor
1937 - 1956	SI 12	Smithsonian rev. 1913	0.9765
1957 - 1967	SI 12	IPS 1956 (Def. 2)[1]	0.9965
1968 - 1980	A 140	IPS 1956 (realized)[1]	1.022
1981 - 1982	A 140	WRR	1.000
1983 -	PMO 6	WRR	1.000

[1] For more details see Fröhlich 1975

Unfortunately, the radiation measurements, except of sunshine duration, were not carried out all over the time at the same place at Potsdam. From 1937 up to 1967 all components were measured at the Telegraphenberg ($\varphi = 52°23'$ N; $\lambda = 13°04'$ E; h = 81 m). Between 1968 and 1984 global, diffuse and direct radiation were recorded about 2,5 km easterly at the Schlaatz. Since the 1st of August 1984 the components have been recorded at the Strahlungs- und Ozonstation Ravensberge (SOR). These three locations form a triangle with nearly equal side length less than 2,5 km. The third location in south direction between the first two points. The microclimate is similar at the first and third location because they are situated in a nearly equal height and the same closed forest area south of the town. The second location, at nearly 50 m lower altitude was surrounded by meadows.

2.2 Estimate of Global Radiation from Sunshine Duration

Because it will be discussed the long time series of the global radiation, it is necessary to extend the measured series backward. Using the close correlation between duration of sunshine and global radiation it was possible to extend the global radiation series backwards till the beginning of sunshine records in 1893. However, this procedure allows reasonably estimates only of monthly means or totals. The monthly totals of global radiation from 1893 to 1936 were calculated using the following regression equation

$$G = G_R (a + b S_r)$$

with G calculated global radiation, G_R global radiation in the Rayleigh-Atmosphere, a and b regression parameters, S_r relative sunshine duration.

Relative sunshine duration and relative global radiation (G/G_R) are highly significant correlated. The standard error of estimation is between 3,2 % in July and 9,4 % in December. From April to September this error is less than 4 %. The annual totals were calculated from the monthly totals.

3 The Homogeneity of the Potsdam Global Radiation

One of the most important supposition for analysing time series is their homogeneity. The Potsdam global radiation series consists of indirectly derived values (from 1893 - 1936) and direct measurements, made, however, with different devices and at slightly different places. An overview of all these changes is given in Figure 1. These different factors may change the stability of the mean and of the dispersion. Therefore we have to test these statistic elements of the time series. It is obvious, that this homogeneization check was done after

levelling (WRR, SI-Units) and supplementing the measurements. The well-documented history of the Potsdam radiation series allowed the level corrections (pyrheliometric scales, reduction of units) without any difficulties.

The test of homogeneity has two main goals, to check

(i) whether the direct measurements are influenced by the different places, the different instruments and data aquisistion methods as well as the processing methods.

(ii) whether the whole series, the direct measured and the calculated values, describe the same sample.

Therefore, the check was splitted in two steps. At first we examined the monthly totals of the direct measurements and at a second stage the whole data ensemble.
A test of the monthly time series is recommended, instead of the annual totals, because the different influences could affect the series in a different manner all over the year.
As above described, the measurement of the sunshine duration was carried out in the last 100 years at the same location and since 1915 with the same instrument. This circumstance and the high correlation between global radiation and duration of sunshine was used to investigate the different influences at the measurement of global radiation especially between 1937 and 1992. Therefore the quotient of these two elements was checked.

The homogeneity was tested (Sneyers 1975, Stellmacher 1983) using the

WALD-WOLFOWITZ-Test

for checking the 1st order autocorrelation, and the

MANN-KENDALL-Test and the

progressive analysis

for examination the stability of mean and dispersion (absolute deviation from the mean). Additionally the mean was checked by the

WILCOXON-Test (U-Test)

(Taubenheim 1969, Weber 1980).
These non-parametric tests do not assume the GAUSSIAN or normal distribution.

The analysis of the homogeneity tests reveals

(i) there are a couple of months (e. g. April) whose homogeneity can be assumed

(ii) if inhomogeneities are stated, they occur mostly in global radiation and in sunshine duration

(iii) surprisingly, the indicated inhomogeneities do not coincide with the changes in instrumentation et al. given in Figure 1.

Meaning, that the detected inhomogeneities are a result of different atmospheric conditions. Hence, the effect of the local factors (location, different equipment and methods), influencing the measurement of global radiation at Potsdam are smaller than the changes in the atmosphere.
An inhomogenous dispersion was only detected in January and April for global radiation and in January for sunshine duration, which were not in context with changes in local factors.
As later described, the time series show a long periodic oscillation, occuring in mostly all of the months and in the annual course. There does not exist any inhomogeneity, after the removal of this oscillations. This test of homogeneity was done with the same procedure. This is some evidence, that the detected inhomogeneities are the result of changes in the atmosphere.
The analysis of the monthly total of global radiation of 100 year series shows only some few inhomogeinities, which were not in connection with backward extension of the series.
The checks for inhomogeneity showed, that the changes of the local factors did not disturb the homogeneity. The 100 year record of global radiation can therefore be used for climatological analysis.

4 Time series analysis

Global radiation at the ground is, even if we suppose a constant radiant flux at the top of the atmosphere and if we exclude the daily and annual course, not a stationary element, because it is influenced on its way through the atmosphere by many changing parameters.

In Figure 2 the 100 years time series of the annual totals of the global radiation at Potsdam are shown. This figure contains the 11 year moving average, too. It characterizes the essential pattern of the time series' course. The annual course indicates main points of inflexion (turning-points), which are connected with the minima around 1907 and 1982. The section between the turning-points are three quarters of the observed time.

It is worthwhile mentioned, that the ascending section is longer than the descending one, meaning, that the period is not stable over the whole time or is a result of superposition of oscillations with different frequencies

or phases.
In general, the ascending and descending parts are nearly linear with some breaks. The increasing tendency of the annual totals is interrupted for ten years between 1930 and 1940.

Because of missing global radiation data in the first half of this century in other time series, the decrease from the early fifties up to now will are interpreted as a trend (e. g. Stanhill and Moreshet 1992). Analysing the data from the world radiation network (1958/85), they found a negative trend for the high temperate latitudes (60 - 45° N), which is partial greater then the measurement error.

The estimated changes per year of the annual totals of global radiation are 0.24 %/yr for the ascending and 0.29 %/yr for the descending sections and 0.03 %/yr between the minima of the running mean (1907 and 1982) for Potsdam. (see also Fig. 2)

The described trends are within the measuring error and the climatic noise and show therefore no significant change of global radiation during the last 100 years.

Comparing the time series of global radiation and sunshine duration (Fig. 3), we observe the same structure. A similar structure was found by Wacker (1981), who analysed the sunshine duration at Karlsruhe, Germany, between 1895 and 1977. Figure 3 shows, too, that the ratio between global radiation and bright sunshine changed in the last 100 years, indicating changing transmissivity of the atmosphere.

What are the reason for the changes in global radiation in the past 100 years?
In Central Europe global radiation is mainly influenced by cloudiness and less influenced by atmospheric turbidity. In Potsdam we observe at around 85 % of the days clouds affect sunshine duration in summertime and up to 95 % in winter.

Comparing the moving averages of the annual values of global radiation and cloud amount (Fig. 2 and 4), we observe two different patterns. The global radiation increases nearly steadily from the minimum in 1907 to the maximum in 1952. Similar is the descent trend afterwards. The long term mean was crossed in 1923 and 1973. The moving average of the cloud amount is from the beginning up to 1935 considerably smaller than the long term mean, but afterwards, without a short break between 1965 and 1972, essential higher.

In the period from around 1935 up to the mid-sixties total cloud amount and global radiation (and the independent measured sunshine duration) are together above the long term averages. We conclude, that the optical thickness of the clouds in that time period was lower than during the first decades of the measuring period. Bernhardt et al. (1991) interpreted this effect as a increase of the share of high clouds at the total cloud amount. This interpretation is supported by the 11 year moving averages of total cloud amount (N) and of the ratio of global radiation (G) and cloud cover (Fig. 5). This ratio may serve as a measure of the transmissivity of the atmosphere. This ratio is nearly constant at a low level from the beginning up to 1915. Afterwards the ratio increases rapidly to a distinct higher value with large variations. The first period with high G/N-values between 1922 and 1932 is accompanied by a small cloud amount. The second section (1943/53) of high G/N-values has a above average cloud amount. Both periods are connected with the highest values in global radiation (see Fig. 2).

Global radiation is governed by cloud amount and the optical thickness of clouds. Long term variations in cloud optical thickness can be assessed independently, too, from Figure 5. Both aspects have to keep in mind when analyzing variations in global radiation.

Weber (1990) investigated the temporal variation of sunshine duration in Germany in 1951/87. He explained the decline in sunshine duration in Central Europe with a changed circulation pattern in Europe. The observed variations in global radiation are, therefore, caused by the variations in the circulation regime.

Course of global radiation and cloud amount are only partly in phase. Hence, the variations in global radiation cannot be explained solely by variation in cloud amount. Variations in cloud radiative properties have to be taken into account, too.

5. Conclusions

In the past 100 years the course of global radiation in Potsdam is characterized by periodic oscillations. Removing this oscillation, a small increase of 0.03 %/yr is observed in the annual totals, which is not significant. The reasons therefore we have to see in a changing total cloud amount and in a change of the optical properties of the cloudiness as well as of the cloud-free atmosphere. The main reason seems to be changing circulation pattern, which also affect the cloudiness.

References

Bernhardt, K., Helbig, G., Hupfer, P., Klige, R. K., 1991: Rezente Klimaschwankungen. In: Hupfer, P. (ed.) Das Klimasystem der Erde. Berlin: Akademie Verlag, 464 pp.
Bener, P., 1950: Beiträge zur Strahlungsmeßmethodik III: Untersuchungen über die Wirkungsweise des Solarigraphen MOLL-GORCZYNSKI. Arch. Met. Geophys. Biokl. Ser., B, 2, 188-249.
Fröhlich, C., 1975: Scientific discussions of IPC IV at Davos. WRC Publication No. 543
Gorczynski, W., 1926: Solarimeters and Solarigraphs. Moth. Weath. Rev., 54, 381-384.
Hinzpeter, H., 1952: Bericht über neuere Arbeiten zum Solarimeter nach Gorczynski. Z. Meteorol. 6, 118-121.
Körber, H.-G., 1993: Die Geschichte des Meteorologisches Observatorium Potsdam. Geschichte der Meteorologie in Deutschland Bd. 2, Offenbach, 129 pp.
Raschke, E., 1989: Der Strahlungshaushalt der Erde. Naturwissenschaften, 76, 351-357.
Robitzsch, M., 1932: Über den Bimetallaktinographen Fuess-Robitzsch. Gerl. Beitr. Geophys., 35, 387-394.
Schieldrup Paulsen, H., 1968: A study of the radiation climate of Southern Norway. Part II: On the calibration of radiation instruments. Arbok for Univ. i Bergen Mat.-Naturw. Serie 2, 74 pp.
Schöne, W., 1973: Über Vergleichsmessungen zwischen Angström- und Silverdisc-Pyrheliometern. Unveröffentl. Bericht, Potsdam, 14 pp.
Sneyers, R., 1975: Sur l' analyse statistique des séries d' observation. WMO, No. 415, TN 143, 189 pp.
Sonntag, D., 1963: Ein Pyranometer bzw. Effektivpyranometer mit galvanisch erzeug-ter Thermosäule. Z. Meteorol., 17, 49-56.
Sonntag, D., 1975: Pyranographen bzw. Effektivpyranographen mit galvanisch erzeugter Thermosäule und ihre Erprobung in Berlin, Potsdam, Stockholm, Leningrad und Bergen. Abh. Meteorol. Dienst DDR, Nr. 115, 80 pp.
Spänkuch, D., 1993: 100 Jahre Meteorologisches Observatorium Potsdam. promet 1/2, 2-7.
Stanhill, G., Moreshet, S., 1992: Global radiation climate changes: The world Network. Climatic Change, 21, 57-75.
Stellmacher, R., 1983: Prüfung der Homogenität und statistischen Analyse von Zeitreihen, vorgestellt am Beispiel klimatologischer und hydrologischer Reihen. Diss. (B), Adw der DDR, Berlin 1983, 117 pp.
Taubenheim, J., 1969: Statistische Auswertung geophysikalischer und meteorologischer Daten. Leipzig: Akad. Verlagsges. Geest & Portig, 386 pp.
Wacker, U., 1981: Untersuchungen langfristiger Schwankungen der Sonnenscheindauer. Arch. Met. Geoph. Biokl., Ser. B, 29, 269-281.
Weber, E., 1980: Grundriß der biologischen Statistik: Anwendungen der mathemati-schen Statistik in Forschung, Lehre und Praxis. 8. überarb. Aufl., Jena: Fischer, 652 pp.
Weber, G.-R., 1990: Spatial and temporal variation of sunshine in the Federal Republic of Germany. Theor. Appl. Climatol. 41, 1-9.

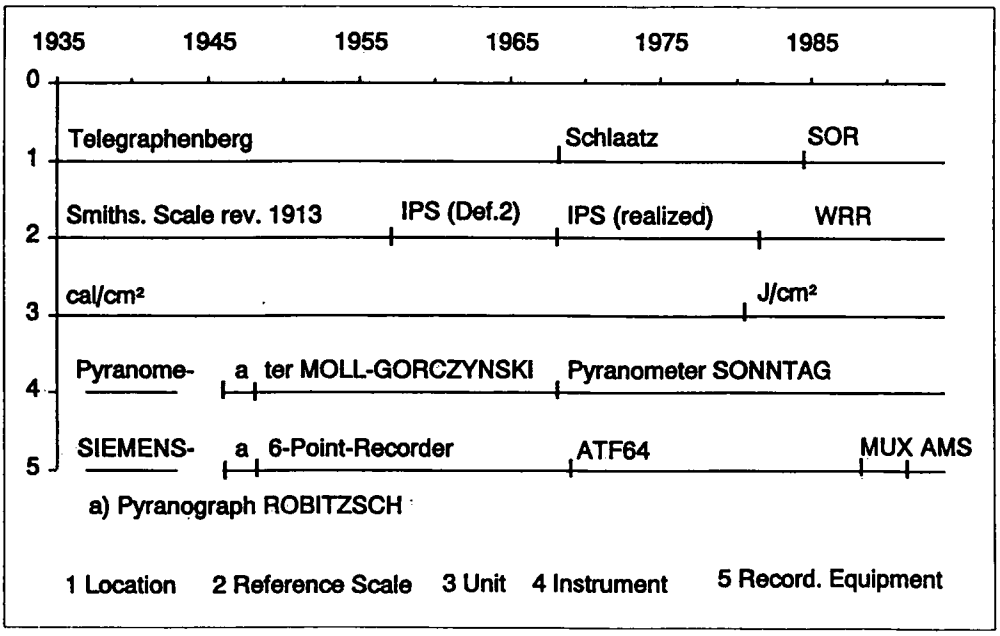

Fig. 1: Overview about the local parameters influenced the Potsdam radiation measurement

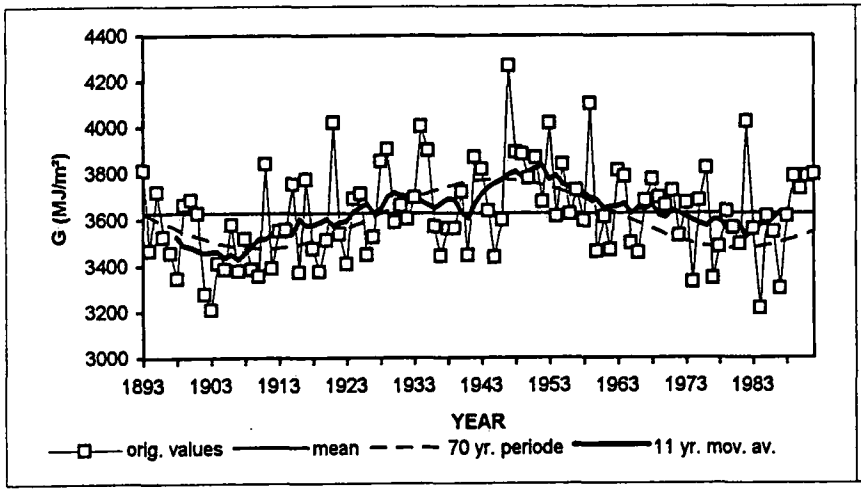

Fig. 2: Annual totals of global radiation (G) at Potsdam (1893/1992)

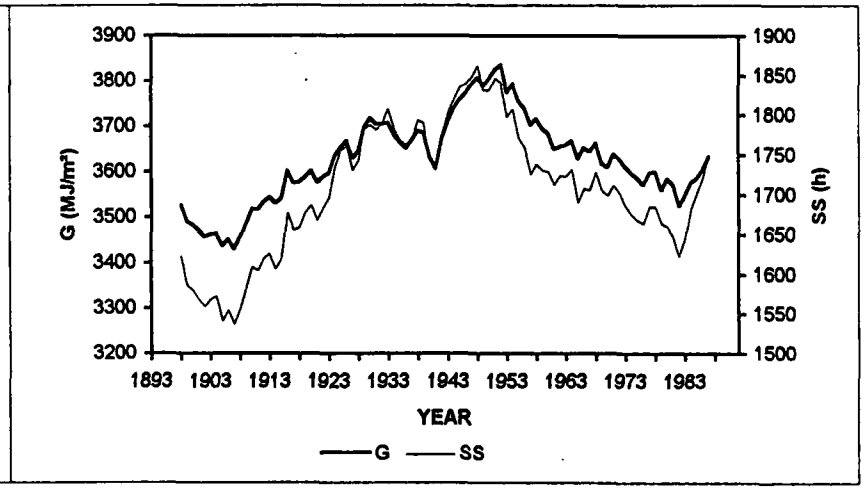

Fig. 3: 11 year moving averages of the annual totals of global radiation (G) and sunshine duration (SS) at Potsdam (1893/1992)

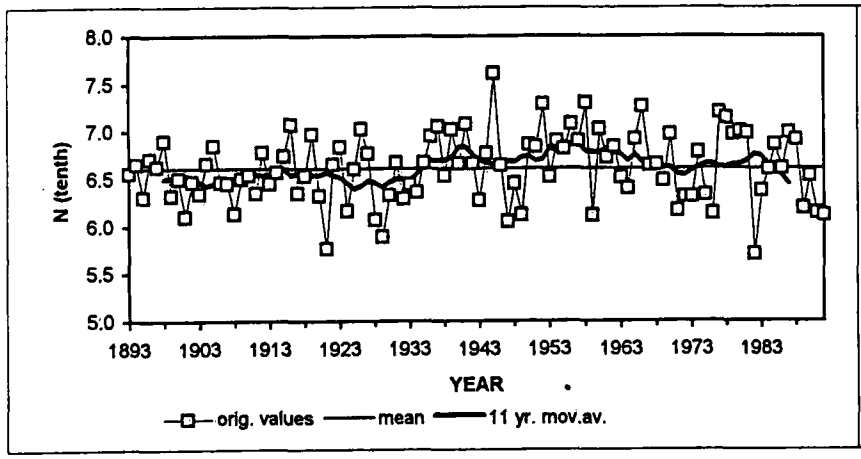

Fig. 4: Annual means of total cloud amount (N) at Potsdam (1893/1992)

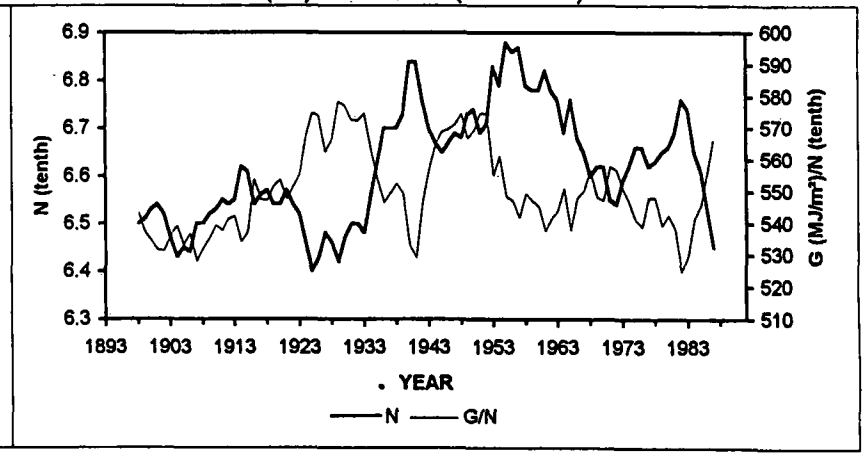

Fig. 5: 11 year moving averages of the annual means of total cloud amount (N) and the ratios of annual totals of global radiation (G) and annual means of total cloud amount (N) at Potsdam (1893/1992)